

Modelling alongshore variable dune erosion with XBeach



Rems Neele - 6266665

19-07-2019

Msc Thesis Earth, Surface & Water

Utrecht University - Faculty of Geosciences - Department of Physical Geography

Under supervision of

- dr. Timothy Price
- prof. dr. Gerben Ruessink



Utrecht University

Abstract

Dune erosion due to storm events have been comprehensively studied in recent history. With the use of measured data about bed level, water level and wave characteristics, further understanding about the processes that drive dune erosion can be achieved. These measured values can be implemented in dune erosion models. Commonly used dune erosion models are one-dimensional, meaning a single cross-shore section of the coastal area. However, a 1D model does not take alongshore variations into account. Hydrodynamics and sedimentation vary alongshore and are affected by each other. Meaning dune erosion varies alongshore as well, resulting in so-called erosional hotspots. What dominantly drives these erosion hotspots is uncertain for dunes impacted by storms in the collision regime. A modelling method that is capable of implementing alongshore variations is XBeach. XBeach is a two-dimensional model for wave propagation, long waves and mean flow, sediment transport and morphological changes of the nearshore area, beaches, dunes and back-barrier during storms. Recent studies have implemented XBeach to study, for instance, barrier island response after a storm that fall under the overwash regime. XBeach has not been validated yet for dunes impacted by storms within the collision regime. For this study, XBeach is used in 2DH (two-dimensional height) area mode. An artificial X-, Y-, Z-grid based on measured data is implemented as model input. The grids consist of an alongshore uniform dune/beach profile, with an alongshore variable nearshore bathymetry. This nearshore bathymetry is varied three times across model runs, to represent different coastal profiles. The generated bathymetries are based on the Dutch and Gironde coast, which fall under the collision regime. Storm events and corresponding wave characteristics are based on these areas as well, giving two separate model conditions. Both wave conditions of the storms are modelled with the three artificial grids for a duration of 48 hours. Giving a total of six separate XBeach models. If only the nearshore bathymetry is varied, and all other parameters are unchanged, the effect on alongshore variations in dune erosion caused by the dimensions of the nearshore bathymetry can be isolated. Furthermore, the effect of change in wave characteristics can be isolated as well because all three bathymetries are modelled with the two storms. The model results implied that erosional hotspots are linked to the outer-bar bays. In terms of wave characteristics, the incoming wave angle shifted these erosional hotspots southward if the wave come in 30-degrees north. Moreover, a higher wave period seemed increase the magnitude of alongshore variations in dune erosion.

Contents

Modelling alongshore variable dune erosion with XBeach.....	1
1.1 Introduction.....	5
2. Literature review – dune erosion.....	6
2.1 Alongshore uniform dune erosion.....	6
2.2 Alongshore variation in dune erosion.....	10
2.2.1 Field observations.....	10
.....	14
2.2.2 Modelling of alongshore variable dune erosion.....	15
2.3 Hydrodynamics.....	17
2.4 Dune erosion models.....	19
3. Research questions.....	20
4. Methodology.....	21
4.1 XBeach model.....	21
4.2 Model settings.....	21
4.3 Grid dimensions.....	22
4.4 Model input.....	23
4.5 Model output.....	27
5. Results.....	28
5.1 Reference case – alongshore uniform outer-bar.....	29
5.2 Model results of wave conditions based on Truc Vert storm.....	31
5.2.1 Bed level change of the full grid at storms end.....	31
.....	32
5.2.2 Dune foot change over time.....	33
5.2.3 Hydrodynamics and sedimentation.....	35
5.2.4 Dune foot eroded volume over time.....	38
5.3 Model results of wave conditions based on Egmond storm.....	41
5.3.1 Bed level change of the full grid at storms end.....	41
``.....	42
5.3.2 Dune foot change over time.....	43
5.3.3 Hydrodynamics and sedimentation.....	45
5.3.4 Dune foot eroded volume over time.....	48
5.4 Comparison between results & reference case.....	50
6. Discussion.....	52
6.1 Alongshore variable dune erosion.....	52

6.2	XBeach limits & validity	55
7.	Conclusion	57
8.	Appendix.....	61
8.1	Parameter files XBeach models	61
8.2	Truc Vert storm	63
8.2.1	Bathy750 TV12.....	63
8.2.2	Bathy1500 TV12	66
	66
	67
8.2.3	Bathy375 TV12.....	69
	69
8.2.4	Bathy750 TV8.....	72
8.2.5	Bathy750shallow.....	74
8.3	Egmond storm	76
8.3.1	Bathy750 EG	76
8.3.2	Bathy1500 EG	79
	80
8.3.3	Bathy375 EG	82

1.1 Introduction

Coastlines are important boundaries for the mainland in many ways. Due to urban expansion and an increase in extreme storms caused by climate change, coastlines are becoming prone to irreversible erosion. Especially sandy coasts that consists of a beach-, dune system. These types of coasts also function as a protective barrier for floods caused by a storm surge. Furthermore, sandy coasts provide recreational activities and a thriving ecosystem if not exposed by irreparable hazards. Therefore, shoreline change along sandy coasts has been an important subject for the last 10 tot 50 yeas in terms of understanding future developments. (Castelle et al., 2017)

Erosion of sandy coastlines has been investigated and researched in many ways over the last century, and new findings are reported every year. Moreover, a lot of new questions arise with these findings, meaning that there are fields and topics within erosion of sandy coasts where further research is needed. Alongshore variation in dune erosion is one of them. This field is of importance because dunes show different erosional patterns in the alongshore direction, on both small (10-1000 meters) and larger (kilometres) scales. On spatial scales of tens to hundreds of kilometres, beach and dune erosion is variable alongshore due to a variety of causes such as gradients in longshore drift, alongshore variability in wave conditions, sediment supply or geological constraints such as headlands or rocky outcrops. At smaller scales, from tens of metres to a few kilometres, variability in beach width can appear along the coast with sometimes a striking alongshore rhythmicity. These shoreline rhythms are observed on rip-channelled beaches associated with surfzone crescentic sandbars or transverse bars (e.g., Aagaard, 1988; van de Lageweg et al., 2013) with the megacusp embayments, where maximum erosion occurs, in the alignment of the rip channels. (Castelle et al., 2015) In what magnitude these parameters influence alongshore variable dune erosion, is different for every location. For this research, we look in into the Dutch coast and the south-western coast of France. The dunes along these coasts are relatively high, meaning that there is no overtopping during storms. In terms of scale, the Dutch coast consist of about 150 km of dunes, the French south-western coast about 250 km. Variations of about 100 to 1000 meters alongshore, and 100 to 500 metres cross shore will be researched. As the variation of dune erosion as a result of the alongshore variability in sandbar morphology is studied herein. Outer bars tend to have shallow and deep parts on this scale which relate to the alongshore dune profile. (e.g. Castelle et al., 2015)

In the next chapter the principles of dune erosion along the Dutch and French coast will be explained. In chapter three we will look into alongshore variations of this erosion, with the knowledge of recent studies taken into account. After that, the storm characteristics with the corresponding wave conditions will be quantified. In chapter five the multiple options of how this erosion can be modelled will be discussed. With the knowledge of the previous chapters, further research topics with corresponding open questions can be formulated. These subjects are the focus of this research and are further explained, including expectations in the form of hypotheses. Furthermore, the methodology will be thoroughly described in the sense of how the XBeach models are generated. The outcomes are stated afterwards, in the results chapter. With the use of the results, research questions and new topics found along the way are discussed and concluded in the last two chapters.

2. Literature review – dune erosion

2.1 Alongshore uniform dune erosion

Erosion of the dunes occurs during storms. The eroded sand is transported dominantly offshore, where it is deposited on the beach and foreshore during the duration of the storm. These storm conditions are mainly described by a storm surge (increase in water level, see Figure 1) and extreme wave characteristics. During a storm event the cross-shore profile of the dunes & beach change in dimensions rapidly. The combination of a higher water level and stronger waves cause the dune foot to erode significantly. In Figure 1 it can be seen that the eroded sand is deposited seaward, with the assumption that the cross-shore section is unaffected by alongshore processes. (De Vries, 2011)

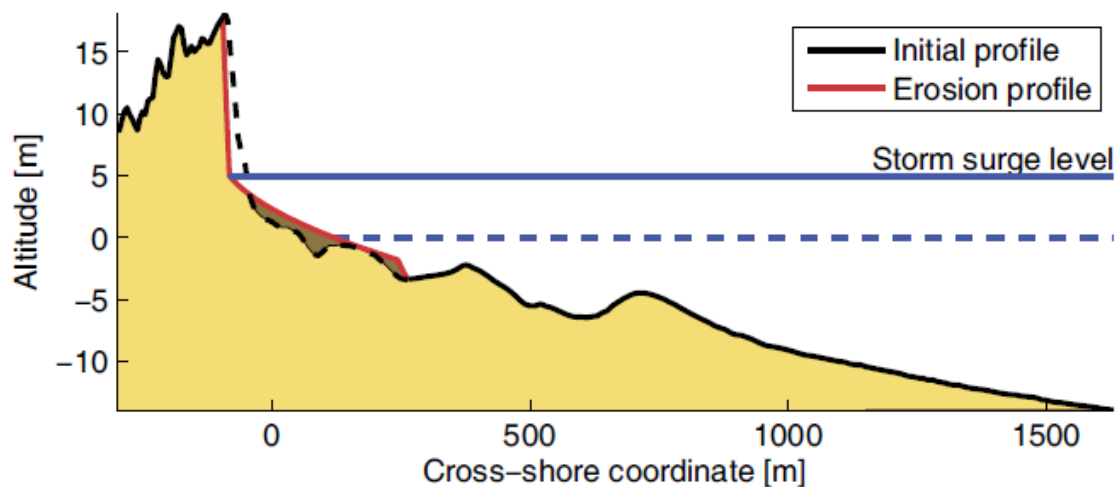


Figure 1 - Principles of dune erosion during a storm (Den Heijer, 2013)

The cross-shore profile is in balance during normal conditions. Meaning that the amount of sand transported out of the system is of the same magnitude as what is transported in. The bed level of the foreshore, beach and dunes have reached an equilibrium with the normal wave conditions. During storm conditions the system is out of balance. The cross-shore profile wants to reach an equilibrium based on the extreme wave characteristics. However, the time scale of a storm is usually too short to reach this new equilibrium. After the storm, the coastal profile wants to reach the initial equilibrium of normal conditions again. As said before, in most cases the dune foot is significantly eroded, and its sand is deposited seaward. The waves transport the eroded sand from the foreshore back to the dunes, where it is picked up by the wind and transported to the dunes. This wind-sand action is also known as aeolian transport. Consequently, aeolian transport results in dune recovery. However, the process of dune recovery can take a significant amount of time, which fully depends on the intensity of erosion caused by storms. In some cases, the dunes fully recover over time, giving a natural balance of the dune coast. If a second storm event occurs shortly after the last, before the dunes are recovered, the severity of erosion significantly increases. Therefore, multiple storm events with a relatively short interval can result in structural and (partially) irreversible erosion of a sandy coast. The large amount of deposited sand on the foreshore can be transported alongshore and thus out of the system, making it irreversible. Therefore, the process of dune erosion gets particularly complicated when cross-shore processes are influenced by an alongshore current. This alongshore flow can be generated by the tide, oblique incoming waves and an alongshore water level gradient. Sedimentation and stirring of the sediment are also influenced by alongshore processes. Furthermore, alongshore differences in near-shore bathymetry can

generate or enhance alongshore flow, which feeds eroded sand being transported in the lateral direction. (De Vries, 2011). (Den Heijer, 2013)

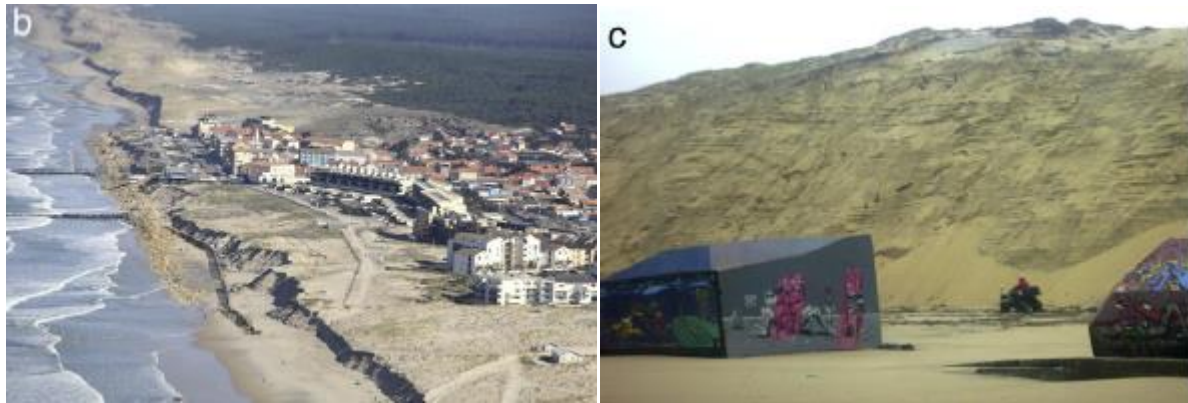


Figure 2 – Dune erosion scraps caused by subsequent storms along the Gironde coast (Castelle et al., 2015)

As said before, erosion during subsequent storms can lead to structural erosion. Meaning that seaward part of the foredune can be completely washed away, resulting in erosion scraps (see Figure 2). Within balanced coastal systems, the foredune will recover over time. The dune foot is both a source of sand and capable of transporting sediment inland (Aagaard et al., 2004). Therefore, the natural dynamics of dune evolution and generation consist of phases of accretion and erosion. Vegetation plays an important role for dune generation. For example, along the Dutch coast marram grass is capable of 'catching' sand transported by the wind and holding on to it, leading to dune generation or recovery. The natural process of establishing foredunes with marram grass can take up to ten years (Woodhouse et al., 1977; Maun, 2004). Moreover, long-term beach sediment budget is important in determining the availability of sediment and the frequency at which the dune is attacked (Psuty, 1988; Hesp, 2002). Dune systems can be categorized in three separate regimes. Sandy coasts with a negative, balanced or positive sediment budget. With negative corresponding to a decrease of sediment budget (erosion). "If the beach sediment budget is strongly negative, dune erosion is relatively frequent and the dune crest may be over washed, with sediment displaced landward (Fig. 3a). On shores where the volume of sediment supplied to the beach is balanced or slightly negative, beach width is moderate and significant dune foot erosion occurs during extreme storms. Subsequent aeolian transport will replenish the sand of the dunes and the dune will be characterized by a high, wide foredune ridge (Fig. 3b). On sandy coasts where the volume of sand delivered to the beach exceeds outputs, a seaward propagation of the shoreline occurs, resulting in formation of multiple foredune ridges separated by lower slacks (Fig. 3c)" (Coastal Dunes, 2004). Furthermore, these regimes are often related to general storm characteristics of the coastal dune development scenarios. Sallenger et al., (2000) created a Storm Impact Scale (SIS) which categorizes storm events to their effect on sandy coasts of barrier islands (see Figure 4 & 5).

To summarize this section, the main processes that can influence cross-shore sandy dune profile erosion and accretion have been discussed. These processes also have an effect on alongshore differences in dune propagation and near-shore bathymetry. However, more factors come into play when alongshore variations in dune erosion are being studied. In the next section multiple studies within this field will be reviewed. With the knowledge of cross-shore dune profile development, the alongshore variability in dune development can be analysed.

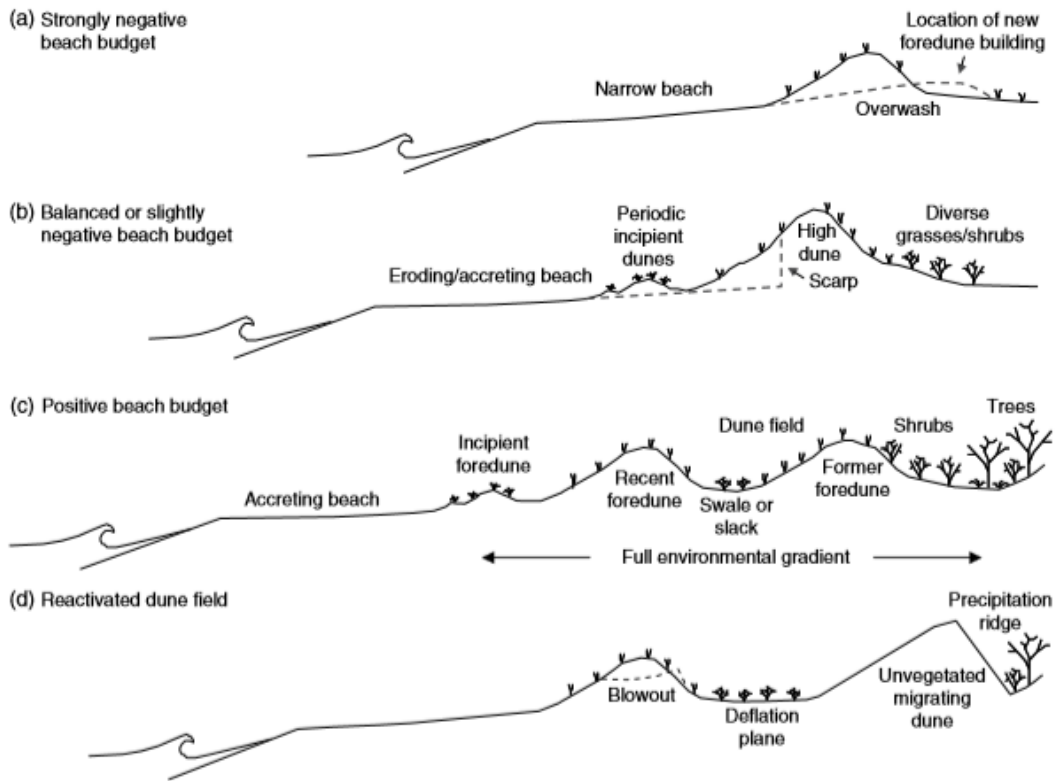
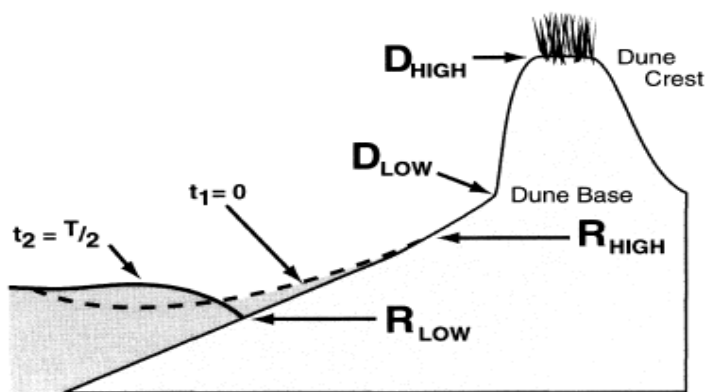


Fig. 8.6 Scenarios for development of coastal dunes, based on beach and dune sediment budgets. (a) A narrow eroding beach leads to frequent dune erosion and overwash. New incipient dunes may form on the wrack lines delivered landward of the former crest, leading to an irregular, low and hummocky foredune that contributes to further overwash. (b) A balanced or slightly negative sediment budget leads to frequent wave erosion and scarp formation on the front of the dune followed by rebuilding by aeolian transport, resulting in a high foredune ridge. (c) Beach progradation allows new foredunes to grow seaward, leaving multiple foredune crests and intervening moister swales (or slacks) with different habitat value. Wide dune fields can be characterized by a complete environmental gradient, from the few species that can survive the stresses on the beach to the species-rich environment farther landward where trees can also survive. (d) A dune field can also be reactivated due to loss of stabilizing vegetation. The former dune surface can be deflated down to the water table, and an unvegetated ridge can migrate into adjacent areas, including developed lands. [Source: Adapted from Nickling and Davidson-Arnott 1990.]

Figure 3 - Development of coastal dunes for different scenarios (Coastal Dunes, 2004)



The Storm Impact Scale (SIS) is a method to describe the impact of storms on barrier islands. It can be used to qualitatively compare different situations with corresponding storms with each other. The figures below show how the scales are determined and what regime it belongs to. (Sallenger et al., 2000)

Figure 4 - Variables used to calculate the SIS

Impact Level	Range of R_{HIGH}/D_{HIGH} and R_{LOW}/D_{HIGH}	Regimes and Predictions of Beach Changes
1	$R_{HIGH}/D_{HIGH} = 0$ to D_{LOW}/D_{HIGH}	SWASH REGIME: <ul style="list-style-type: none"> • Runup is confined to the foreshore of the beach. • During storms, the foreshore typically erodes and sand is transported offshore. • Following the storm, sand is transported onshore gradually, over weeks to months. Hence, the eroded sand is replaced and there is little net change to the beach.
2*	$R_{HIGH}/D_{HIGH} = D_{LOW}/D_{HIGH}$ to 1	COLLISION REGIME: <ul style="list-style-type: none"> • Runup collides with the base of the foredune ridge (if no foredune is present see note, *, below). • The collision forces sand to be eroded from the dune and transported offshore (&/or longshore). • Eroded dune sand is not readily returned to the dune, hence there is net erosion (relative to Impact Level 1).
3	$R_{HIGH}/D_{HIGH} > 1$ and $R_{LOW}/D_{HIGH} < 1$	OVERWASH REGIME: <ul style="list-style-type: none"> • Runup exceeds the elevation of the 'first line of defense', either dune ridge or, if dune is not present, the berm crest. • Sand is transported landward (tens to hundreds of meters) contributing to the net migration of the barrier beach landward (i.e. there is net erosion of the beach foreshore & net deposition landward of dune).
4	$R_{HIGH}/D_{HIGH} > 1$ and $R_{LOW}/D_{HIGH} > 1$	INUNDATION REGIME: <ul style="list-style-type: none"> • Elevation of the base of swash motion, R_{LOW}, exceeds the elevation of the 'first line of defense', D_{HIGH}, hence the entire beach/foredune ridge system is continuously subaqueous; • Limited observations suggest that massive net onshore transport occurs with landward migration of sand bodies on the order of 1 km.

Figure 5 - The four impact levels and corresponding regimes

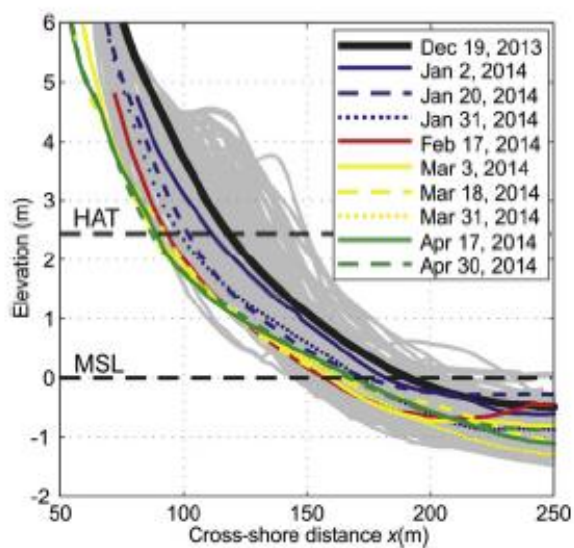
2.2 Alongshore variation in dune erosion

A complete coastal profile that consist of sandy dunes can be separated in two main compartments. The dune/beach topography, and the nearshore bathymetry. Both vary alongshore and are affected by each other's behaviour. However, this behaviour can be different for each case, meaning that there is no generalized connection between the two, in terms of predicting alongshore variable dune erosion. Furthermore, the characteristics and spectrum of the high-energy waves that cause erosion also play a great role in alongshore variable dune erosion. These three components are the main focus of this section. Furthermore, recent findings of the influence of said components that determine alongshore variable dune erosion for different cases will be discussed, giving a clearer image to what dominantly drives variations in alongshore dune erosion. Alongshore variable dune erosion basically means that certain alongshore parts of the dunes erode more than others. These heavier eroded parts are known as erosional hotspots.

2.2.1 Field observations

The presence of sandbars or other geological features offshore may impact the overall erosion response during a storm (Stockdon et al., 2007; Harley et al., 2009, 2015; Houser et al., 2008; Schupp et al., 2006). For example, previous studies at Narrabeen-Collaroy have shown that the presence or absence of a sandbar is related to the magnitude of shoreline erosion response (Harley et al., 2009). The lack of a sand bar is correlated to highly accreted beaches and low-energy conditions, far from a storm-energy equilibrium, thus a larger erosion response is expected (Harley et al., 2009, 2015; Davidson et al., 2013). This is in contrast to a beach with a well-developed storm bar that is more in equilibrium with storm conditions, and thus experiences less erosion (Harley et al., 2009, 2015; Davidson et al., 2013). Similarly, the presence of mega-rips (a localized deep channel and lack of bar) have also been shown to influence the erosion response of embayed beaches (Loureiro et al., 2012; Thornton et al., 2007).

It is frequently observed that alongshore differences in storm-induced dune erosion at scales of 10s-1000s of meters can be due to alongshore variability in offshore and near shore bathymetry, localized rip currents and alongshore gradients in wave height (Castelle et al., 2015; Loureiro et al., 2012; Coco et al., 2014; Senechal et al., 2015; Harley et al., 2015). As well as morphological characteristics of the subaerial beach such as the elevation of the dune toe, dune height and beach slope. (Splinter et al., 2017). *“Claudino-Sales et al. (2008) and Houser et al. (2008) suggested that the alongshore erosion differences at Santa Rosa Island after hurricane Ivan were mainly caused by offshore bathymetry differences (e.g. transverse ridges on the inner shelf) that locally focus wave energy and therefore cause alongshore variations in dune erosion. Similar findings have also been reported by Bender & Dean (2003), Schupp et al. (2006) and (Galal & Takewaka (2011)).”* *“For example, Galal & Takewaka (2011) found that the short-scale variability of cross-sectional change (dA) for the areas without coastal works showed a systematic correlation with the distribution of the short-scale alongshore currents and water level gradients, which is induced by the presence of the ridges within the shallow areas between the depth of 20 and 30 m”.* *“Furthermore, Thornton et al. (2007) related localized erosional hot-spots to the presence of persistent rip channels. Where the beach is narrower at the embayment of the mega-cusps, which are coupled to the rip channels”.* *“However, Van Thiel De Vries et al. (2011) and Den Heijer (2013) suggest that alongshore erosion differences are largely determined by the upper part of the profile, for example, dune height.”*



Superimposed alongshore-averaged beach profiles surveyed at Truc Vert beach from April 2005 to May 2014 in grey, with indication of the Mean Sea Level (MSL) and Highest Astronomical Tide (HAT) level. The alongshore-averaged profiles surveyed throughout the erosive winter 2013/2014 are coloured.

Figure 6 - Coastal profiles at Truc Vert beach over the years, 2013/2014 storms highlighted (Castelle et al., 2015)

Castelle et al. (2015) studied the response of Truc Vert beach to the extreme 2013/2014 storm waves and is further used to diagnose the erosion patterns along the 110 km-long Gironde coast (see Figure 6 for alongshore averaged beach response). At Truc Vert beach, beach megacusps couple to the inner bar during moderate-energy wave conditions, with megacusp embayments facing inner-bar rip channels (see for instance Fig. 4b in Castelle et al., 2014), here megacusp embayments and resulting dune erosional hotspots caused by a 10-year return period shore-normal storm swell ('Hercules') are found to couple to the outer bar with embayments facing outer-bar bays (Figure 8). A detailed visual inspection of satellite images (Fig. 7 in Castelle et al., 2015) and aerial photographs shows that following the 'Hercules' storm in early January 2014

the inner bar was rather flat and coupled to the outer bar with offshore-protruding inner-bar sections facing the outer-bar horn, with the notable absence of inner-bar rip channels. This coupling is therefore similar to the out-of-phase downstate terraced coupling observed by Price et al. (2013) on the Gold Coast, Australia. Sandbar-sandbar coupling (e.g., Ruessink et al., 2007; Castelle et al., 2010a, 2010b; Price and Ruessink, 2013; Price et al., 2013, 2014) and sandbar-shoreline coupling (e.g., Coco et al., 2005; Thornton et al., 2007; van de Lageweg et al., 2013) have been studied rather extensively. *"Here, there is evidence of a sandbar-sandbar- shoreline coupling with the outer bar acting as a morphological forcing template for the inshore flow patterns and, in turn, for the inner bar and shoreline rhythms. This is important for understanding and further predicting erosional hot-spots on multiple-barred beaches. Antecedent outer-bar morphology and storm wave conditions, including significant wave height, peak wave period and incidence angle with respect to the shore, are found to be of critical importance for dune response."* (Castelle et al., 2015)

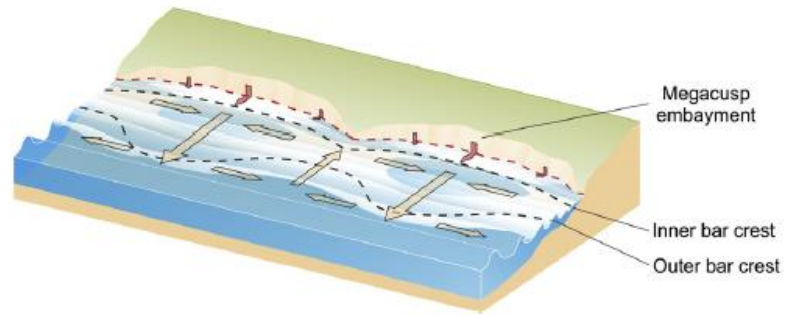


Figure 7 - Schematic diagram of sed. transport between the inner- and outer bars (Castelle et al., 2015)

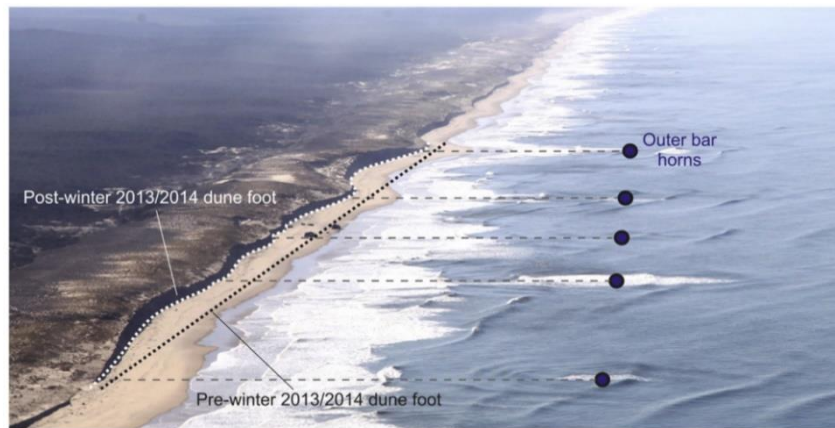


Figure 8 - Megacusp horns with outer-bar horns (Castelle et al., 2015)

Another research that investigated drivers of alongshore variable dune erosion, is the one of Splinter et al. (2017). Here daily observations of alongshore-variable dune erosion are presented, obtained by rapid-response airborne Lidar deployed within a single 3.6 km long embayment during a 6-day storm wave event. Utilizing a simple model framework (Palmsten and Holman, 2012; Splinter and Palmsten, 2012), the key drivers with respect to hydrodynamic (tides and run-up) and morphological (beach slope and dune toe elevation) drivers that account for the observations explored.

Considerable alongshore variability in the observed erosion response to a single storm event along a 3.6 km embayment was captured by daily airborne Lidar surveys over a 6-day period (see Figure 9 & Figure 10). Pre-storm morphology, such as beach slope, dune toe elevation, and dune height varied considerably alongshore. Using the unique high spatial and temporal resolution 3D surveys of the beach, several key observations were made. First, at alongshore locations where the pre-storm dune toe was lower, total water levels during the storm exceeded the dune toe and waves collided with the dune resulting in greater dune erosion. Conversely, where dune toes were elevated above the water line and wave run-up was predominately limited to the swash regime, very little to no erosion was observed. *“Considerable alongshore variability in the magnitude of inshore wave heights was not observed to be the primary determinant of localized maximum dune erosion. These observations are consistent with the Storm Impact Scale (see Figure 4) concept of Sallenger (2000), whereby dune erosion scales with the Total Water Level (sum of ocean water level and 2% run-up exceedance) above the elevation of the pre-storm dune toe. Second, beach erosion varied through time. While waves were directly colliding with the dune, the dune eroded and the dune toe receded upwards and landwards as the storm progressed. When water levels no longer reached the dune toe, erosion decreased or ceased all together. These*

field observations are in agreement with lab experiments, such as Palmsten and Holman (2012) and references therein. Third, at the tail end of the storm, some alongshore locations of the beach were observed to show the initial stages of recovery and sand deposits around the mean water line, highlighting how fast a beach may begin to recover from storm erosion.” (Splinter et al., 2017)

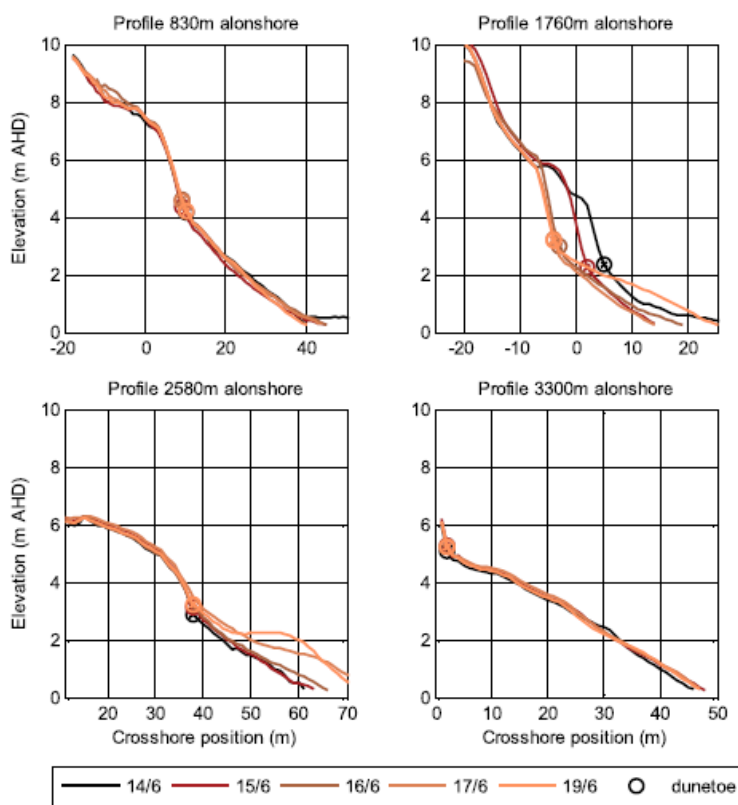


Figure 9 - Dune response during the 5-day long storm (Splinter et al., 2017)

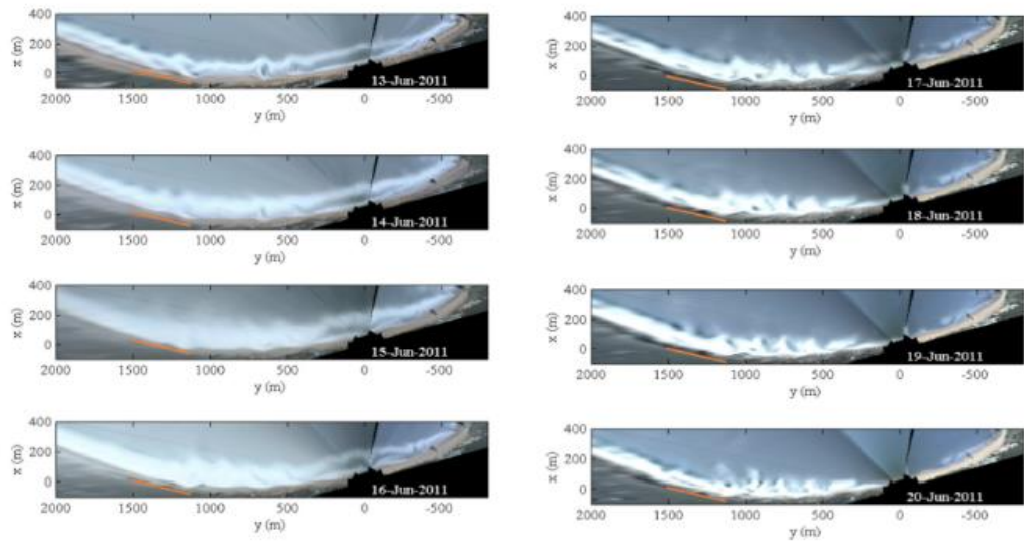


Figure 10 - Daily top view images of a sandy beach during a storm at the Gold Coast, Australia (Splinter et al., 2017)

2.2.2 Modelling of alongshore variable dune erosion

In recent history, dune erosion usually has been computed with empirical 1D equilibrium models. The computational ease of these one-dimensional (i.e., cross-shore profile) models allows them to be embedded in a probabilistic setting (e.g. Den Heijer et al., 2012) and to be applied in operational coastal safety assessments, such as in the Netherlands. However, the underlying assumption of alongshore uniformity in waves and morphology is rarely met in nature. Furthermore, multiple 1D cross-shore models of the same coastal section, but different alongshore positioning, are not sufficient to study alongshore variations in dune erosion. Variables like cell circulation and (rip) currents between the cross-shore profiles are not taken into account, since the 1D profiles are not connected with each other.

“De Winter et al. performed XBeach simulations for Egmond aan Zee, to explore the underlying causes for the differences in alongshore erosion volumes at these relatively high dunes under storm surge. With the model being calibrated for the storm surge at Egmond, three simulations were run to consider the reasons for the observed alongshore variability in erosion volume. In the first run, termed ALL_UNI, the morphology is entirely alongshore uniform. In the second run, called BATHY_UNI, the measured (and thus alongshore variable) dune profiles were used, but the intertidal and subtidal bathymetry was made alongshore uniform. In the third run, DUNE_UNI, the initial bathymetry comprised the measured intertidal and subtidal bathymetry, but an alongshore uniform dune profile.” (De Winter et al., 2015)

Figure 11 below shows the modelled versus measured alongshore erosion volume. The run with an alongshore uniform bathymetry comes closest to the observed values. Overall, these simulations suggest that the measured alongshore variation in dune erosion was primarily steered by the pre-storm dune topography (i.e., presence of embryo dune field and the steepness of the dune front). With variation in the intertidal and subtidal bathymetry playing a secondary role. But not negligible during the initial stage of the storm, when the surge level was still low. (De Winter et al., 2015)

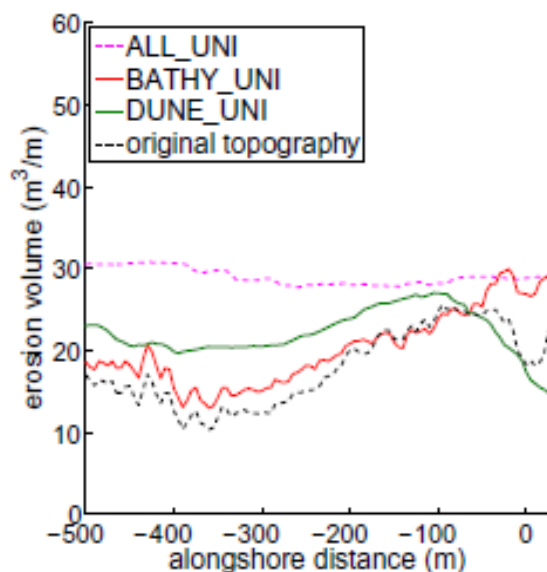


Figure 11 - Results of the model runs for the storm at Egmond aan Zee

Splinter et al., (2017) used a simpler empirical model that attempts to quantify the volume of sand eroded from a coastal dune during storm attack that requires less forcing data and have fewer parameters to be calibrated. (Overton and Fisher, 1988, 1994; Larson et al., 2004; Palmsten and Holman, 2012). Here, the simple empirical dune erosion model presented in Palmsten and Holman (2012) is used to further explore the temporal and alongshore-variable morphological response that was observed during the June 2011 ECL.

The observations and modelling results presented in Figure 12 confirm that knowledge of the pre-storm subaerial profile, in particular the elevation of the dune toe with respect to time-varying water levels during a storm, is a driver of alongshore variability in the erosion response along dune-backed sandy coastlines. (Splinter et al., 2017)

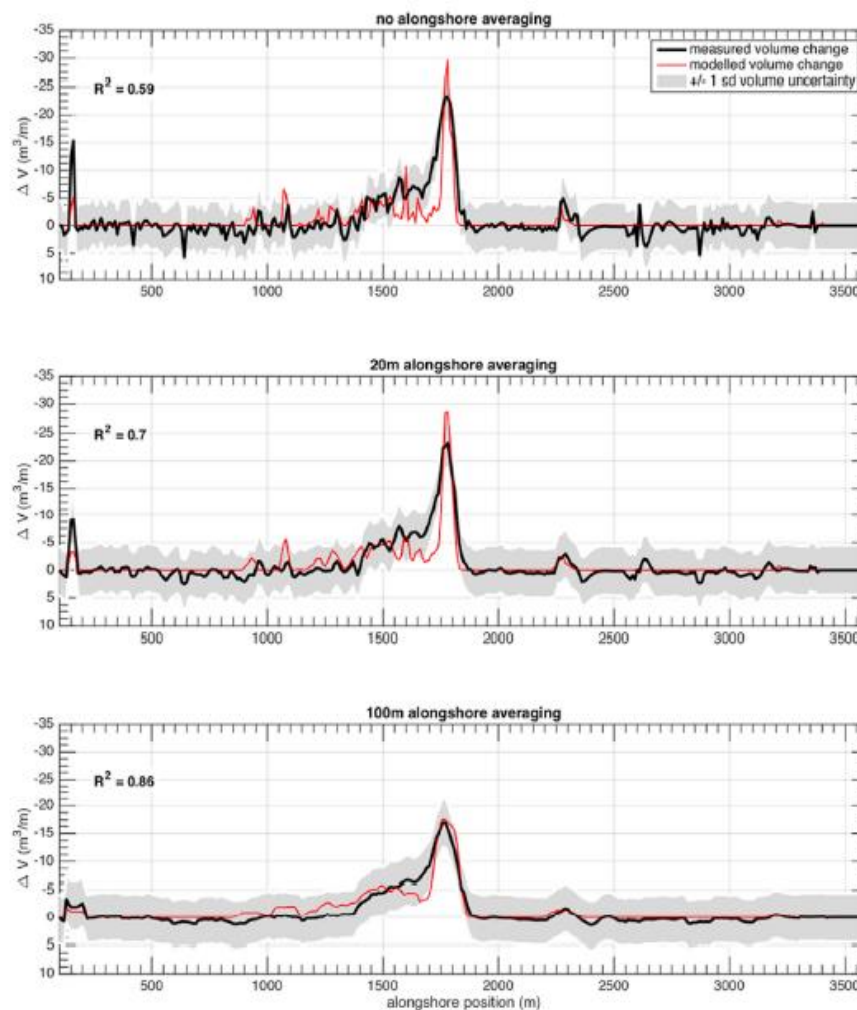


Figure 12 - Observed vs. measured erosional volume for the June 2011 ECL

All the observations and findings of the variety of studies stated above show similar remarks. Alongshore variations in dune erosion can be driven by all the three components stated in 2.2, but which one dominates is different for each situation. Every beach has its own unique combination of near-shore bathymetry, dune/beach profile and wave characteristics. An open topic which requires more research is to achieve a more generalised relation between the components that drive alongshore variations in dune erosion. For instance, by creating an artificial situation where all sections can be individually altered to study their specific influence on alongshore variations in dune erosion.

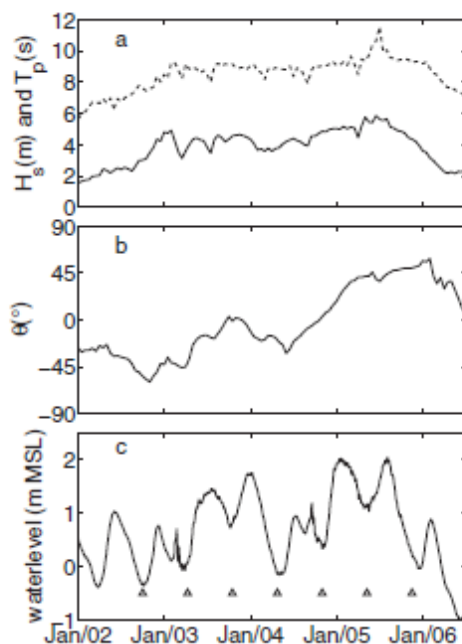
2.3 Hydrodynamics

The studies mentioned in chapter 2.2 investigated certain storm events. These are defined as storms due to their extreme wave conditions. The table below shows all the corresponding wave characteristics, to give a clear overview of the variety of storms that have been studied.

Research paper	H_s (m)	T_p (s)	Θ (°)	Storm duration
De Winter (2015)	2.5 – 5.8	6.2 – 11	-50 (start) - +50 (end)	Five days ¹
Castelle (2015)	4.0 – 9.0	12 – 23	-5 - +5	Multiple storm events (Hercules 2013/14) ²
Splinter (2017)	8.0 – 10	2.0 – 4.0	-40 - +20	Six days
Thornton (2007)	Avg. 3.0	10 – 20	-10 - +10	Period of January – April 2004
Galal & Takewaka (2011)	4.0 – 8.0	7 – 14	0 - -60	October 2006

Some interesting remarks can be made about the wave characteristics above. All components of the storms show a lot of variations between the study areas. No clear resemblances or correlations between the different storms can be observed from their combination of wave height, wave period and angle of incidence. Resulting in a wide variety of morphological response caused by each storm event.

¹ = Wave characteristics of the five-day storm in January 2012.



Offshore hydrodynamical conditions between 3 and 7 January 2012, a solid line: significant wave height H_s (m), dotted line: peak period T_p (s), b. wave angle θ (°) with respect to shore normal, c. water level (m) with respect to mean sea level (MSL), Δ times of bed level output.

Figure 13 - Wave characteristics of the storm in De Winter et al., (2015)

² = Storm clusters during Jan/Feb/March 2014. (Castelle et al., 2015)

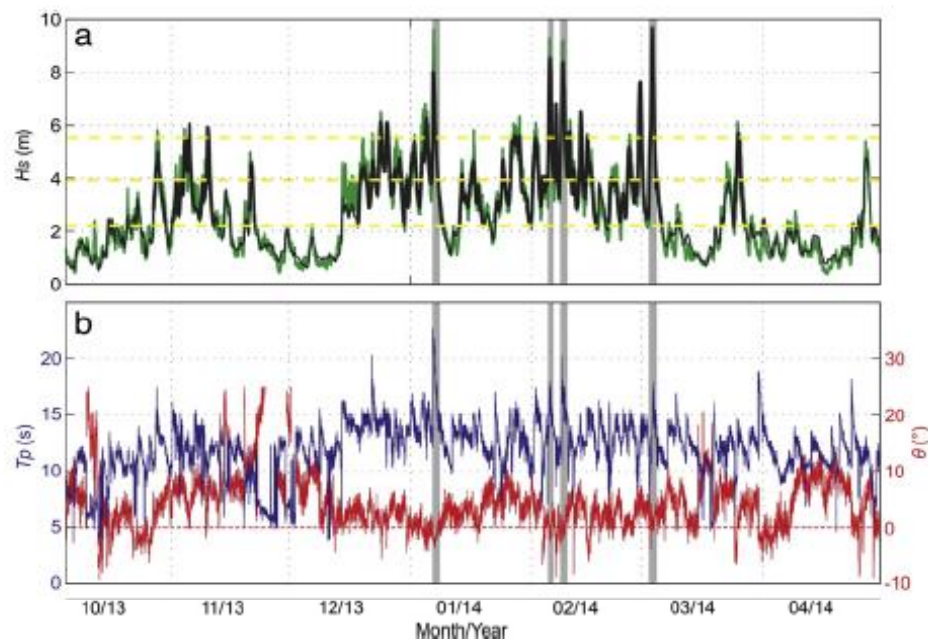


Figure 14 - Wave characteristics of the storm in Castelle et al., (2015)

As said before, every coastal system has its own unique combination of topography, bathymetry and wave/storm conditions. These differences are mostly caused by geographical features and weather conditions. Two coasts that have been discussed in the previous chapters show a lot of resemblance, namely those of the Netherlands and France. The main difference between the wave characteristics of the two coasts are the intensity of storms and the angle of incidence. This due to the Atlantic Ocean being much larger than the North Sea. More wind and a larger area to build up waves, leads to a higher wave height and period. In the North Sea the waves dominantly come from NW and SW direction, because of the dimensions it forms with the United Kingdom. Moreover, the 'funnel' shape of the North Sea causes relatively high storm surges at the Dutch coast,

In general, the French south-western coast receives waves of much higher energy during storms, if compared to the Dutch coast. Secondly, the directional spread of the waves along the Dutch coast is evenly distributed in the NW and SW direction, while in the southwest of France the waves arrive shore normal. In terms of morphological response, some notable differences are present. The Gironde coast has outer-bars relatively close to the coastline, and coupling with the beach/dunes is clearly visible (see Figure 8). In Egmond the outer-bars are positioned much further offshore (1000m to about 300m in Truc Vert). Moreover, the alongshore distance between the outer bars is also much larger in Egmond compared to Truc Vert. Around 1500m in Egmond, while at Truc Vert only about 400m. Heavier storms along the Gironde coast means heavier erosion events compared to Egmond as well.

2.4 Dune erosion models

In chapter 2.2.2 methods to model dune erosion, among which XBeach, were introduced. Multiple dune erosion events have been studied with the use of XBeach. Furthermore, the validity of XBeach has been tested and compared with other modelling methods.

XBeach (Roelvink et al., 2009) is an open source numerical modelling approach to assess the natural coastal response during time-varying extreme storm. It aims at describing the processes relevant for the different regimes defined by Sallenger (2000): swash, collision, overwash and inundation (see section 2.1). The model solves 2DH equations for wave propagation, flow, sediment transport and bathymetry development, for time-varying wave and current boundary conditions. The model resolves the 'surf-beat', i.e. the longwave motions created by the variation in wave height on a wave group time scale, that is responsible for most of the swash waves that actually attack the dune. For short-wave averaged, 'surf-beat' simulations, an improved numerical scheme and a different way of simulating the propagation of directionally-spread short wave groups result in better prediction of the groupiness factor (GF, Funke and Mansard, 1980) of the short waves and the resulting infragravity waves. (Roelvink et al., 2017)

The sediment transport is described by a depth-averaged advection diffusion equation (Galappatti and Vreugdenhil, 1985). Several formulations are available for the equilibrium sediment concentration. By default, the extended Van Rijn (Van Thiel de Vries et al., 2008) formulation is used. Alternatively, Soulsby–Van Rijn (Soulsby, 1997) can be chosen, including both bed load and suspended load transport. (Den Heijer, 2013)

Next to XBeach, there are some other officially validated and often used models to compute dune erosion. DUROS/DUROS+/D++ and DUROSTA for instance, are more traditional dune erosion models. DUROSTA is numerical 2DV cross-shore model, while the DUROS models are empirical 1D equilibrium profile models.

Since alongshore variability in dune erosion is a main topic for this subject, a 1D model would not be able to compute this variability. DUROSTA is like XBeach a 2D numerical model, but it does not take alongshore dimensions into account. Meaning that both DUROS/DUROS+/D++ (or any other empirical models in general) and DUROSTA are not desired methods to compute alongshore variable dune erosion. (Den Heijer, 2013)

Overall XBeach appears to be a viable option to study alongshore variations in dune erosion, since it's primarily designed to study dune erosion in 1D as well as in 2D(H). The largest difference between the dune erosion events discussed above and the dunes relevant for this research is the presence of overwash. XBeach has been validated for erosion of, for instance, barrier islands where waves crash over the dune top. Along the Dutch and French coast such events do not occur. Even though using XBeach to study alongshore differences in dune erosion at the collision regime (see Figure 4) has not been validated yet, but it is not unexplored. For example, de Winter et al. (2015) created 2DH XBeach models to study a storm event along the Dutch coast. The model might not work as well as situations where overwash does take place. However, it is expected that the model will show some interesting results and be considered a viable option to study alongshore differences in dune erosion where no overwash takes place.

3. Research questions

Castelle et al. (2015) came to the conclusion that erosional hotspots are affected by the shape of the inner- and outer bars (near-shore bathymetry). De Winter et al. (2015) found that pre-storm dune topography played the largest role, but that the near-shore bathymetry still significantly affects alongshore variable dune erosion.

For this research two, expectedly, important components that can or may drive erosional hotspots will be studied. Namely, the importance of wave characteristics and near shore bathymetry on alongshore variations in dune erosion. With this in mind, the main research question is as follows:

- How do differences in wave characteristics & near-shore bathymetry affect alongshore variations in dune erosion?

This main question can be split into two sub questions:

- How do wave characteristics (direction, wave height & period) affect alongshore variations in dune erosion?
- How does the initial near shore bathymetry affect alongshore variations in dune erosion?

Based on the findings of previous studies, a hypothesis for the second research question can be formed. Alongshore differences in dune erosion during storms are related to the alongshore shape of sandbar profiles positioned on the bathymetry (see Figure 7). To put it into a more general perspective; it is suspected that shallow sandbars will absorb more of the waves energy, resulting in less dune erosion in the area behind it. Especially for Truc Vert there is a clear pattern in shallow/deep outer bars. Castelle et al. (2015) found that the outer-bars showed a coupling mechanism during storms with the embayments located on the beach. Meaning that this outer-bar pattern is visible in the dune erosion during storms.

In terms of wave characteristics, it is expected that the angle of incidence has the most impact on alongshore dune erosion variations. The waves will refract with the outer-bars and shoreline, resulting in different patterns for different angles of incidence. Other conditions that will be varied are the wave height and wave period. A higher wave height and longer period generally means that the waves carry more energy, and thus result in more erosion. Variations in this will most likely not affect alongshore erosional hotspots. A higher storm surge (water level) probably has the same effect as higher energy waves; more erosion, but not on an alongshore variable scale. To test these hypotheses, multiple XBeach 2DH models will be computed to investigate erosional behaviour.

All results will be compared to a reference case with an alongshore uniform beach/dune topography & near-shore bathymetry. By doing this, the differences in erosion caused by a change in specific properties (i.e. the number of shallow bars & wave conditions) can be qualitatively studied.

4. Methodology

For this research, the latest version of XBeach, 'XBeachX', in 'surf beat mode' is used to compute dune erosion during extreme storms. As stated in chapter 2.4, XBeach is capable of modelling on a two-dimensional-horizontal (2DH) level. Meaning that it consists of a X-, Y-grid with Z-values, combined with user defined wave conditions and model duration. These properties meet the requirements to study the research topics.

In the section below the model will be introduced. Followed by the applied settings, input and output.

4.1 XBeach model

XBeachX is an open source program from Deltares, which can be downloaded from their website. The software is a directory which contains a XBeach executable and driver files to support 'netcdf' output format. To successfully run 'xbeach.exe', the directory needs to contain three types of user defined files. Wave conditions in a .txt format that match the model duration and X-, Y-grid files. The waves, the grid and all other settings and parameters are combined in a third file, 'params.txt'. If everything is set correctly the mode will start computing. XBeach saves output for each specified timestep in a 'xboutput.nc' file which will be generated once the model starts running.

XBeach models are very broad in terms of uses and possibilities. Therefore, it is of utmost importance that all model properties are chosen correctly and substantiated in the way they are set up.

A convenient and user-friendly way to set up model parameters, is to make use of the 'Open Earth Tools' Matlab Toolbox provided by Deltares. XBeach parameter input scripts consists of three main compartments:

- Wave conditions
- Grid parameters
- XBeach settings/parameters

Everything is written and combined in a single Matlab script. This script creates the 'params.txt' file (see appendix 8.1) which is used to execute 'xbeach.exe'. Generating wave conditions defines the wave spectrum, wave height, wave period, angle of incidence, surge level and the wave spectrum. The second part, grid parameters, generates a X-, Y-grid with Z-values. Which are combined in a 'depfile'. A further in-depth clarification of the grid is explained later in this chapter. Finally, all the XBeach settings will be determined. XBeach will automatically set parameters to 'default' if nothing is specified for that said parameter. See 'XBeach masters manual' for all the default values.

4.2 Model settings

For this research, the 'wbctype' (wave boundary conditions) is set as a standard JONSWAP random wave spectrum, with 'roelvink2' as the wave breaking parameter. Wave conditions and the duration of a single spectrum are required to create a JONSWAP table that can be used by XBeach. The JONSWAP table, also known as 'JONSWAP1.txt' at the 'bcfile' setting in XBeach, contains of seven parameters (H_{m0} , T_p , θ , Σ , s , duration, l) with three of them (Σ , s , l) set on default. The duration of a single spectrum is set to 1800 seconds (30 mins). Differences in duration are not important, since the wave conditions remain the same over the full duration of the computation. Varying, for example, the wave height over time, creates an irrelevant effect on how the research questions can be answered. Hence, for this study wave conditions are kept constant (stationary) within each run. The number of JONSWAP spectra matches the computation time of the model run. If the model runs for 30 hours while a single JONSWAP spectrum is 30 minutes, the Matlab script needs to generate 60 rows of the seven-column wide JONSWAP spectra in the 'JONSWAP1.txt' file. A second part of the wave

conditions is the water level, which is the reference of where the waves will be generated from. As default the water surface is set on 'z = 0'. Tidal change over time can also be implemented in XBeach. However, the surge level will be set at a fixed value since tides do not play a role in the research topics. Variations in water level create an undesired effect on the model results. Once the wave conditions are defined and a X-, Y-grid is implemented (see section 4.3), some general model settings and parameters need to be defined before the computation can begin. One of them being model duration. The duration controls for how long the waves will attack the user-defined grid. According to previous studies, a spin-up time ('morstart') of about four hours is necessary for the waves and currents to become stable. During this spin-up the morphology of the whole grid is fixed on the starting Z-value. After four hours the grid becomes unlocked and bed level change due to the waves begins. The total model duration is 52 hours ('tstop'), including four hours of spin-up. Therefore, the storm surge affects the bed level for 48 hours. A storm of two days is chosen because the cross-shore profile will most likely have reached an equilibrium after such an event. Data is measured every ten seconds ('tintg' = 10). Since output for every ten seconds over a period of 48 hours produces a large amount of data, the mean, maximum, minimum and variation over the last 15 minutes is saved in the netcdf file ('tintm' = 900). Thus, this gives 208 values for every data output at all grid points. A detailed description of all output variables will be given later in this chapter. A final important setting under the morphology settings, is the morphological acceleration factor ('morfac'). This factor speeds up the morphological time scale relative to the hydrodynamic timescale. Meaning, when a model is ran for 10 minutes and a morfac of 6 is used, the morphological evolution over 60 minutes is effectively simulated (XBeach Manual, 2018). In other words, if a 'morfac' of 6 is applied, the computation time is a factor 6 faster than with a 'morfac' of 1. For test runs a 'morfac' of 5 is used, to attain results quickly to see if the model is working properly. For the final runs a factor of 2 is chosen. The results show less irregularities if the 'morfac' is lowered. Some test runs have been done with a varying 'morfac', while everything else stayed the same. The difference between a factor of 5 and 2 was noticeable, but the overall erosion trends were comparable. A 'morfac' of 1 would not improve the results in a way to better study alongshore variations in dune erosion, whereas the computation time almost doubles. The bed level deviated about 2-5 cm compared to that of a morfac of 2, while all the erosional patterns and related hydrodynamic behaviour remained the same. Hence the decision of morphological acceleration factor of 2.

4.3 Grid dimensions

Together with the wave conditions, the X-, Y-grid is the main input component. A grid consists of alongshore (Y) and cross-shore (X) points with corresponding elevation values (Z). The artificial bathy-, beach-, dune profile has a cross-shore distance of 3000 meters, with an alongshore distance of 4500 meters. The grid size is 10 by 10 meters, giving a total of 300 x 450 grid points. Since not all grid points are of equal importance to the analysis, a grid size scaling function of Open Earth Tools (OET) is used to decrease number of grid points. This decreases the computation time. In other words, the grid size further offshore is larger (10-15 m) than close to the beach (8 m). In the alongshore direction the grid size is at its finest (10 m) in the middle of the profile, while at the most northern and southern sides the dimensions are the largest (20 m). The OET function 'xb_grid_xgrid/ygrid' generates a new profile with the user-defined minimum and maximum X-, Y-grid sizes. These min/max values gradually scale towards each other along the profile. Even though the number of grid points change, the 'real' dimensions stay the same due to this OET function. A XBeach input grid requires extra space around the research area, because the edges of the grid were found to cause unrealistic deviations in wave run-up. This subsequently resulted in incorrect erosion patterns. Therefore,

the area that was studied is 1500 x 1500 meters, located in the middle of the grid, see Figure 15 for the exact location and dimensions of the research area. To summarize, at an alongshore distance of '0m' and '4500m' the grid size is 20 m. This is evenly scaled to a grid size of 10m between '1500m' and '3000m'.

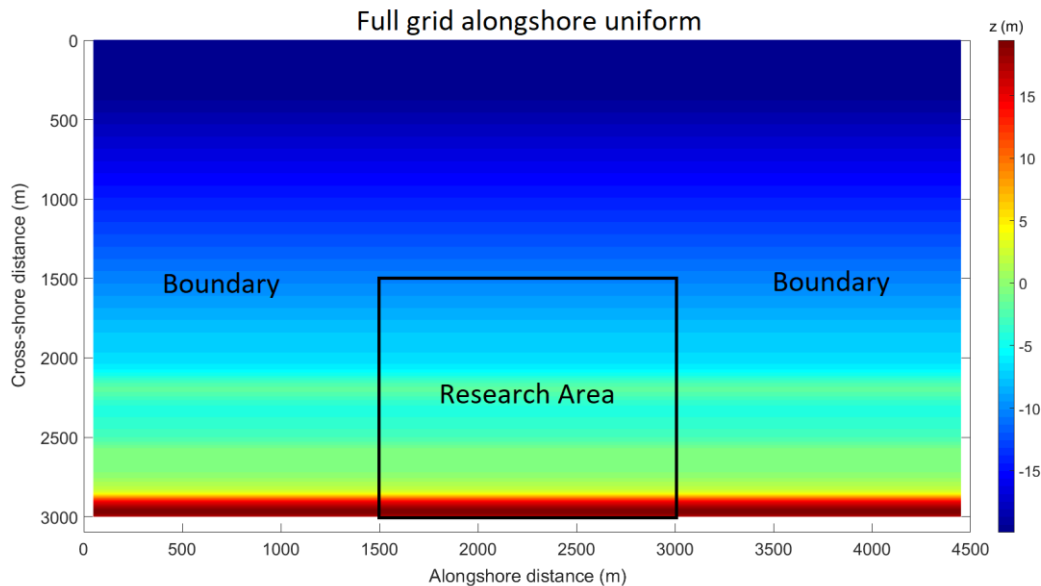


Figure 15 - Full grid dimensions

The boundaries are more or less alongshore uniform. In the next chapter the exact profiles implemented in the grid will be further explained. On the north and south side of the grid the boundaries are 1500 meters wide. This value is based on the paper of de Winter et al. (2015), who used about 1000 meters of extra alongshore uniform bathymetry on both sides. The 1500 extra meters offshore is necessary for the waves to settle in the grid. Furthermore, a water depth of 20 meters must be reached. Because waves might break right at the edge of the grid for the storm wave heights used, which causes errors in the wave propagation further landward. At the sea-ward end of the grid, the bathymetry becomes horizontal for about 50 meters. A sloped edge of a XBeach grid can cause errors in terms of erosion during computation. The different types of bathymetries, that are placed in the grid, will be discussed in the next paragraph.

4.4 Model input

For this research, the coastal profiles and hydrodynamics of Egmond aan Zee (NL) and Truc Vert (Fr) have been used as reference. The reason for this is that these areas are suitable for further research, because of recent studies and their findings (De Winter et al. & Castelle et al.).

The complete grid consists three main compartments. An alongshore uniform dune-, beach profile, an artificial near-shore bathymetry and boundaries as discussed in the previous chapter. The only part of the grid that will be varied across the XBeach models, is the near-shore bathymetry. Furthermore, a Jarkus 2011 profile of the dunes and beach at Egmond aan Zee is extended alongshore and attached to the artificial bathymetry. Jarkus profiles are yearly LIDAR measured cross-shore sections of the Dutch coast. On the seaward side of this artificial bathymetry the profile continues as an evenly sloped seabed that reaches -20 meter.

Three artificial bathymetries were created that resemble the sub-aquatic profiles of Egmond aan Zee and Truc Vert. Two resembling Egmond and Truc Vert, and a third one that is 'in-between' the other profiles. All three grids were compared to an alongshore uniform grid as

reference. The bathymetries are generated with a custom Matlab script. This Matlab script produces an outer- and inner-bar onto a dean profile, with a user-defined along- and cross-shore width. Both bars can also be altered in terms of shape, location, depth, pattern and cross-shore width. Only the shape of the outer bar has been altered for this research. Thereby, the effect of the shape and pattern of the outer bar on alongshore variations in dune erosion can be isolated. The dean profile, outer-bar location & width and location & shape of the inner-bar remained the same for all three bathymetries. The Matlab script has been slightly edited with the help of Bruno Castelle to create the desired crescentic pattern of the outer bar. An important aspect of the outer-bar pattern is that it consists of shallow and deep parts. As stated in the hypothesis, less erosion is expected at the dunes behind shallow parts of the bar. The depth difference between shallow and deep bars was a fixed value of about three meters for all bathymetries. For the three different runs, the number of shallow bars along the 1500-meter profile were varied. Therefore, the alongshore distance between shallow and deep parts varied as well. If every other aspect of the bathymetry stays the same, the differences in beach/dune response should only be caused by the variations in shallow and deep bars in the alongshore direction of the outer-bar.

The first bathymetry is based on Truc Vert, with four shallow bars along the 1500-meter profile. The third bathymetry has only one shallow bar, which is based on Egmond aan Zee. The other bathymetry is, as said before, in-between the others, with two shallow outer-bars. See figures below for a visualisation of the three grids. All artificial bathymetries are integrated in the grid of Figure 15. The bathymetry of Figure 16 will be referenced to as 'bathy375', Figure 18 as 'bathy750' and Figure 17 as 'bathy1500'. With the number indicating the alongshore wavelength of the outer-bar patterns.

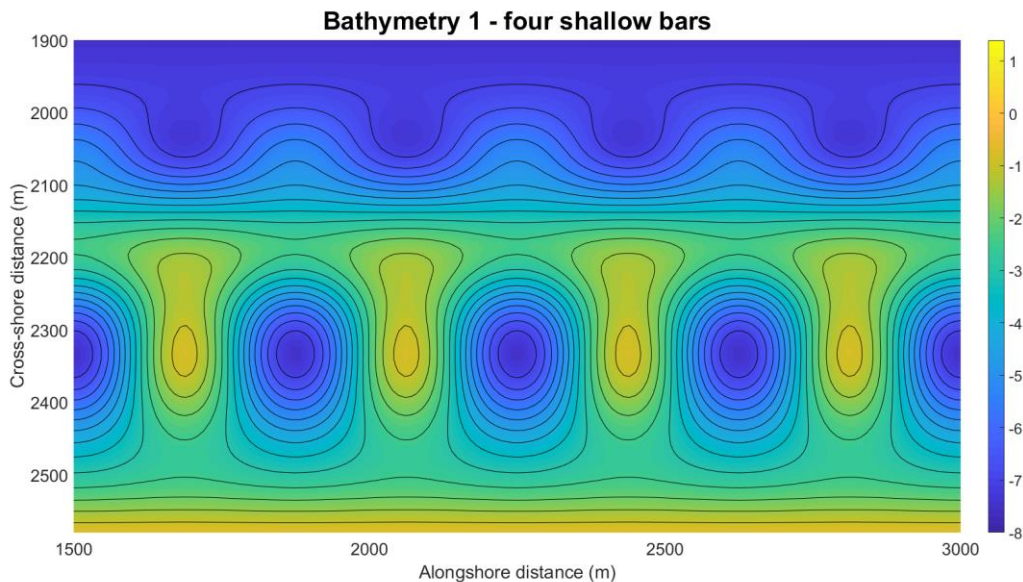


Figure 16 – Outer bar profile with 375m between shallow bars

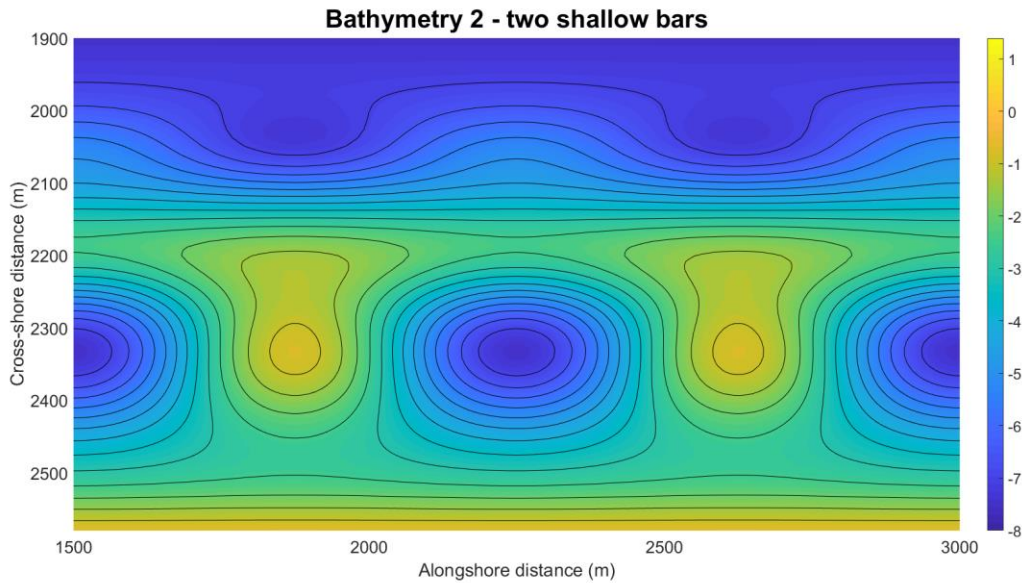


Figure 18 – Outer bar profile with 750m between shallow bars

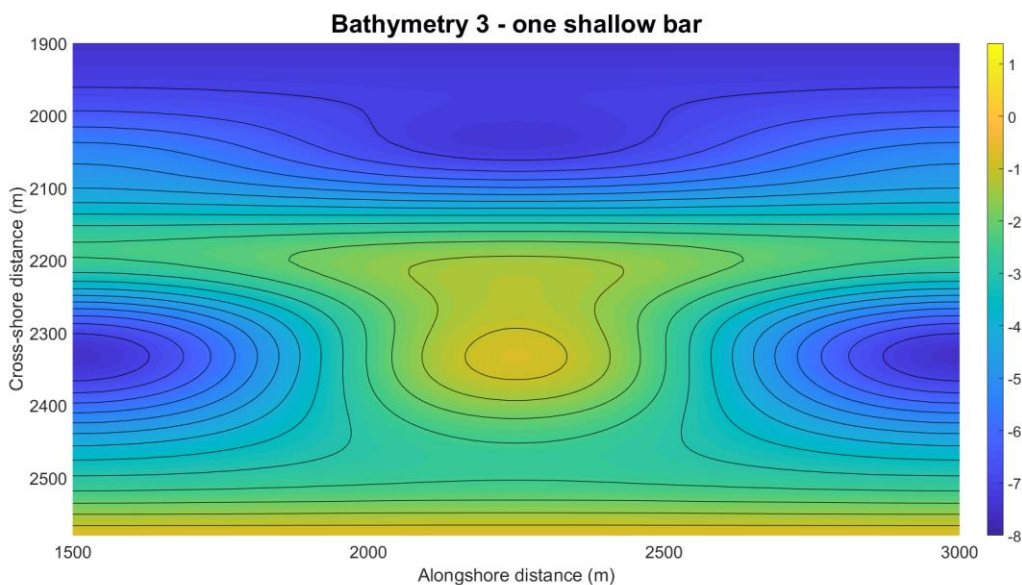


Figure 17 – Outer bar profile with 1500m between shallow bars

All three grids were ran with two separate wave conditions based on extreme storms of Egmond aan Zee and Truc Vert. Giving a total of six model runs, with an additional two reference runs. The two storm conditions are taken from the papers of Castelle et al. (2015) & De Winter et al. (2015). For both storms the surge level (water level above reference) was fixed on 4 meters. The dune foot is located at about 4 metres above reference level, which means it will be inundated during the storm event. Lower surge levels showed less overall erosion. A four-metre surge fits better among extreme wave conditions and is realistic for both sites (Truc Vert & Egmond). As said before, the wave conditions remain the same over the full 48 hours of the model duration.

In general, the dune profiles along the French and Dutch coast show similarities, but the wave spectra and the corresponding hydrodynamics are different. The table below shows the hydrodynamics along the Dutch and French coast during heavy storms, compared to a standard situation at both sites.

<i>Wave conditions</i>	Egmond aan Zee (NL)		Truc Vert (FR)	
	Storm ¹	Standard	Storm ²	Standard
H _s (m)	2.5 – 5.8	~0.5 – 1.0	4.0 – 9.0	~0.5 – 1.0
T _p (s)	6.2 – 11	~4.0	12 - 23	~8.0
Θ (°)	-50 (start) - +50 (end)	SW (-45) & NW (+45) dominant	-5 - +5	Shore normal (0) dominant
Surge level (+m MSL)	Max. 4.0	-		-

^{1 2} = See chapter 2.3.

With the use of the measured storm data above, the following two separate wave conditions have been set into XBeach.

Wave conditions based on Truc Vert storm:

- Wave height (H_s) = 5 meters
- Wave period (T_p) = 12 seconds
- Angle of incidence (θ) = 0 degrees (270 in XBeach)
- Surge level = 4 metres

Wave conditions based on Egmond aan Zee storm:

- Wave height (H_s) = 5 meters
- Wave period (T_p) = 8 seconds
- Angle of incidence (θ) = 30 degrees towards north (300 in XBeach) – not 45 degrees because XBeach has problems with higher angles of incidence.
- Surge level = 4 metres

It can be observed that only the wave period and angle of incidence are different for both storms. This is because the validity of this specific model is uncertain for more extreme wave heights. Test runs showed that relatively high energy waves (i.e. H_s = 8 m & T_p = 16-20 s) gave unrealistic results with the artificial bathymetries discussed earlier in this paragraph. The table below shows a clear overview containing all discussed model runs and their characteristics. Model nickname is their reference name which will be used in the results.

<i>Model nickname</i>	H_s (m)	T_p (s)	Θ (deg)	Surge (m)
Ref. Truc Vert (bathyUniTV)	5.0	12	0.0	4.0
Ref. Egmond (bathyUniEG)	5.0	8.0	30	4.0
bathy750TV	5.0	12	0.0	4.0
bathy1500TV	5.0	12	0.0	4.0
bathy375TV	5.0	12	0.0	4.0
bathy750EG	5.0	8.0	30	4.0
bathy1500EG	5.0	8.0	30	4.0
bathy375EG	5.0	8.0	30	4.0

4.5 Model output

A final and important aspect of setting up a XBeach model, is defining the model output. XBeach has many output variables, which needs to be carefully chosen. Because if the variable is not stated in the 'params.txt' file, the model needs to be ran again to attain said output variable. All variables are saved for every grid point and corresponding timestep.

To fully examine all research topics and substantiate erosional patterns, the following seven output variables have been chosen.

- **H** – Wave height (H_{rms}) in meters. Shows the short-wave height. Important to observe where the waves are breaking and alongshore difference in wave height occur.
- **Zs** – Water level in meters with Zb as reference. Mainly used to calculate long-wave (infragravity) height, with the use of 'zs_var'. (see results)
- **Zb** – Bed level in meters. Main variable to study erosion, since it displays bed level change over time.
- **u** – GLM (generalized lagrangian mean) velocity in meters per second. Gives the wave induced currents on the water surface, cross-shore component (X).
- **v** – Same as 'u', but then the alongshore component (Y). 'u' and 'v' are used to create quiver plots in Matlab. Resulting in a figure displaying the direction and magnitude of the currents.
- **Sutot** – Suspended + bed load sediment transport in cubic meters per second. 'S' stands for sediment and 'u' for the cross-shore component (X).
- **Svtot** – Same as 'Sutot', but then the alongshore component (Y). Similar to the currents, a quiver plot can be generated with both the X and Y component. This figure shows in which direction and magnitude the sediment is moving.

These output variables will be used to visualise and analyse results, as to find links between short- & long wave height, currents and sediment transport and erosional behaviour.

5. Results

As said in the previous chapter, seven output variables are used to create plots and display the results. A reference case is shown first with X-, Y-, Z-grid plots, where X & Y stands for cross- and alongshore dimensions. Note; alongshore distance (Y) is plotted on the X-axis, with cross-shore distance (X) on the Y-axis. The Z-values show change in bed level (dZ_b), with the initial bed level (Z_b) as reference. The model results of the three artificial bathymetries will be split up into Truc Vert & Egmond storm conditions. Starting with the bathymetry containing two outer-bar horns (bathy750), followed by one outer-bar horn (bathy1500) and four outer-bar horns (bathy375). Within these sections, alongshore differences in dune erosion is the main topic and will be linked to hydrodynamics and initial morphodynamics. The hydrodynamics and sedimentation rate are taken from the spin-up time, where the bed level is stationary. A mean value of all time-steps between $t = 1$ hr and $t = 3$ hrs are used to minimize unwanted deviations caused by the random wave spectrum. By doing this, the effects of the initial bathymetry on hydrodynamics and sedimentation can be studied. Figure 19 below displays the location of characteristic components in the grid, where references will be made to in this chapter. For instance, the 'shallow bar section' is a cross-shore profile on-top of the outer-bar horns. The dune foot is studied to investigate erosional behaviour, located at a cross-shore distance of 2850m.

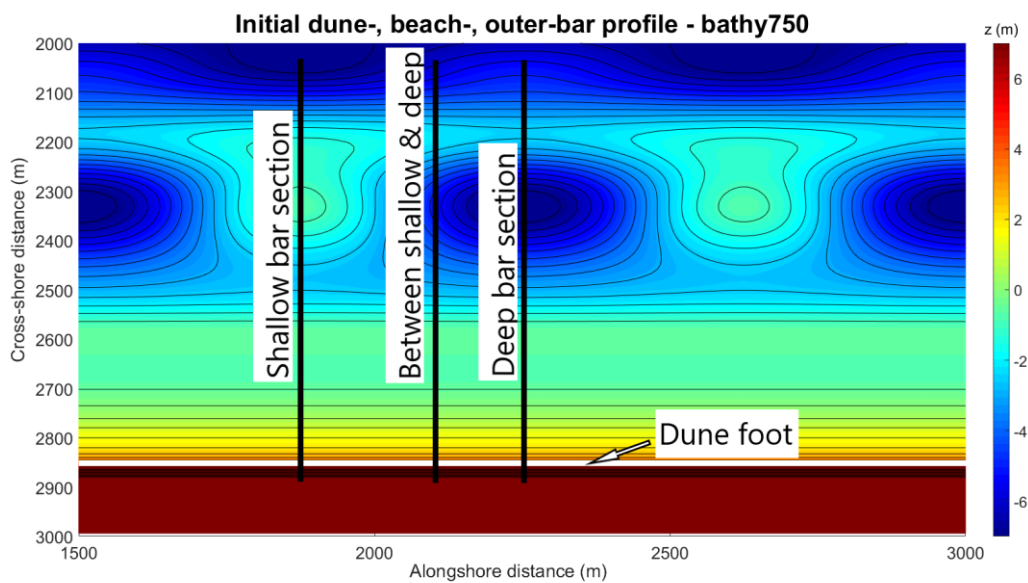


Figure 19 - The dune foot (white line) is located at $x = 2850$ m, with a $Z_b = 3,9$ m (the same for all three bathymetries). The alongshore locations of the shallow, deep and in-between sections are different for every bathymetry.

5.1 Reference case – alongshore uniform outer-bar

To compare and verify results, a grid with an alongshore uniform outer-bar was used as input in XBeach and ran with the same two separate 48 hours long storm conditions. Here, alongshore uniform bars implies that the whole grid is alongshore uniform. The figures below show the bed level change resulting from the both storm events. The colourbar represents bed level change at storms end, with 0 (white) meaning no change. Red areas (negative) stand for erosion and blue (positive) for deposition. The arrows display sedimentation rate.

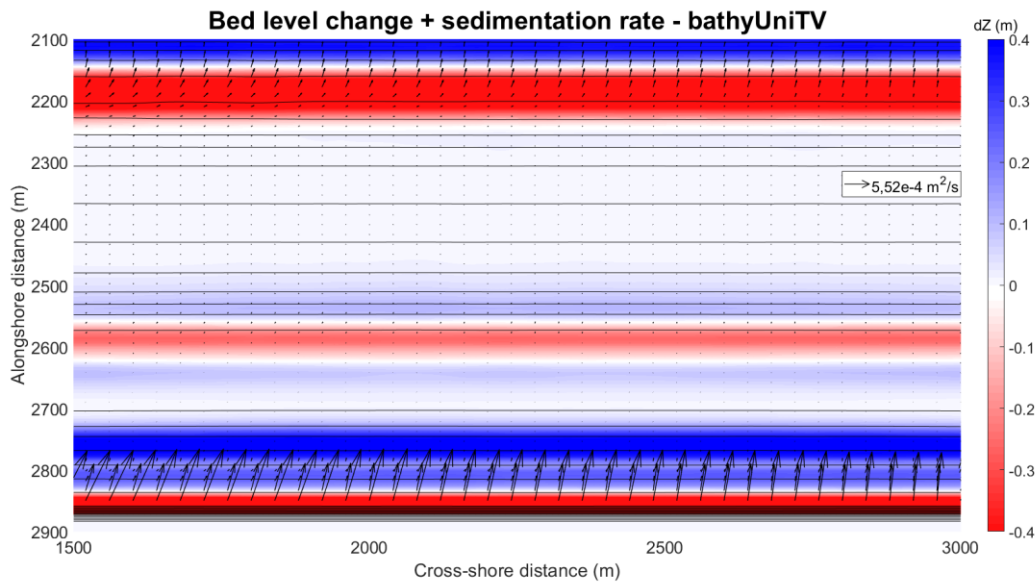


Figure 20 – bathyUniTV: Bed level change (dZ_b) after 48 hours for an alongshore uniform grid – Truc vert storm. Initial bed level is used as reference ($dZ_b = 0$). Quiver shows the sedimentation rate for a given grid point.

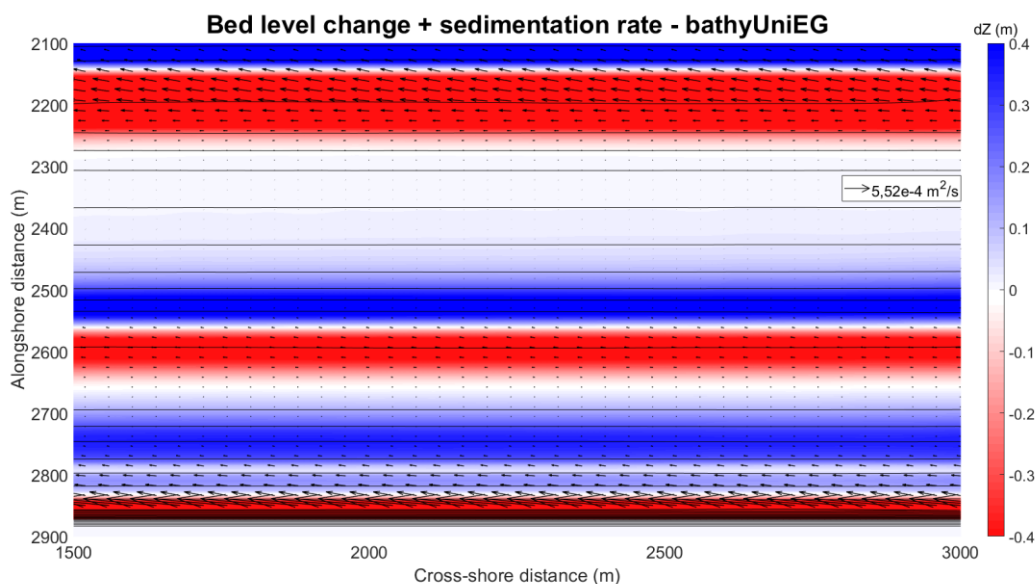


Figure 21 – bathyUniEG: Bed level change (dZ_b) after 48 hours for an alongshore uniform grid – Egmond storm. Initial bed level is used as reference ($dZ_b = 0$). Quiver shows the sedimentation rate for a given grid point.

Interesting to note is that for the Egmond storm significantly more erosion takes place. This can be seen from the heavier colouration across the grid. In terms of eroded volume, the dune foot of bathyUniEG eroded $31,5 \text{ m}^3/\text{m}$, bathyUniTV only $26,6 \text{ m}^3/\text{m}$. While the wave period is lower and the wave height unchanged. Meaning that the 30-degree angle of incidence by itself has a large impact on erosional volume. See chapter 5.4 for a further clarification of this.

Furthermore, the Egmond storm causes the dunes to slump after about $t = 24$ hrs. Before this slumping event, erosion build up much slower than that of the Truc Vert storm. See Figure 22 and Figure 23 up until $t = 24$ hrs.

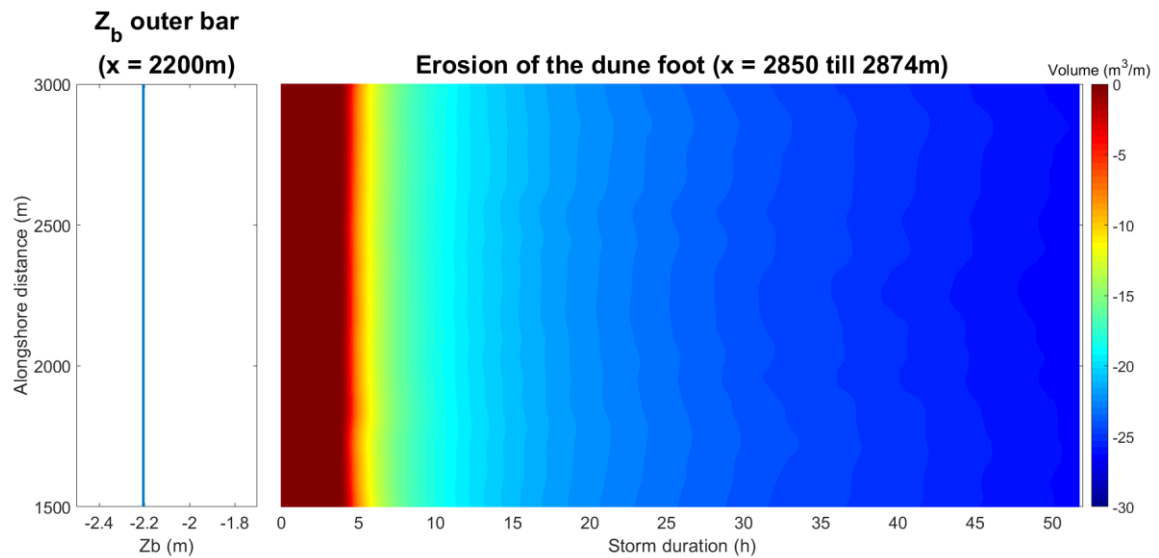


Figure 22 – Dune foot change for alongshore uniform grid – Truc Vert storm

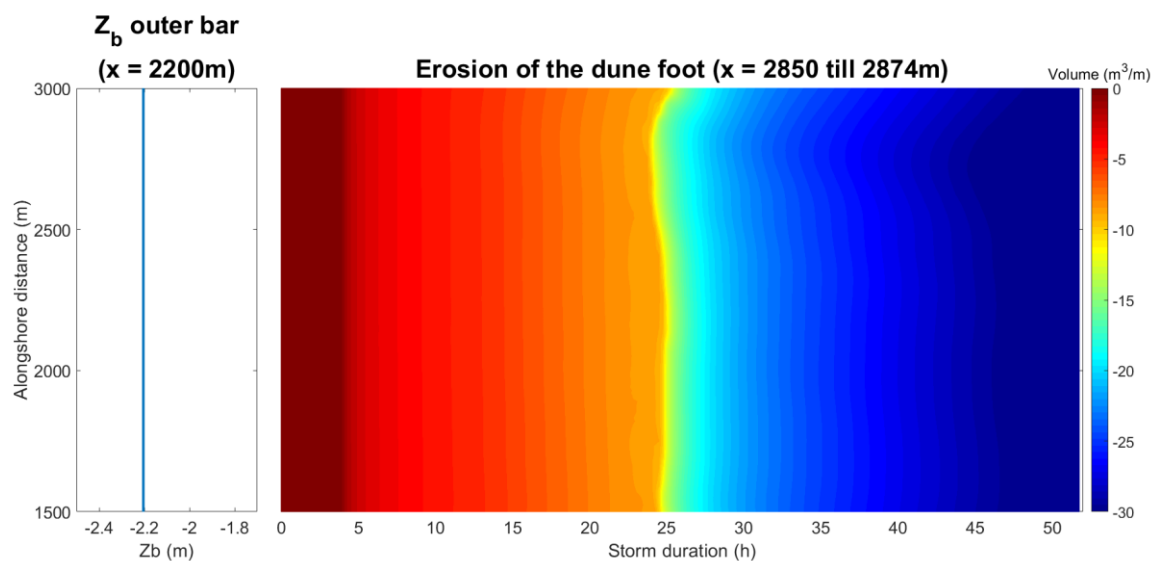


Figure 23 - Dune foot change for alongshore uniform grid – Egmond storm

The plots above show a timestack of the eroded volume of the dune face. How this is calculated will be further explained in 5.2.4. In Figure 23 slumping can be clearly observed, which will be addressed in sections 5.2.1 and 5.2.2. Therefore, the larger magnitude in eroded dune foot is caused by this slumping event.

5.2 Model results of wave conditions based on Truc Vert storm

At first, visualisations and observations of the model output from the three artificial bathymetries computed with the Truc Vert storm will be explored. These will be compared with the reference case in chapter 5.4.

5.2.1 Bed level change of the full grid at storms end

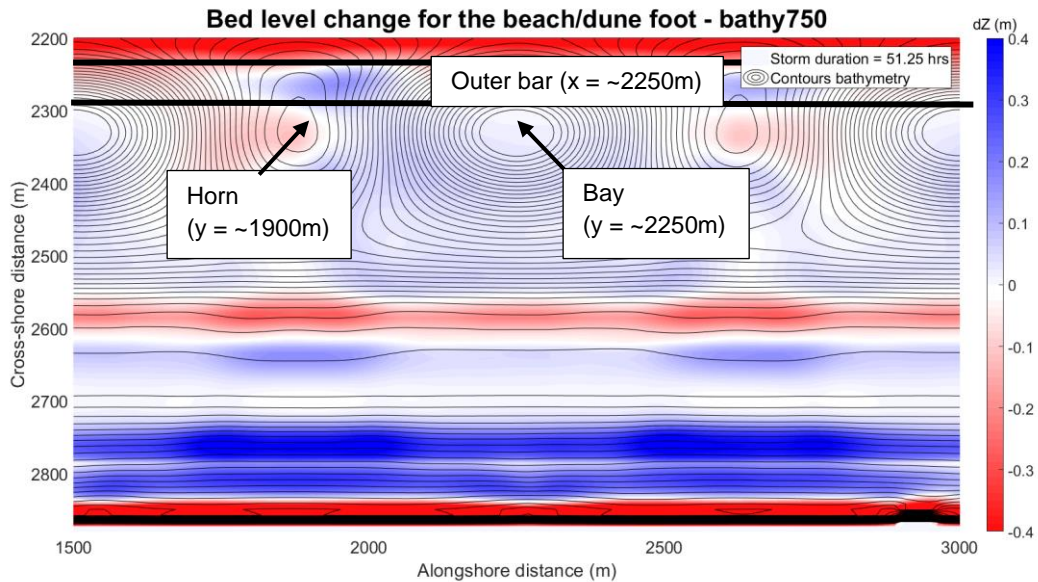


Figure 24 – bathy750TV: Bed level change (dZ_b) after 48 hours for bathy375. Initial bed level is used as reference ($dZ_b = 0$)

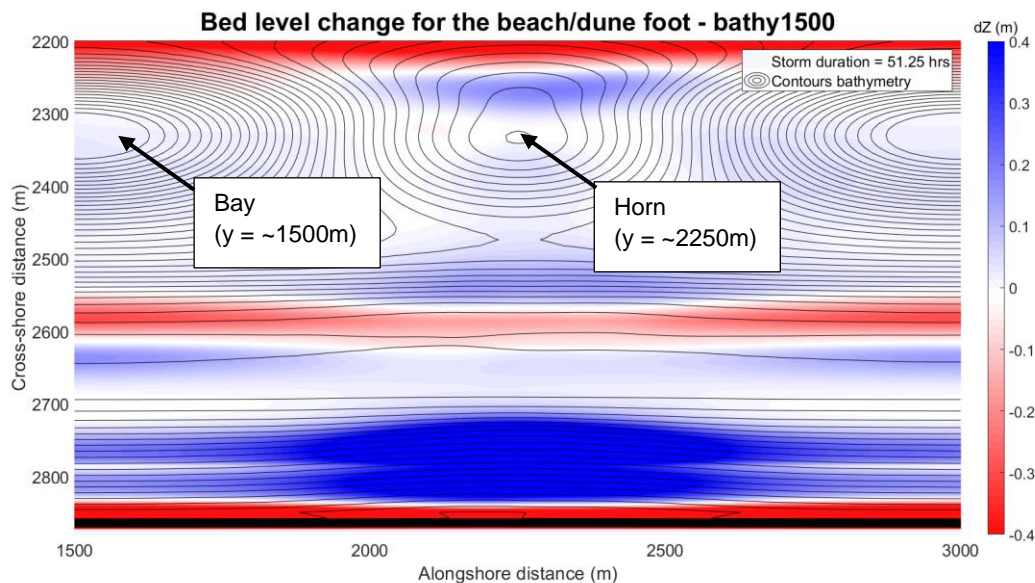


Figure 25 – bathy1500TV: Bed level change (dZ_b) after 48 hours for bathy750. Initial bed level is used as reference ($dZ_b = 0$)

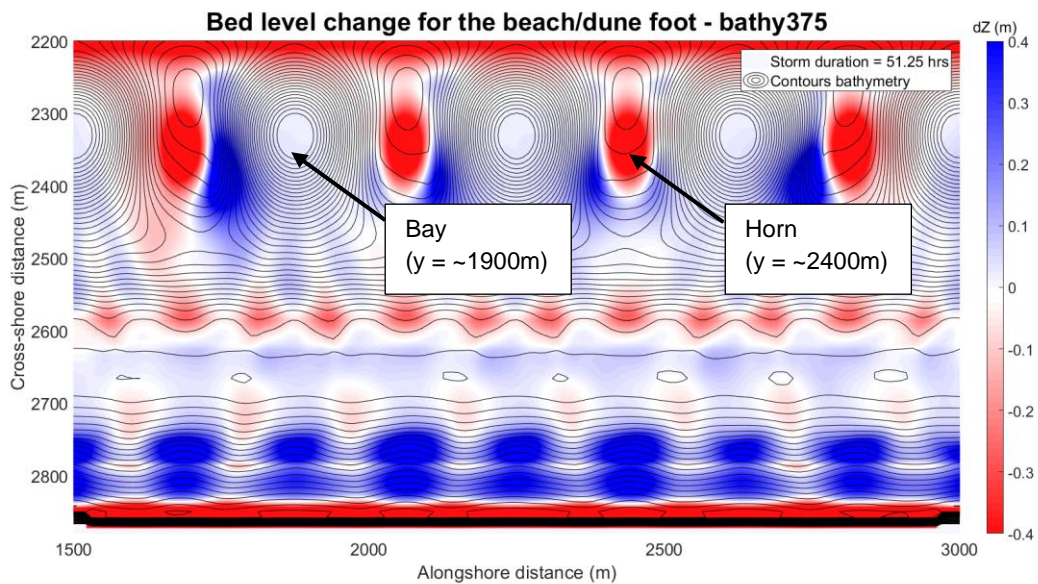


Figure 26 – bathy375TV: Bed level change (dZ_b) after 48 hours for bathy1500. Initial bed level is used as reference ($dZ_b = 0$)

It can be observed for every bathymetry that heavy erosion takes place at the dune foot, which is deposited on the beach. Alongshore variations in dune foot erosion are difficult to notice within these figures, this will be discussed in the next sections. These full grid plots are used to visualise bed level response during a storm on of the complete bathymetry. An interesting remark about the dunes is that slumping or also known as avalanching occurs after about 15-24 hours of storm, which is not visible in these plots. See section 5.2.2 for a visualisation of this occurrence. Alongshore difference in deposition on the beach (between $x = 2720$ and 2820m) do show in these figures. All deposited sand on the beach originates from the eroded dunes. Behind the outer-bar horn (shallow part, see Figure 19) is considerably more deposition for all bathymetries. Meaning that the resulting bed level on the beach caused by the storm surge, is situated lower behind the outer-bar bays (deep parts) of the outer-bar. In other words, sand that is deposited on the beach accumulates behind shallow parts of the outer-bar. A further explanation about related wave-induced currents and sedimentation will be given in section 0.

As said before, remarks about erosional hotspots of the dunes are difficult to make with full grid plots. However, the depositional areas on the beach (dark blue) show a clear relation with the outer bar pattern for bathy750TV and bathy1500TV, but this is not the case for bathy375TV which shows some particularly interesting results. The bathymetry consists of four shallow bars, while the alongshore beach section shows depositional areas. This might be caused by a morphological coupling at half of the outer-bar wavelength, instead of an in-phase coupling. *Castelle et al. (2009, part 1)* found that the regime where this type of coupling is most likely to occur is for an outer-bar with a crescentic pattern with a wavelength of 400-500m. bathy375TV has a crescentic wavelength of 375m, which is close to this regime.

5.2.2 Dune foot change over time

Figure 27 till Figure 29 are so called timestacks of the dune foot. These plots clearly show how the dune foot changes over time, with the initial outer-bar dimensions as reference on the left. Furthermore, the slumping of the dunes mentioned in the previous section is clearly visible with the use of timestacks. The red area from $t = 0$ hrs till $t = 4$ hrs is during the spin-up time, where the dune foot is positioned at an alongshore uniform height of $Z_b = 3,9$ m.

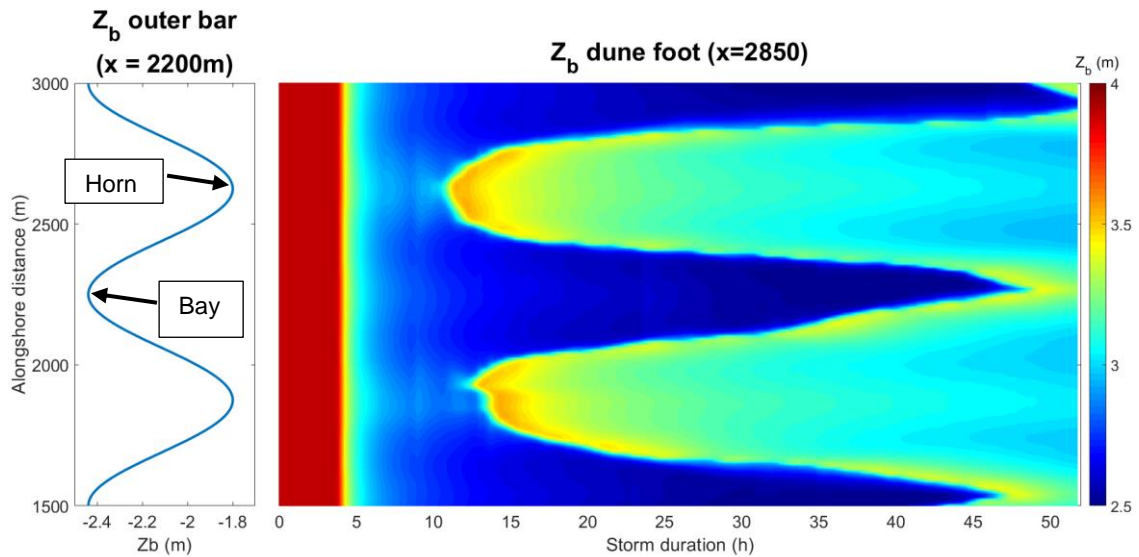


Figure 27 – bathy750TV: Timestack of dune foot change with the outer bar dimensions as reference

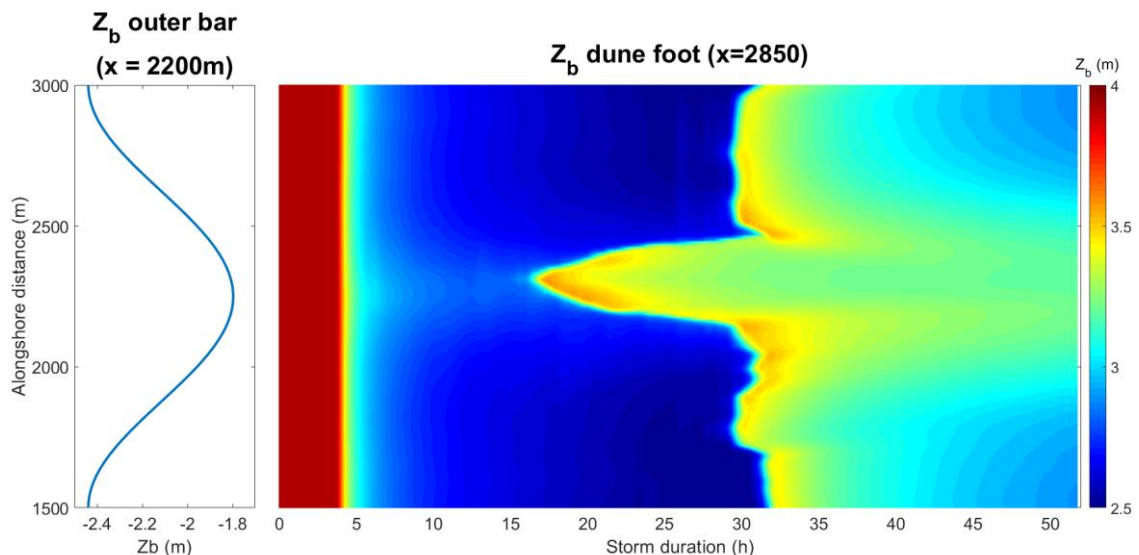


Figure 28 – bathy1500TV: Timestack of dune foot change with the outer bar dimensions as reference

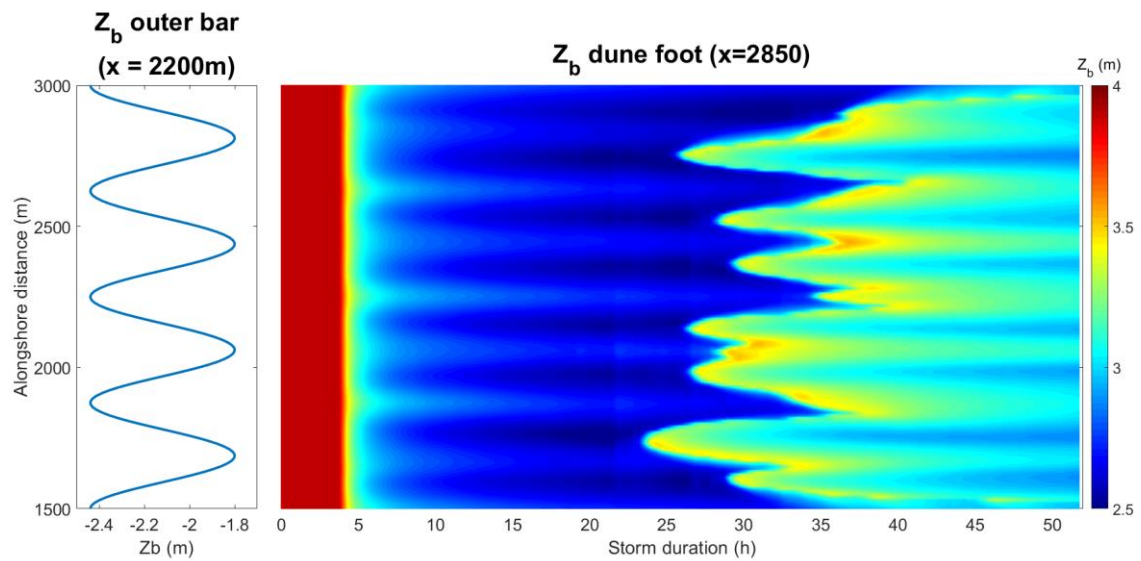


Figure 29 – bathy375TV: Timestack of dune foot change with the outer bar dimensions as reference

Right after the spin-up time ($t = 4$ hrs), heavy erosion takes place for all three bathymetries. After about 6-7 hrs (including spin-up) alongshore variations become visible. The magnitude of bed level change is about the same for every bathymetry. After a certain storm duration, a sudden and extreme rise in dune foot can be observed at various alongshore locations. This sudden rise is caused by slumping. The dune foot height increases because the dune face above the dune foot ($x = 2850$ till 2874 m) collapses seaward, instantly rising the bed level of the dune foot. From just one alongshore section the total eroded volume of the dune is not considered, which will be quantified in section 5.2.4.

Figure 27 shows the dune foot of bathy750TV, where from $t = 5$ hrs till $t = 10$ hrs slight variations in bed level can be observed. Behind the outer-bar horns ($y = 1900$ m & 2600 m) the dune foot is positioned about 20 cm higher than behind outer-bar bay ($y = 2250$ m). At around $t = 12$ hrs slumping occurs behind the shallow sections of the bar, which evenly spreads out over the whole dune foot during the remaining duration of the storm. At storms end $y = 2250$ m is positioned about 25 cm higher than $y = 1900$ m & 2600 m, because the dune has not fully slumped yet.

Bathy1500TV (Figure 28) displays the higher dune foot between $t = 5$ hrs and $t = 10$ hrs for the shallow outer-bar section ($y = 2250$ m) more clearly. Once again, the dunes starts to slump behind the outer-bar horns, but in this case a little later ($t = 16$ hrs). Furthermore, the slumping spreads out alongshore. However, at $t = 30$ hrs the whole alongshore profile of the dune foot slumps abruptly, which is different from bathy750TV. At storms end the dunes are fully slumped, and the dune foot behind the outer-bar horn is about 20 cm higher than behind the bays.

In Figure 29 the morphological coupling with the outer bars at half the wavelength of the crescentic pattern is clearly visible. In-between the shallow and deep part additional erosional hotspots occur, giving a total of 8 locations where dune foot is positioned higher compared to the erosional hotspot. After about 24 hrs of storm duration, slumping starts behind the in-between parts and shallow parts. At storms end, when the full dune foot profile is slumped, the morphological coupling is still visible.

5.2.3 Hydrodynamics and sedimentation

To clearly visualize and link wave heights, currents and sedimentation with erosional patterns, figures consisting of five subplots were made. All plots are from the alongshore section of the dune foot ($x = 2850\text{m}$) except the one of the outer-bar profile ($x = 2200$), which is used as a reference point (subplot a). Subplot b shows the infragravity wave height, which is at its highest near the collision regime. The short wave height, displayed in subplot c, are on its lowest magnitude at the collision regime. Subplot d gives a quiver plot of the wave induced currents, with a X-, Y-, Z-grid of the bed level at storms end ($t = 48\text{h}$) as background. Subplot e has the same background, but with sedimentation rate and direction displayed with quiver arrows. Furthermore, the current velocity (u & v) is taken from the water surface level. Sedimentation rate is that of the bed level, including suspended sediment above that said grid point. With the use of these subplots, clear correlations between alongshore variations in hydrodynamics and sedimentation can be linked to erosional patterns. See appendix 0 for full grid plots of these cross-sections.

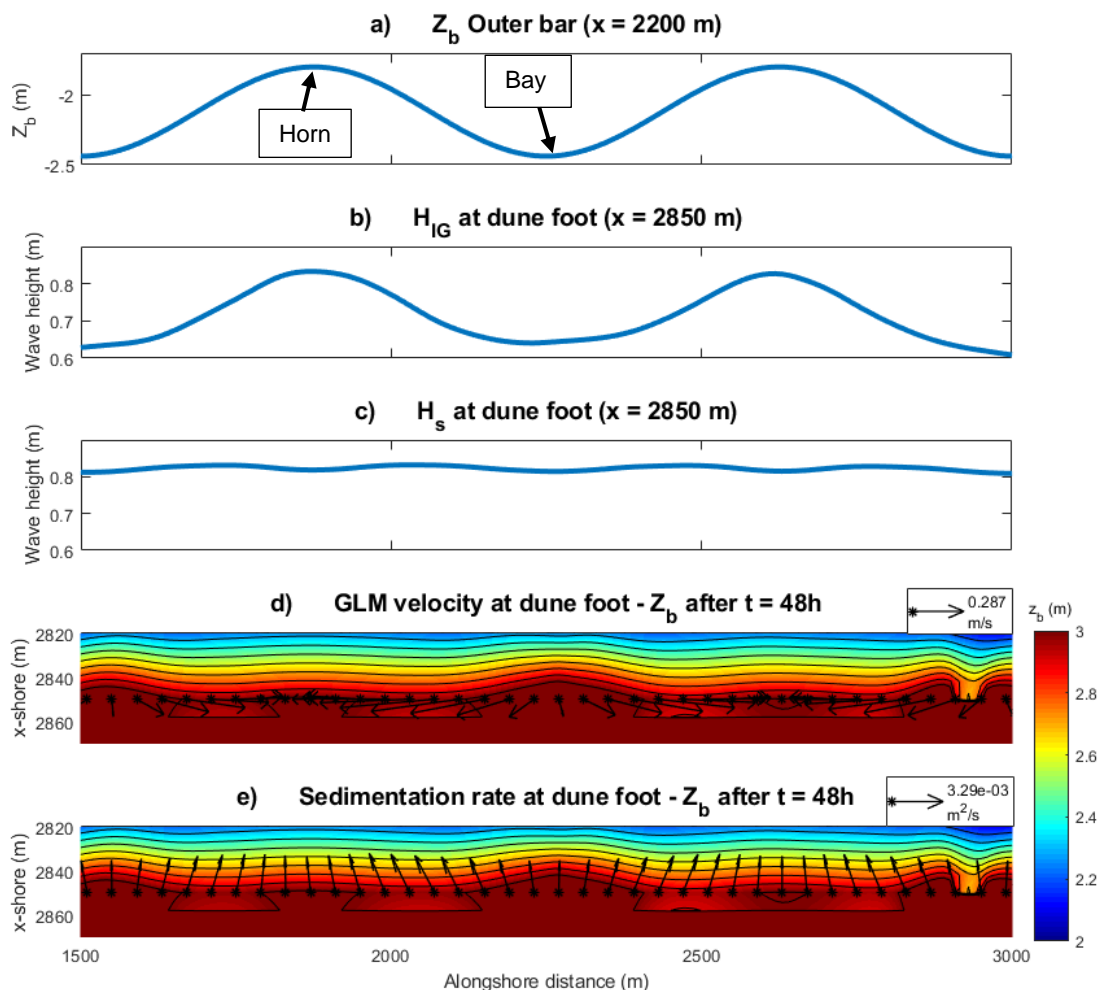


Figure 30 - bathy750TV: Five subplots containing wave heights, wave induced currents and sedimentation rate, with the outer-bar as reference

Figure 30a & b show a clear resemblance in alongshore pattern. The infragravity wave height is at its highest at the alongshore location of outer-bar horns. However, less erosion takes place at these locations. Infragravity waves are expected to impact dune erosion, but these results suggest the exact opposite. The bed level from Figure 32d & e show that the dune foot is at its highest behind the outer-bar bay at storms end. Although, this is caused by the slumping of the dune, which start behind the outer-bar horns. As discussed earlier, Figure 27 shows that the dune foot is positioned higher behind the outer-bar horns before slumping occurs. The short waves show little to none alongshore variations, which is expected since they lose all its energy in the collision regime. The quiver plots show some interesting results as well. Wave induced currents seem to circulate and move towards areas behind the outer-bar horns. Moreover, the sedimentation rate clearly converges towards the outer-bar horns. This explains the heavily deposited areas behind shallow parts of the outer-bar discussed in section 5.2.1.

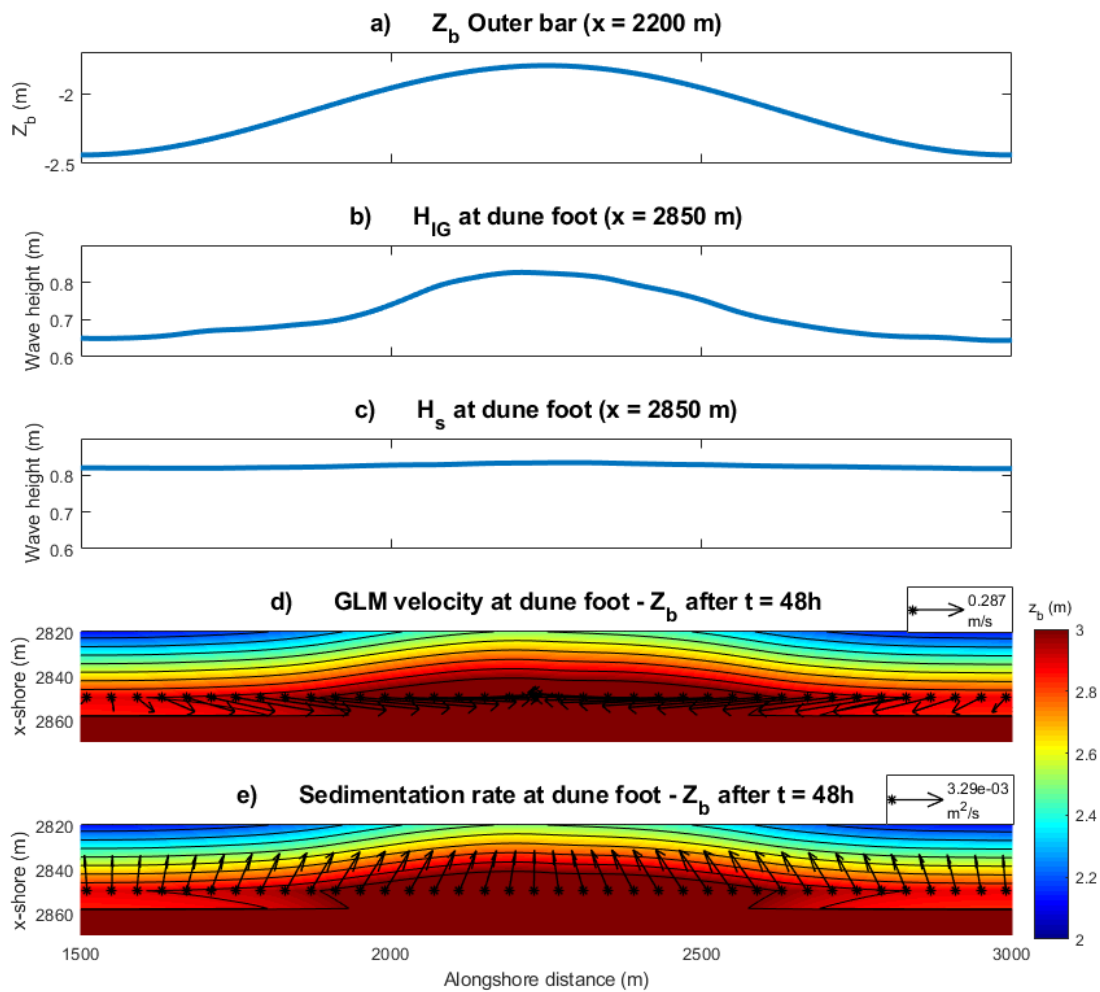


Figure 31 – bathy1500TV: Five subplots containing wave heights, wave induced currents and sedimentation rate, with the outer-bar as reference

Figure 30 and Figure 31 show some clear similarities. Infragravity waves follow the pattern of the outer bar, short waves are alongshore uniform, currents circulate towards the outer-bar horn and sedimentation converges to the horn as well. However, bathy1500TV does clearly show a higher located dune foot behind shallow part of the outer-bar. This can be caused by its different behaviour in slumping compared to that of bathy750TV. Furthermore, the alongshore variations in dune erosion are more present with only one outer-bar horn.

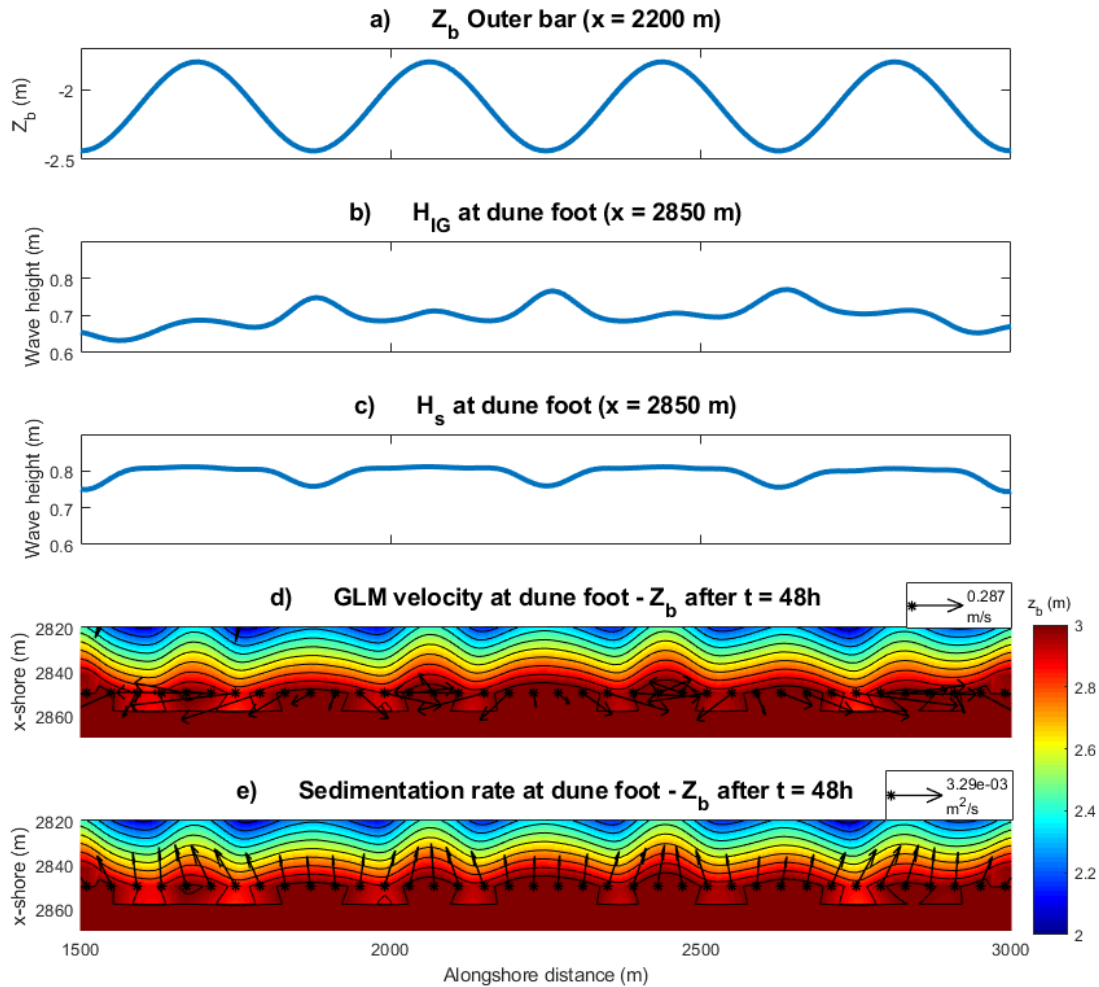


Figure 32 – bathy375TV: Five subplots containing wave heights, wave induced currents and sedimentation rate, with the outer-bar as reference

As stated before, bathy375TV is an interesting one since its morphological coupling is double the outer-bar crescentic wavelength. The infragravity waves do show peaks at the bays, but only slightly to none at the doubled locations (in-between horn & bay). Moreover, the short wave height does show some alongshore variations. About 5 cm lower at the outer-bar bays. Lower is as expected, but a 5 cm variation with a short wave height of 80 cm is most likely insignificant. However, bathy750TV and bathy1500TV did not show any variations at all. Figure 32d displays a slight circulation towards the outer-bar horns, but is somewhat unclear due to its number of erosional hotspots. The dune foot is located at its highest point behind the horns, with the half wavelength coupling locations slightly lower. Sedimentation converges towards the horns but also, in lesser magnitude, towards the bays. Hence, the doubling in deposition on the beach visible in Figure 26.

5.2.4 Dune foot eroded volume over time

The eroded volume is taken from a cross-shore section between $x = 2850$ & 2874 over the complete alongshore distance. The initial dune foot is compared with the eroded dune foot over the duration of the storm. See Figure 36 for a cross section. The surface area between the two profiles has been calculated for each timestep to quantify the amount of eroded sand of the dune foot per metre alongshore (m^3/m).

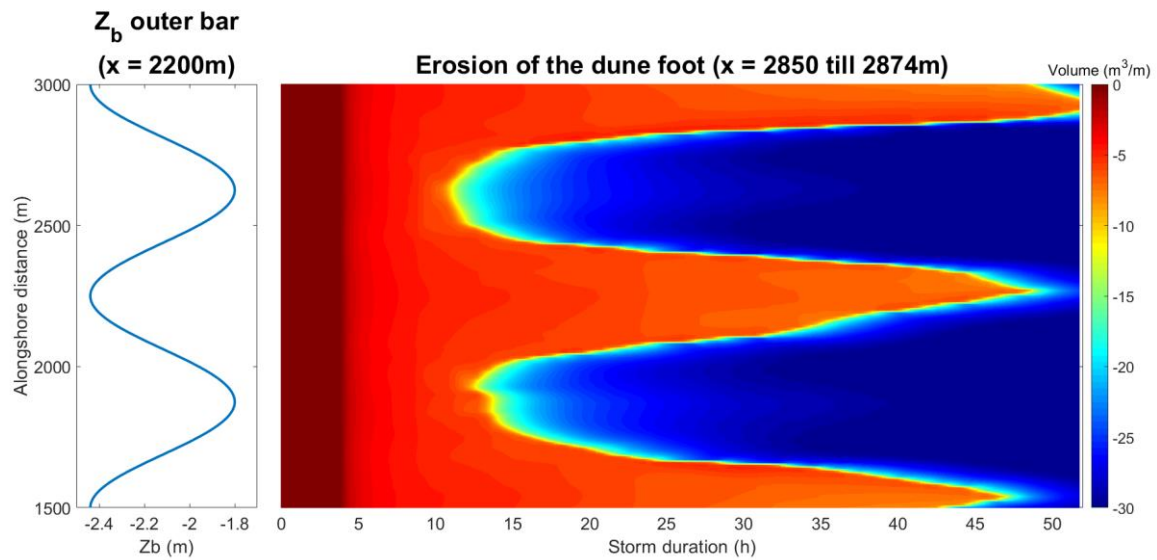


Figure 33 – bathy750TV: accumulated eroded volume of the dune face

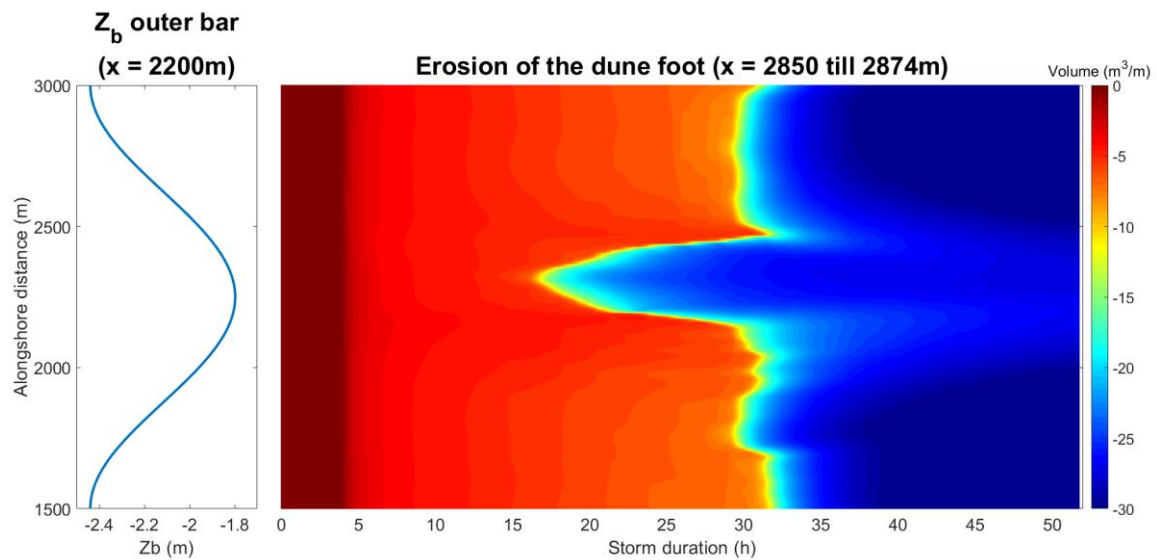


Figure 34 – bathy1500TV: accumulated eroded volume of the dune face

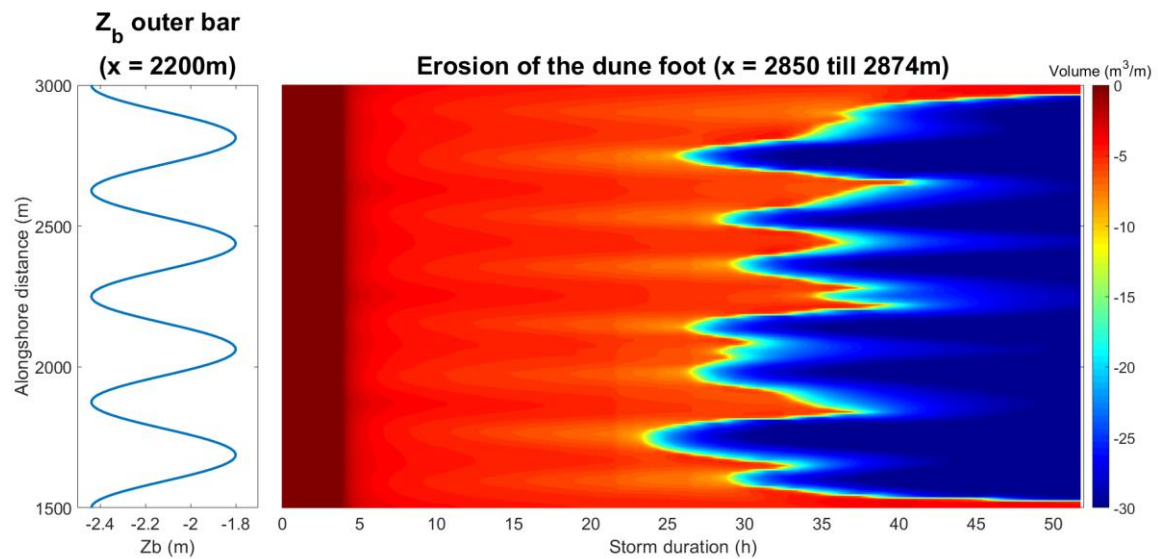


Figure 35 – bathy375TV: accumulated eroded volume of the dune face

The eroded volume plots are similar in terms of pattern to those of section 5.2.2. However, a sudden rise in eroded volume at the step where slumping occurs is visible, instead of a jump in dune foot height. Due to the range of the colourbar, alongshore variations in eroded volume are hardly visible before slumping occurs. The following table below was made to quantify the alongshore variations in dune erosion, at a storm duration of 5 hours (after spin-up time).

Total eroded volume of the dune foot (between x = 2850 & x = 2874) for t = 10 hrs	<i>Eroded volume bathy375 (m³/m) + alongshore location</i>	<i>Eroded volume bathy750 (m³/m) + alongshore location</i>	<i>Eroded volume bathy1500 (m³/m) + alongshore location</i>
<i>Shallow section</i>	4,40	4,72	4,23
	<i>y = 2100m</i>	<i>y = 19000m</i>	<i>y = 2250m</i>
<i>Between shallow & deep</i>	4,67	4,70	4,26
	<i>y = 2200m</i>	<i>y = 2100m</i>	<i>y = 2700m</i>
<i>Deep section</i>	3,94	4,46	4,23
	<i>y = 2250m</i>	<i>y = 2250m</i>	<i>y = 2940m</i>

The values from the table show no significant variations in erosion. Except for bathy375TV, where less erosion takes place behind the outer-bar bays. However, this is caused by the doubling in morphological coupling. Furthermore, for bathy750TV and bathy1500TV the dune foot height was situated lower behind outer-bar bays, creating erosional hotspots. Nonetheless, this is not reproduced when the eroded volume was calculated. The minimal variations in dune foot height (max. 20 cm) are most likely insignificant when calculating a surface area between two cross sections of 24 metre long. However, after only 12-16 hours of storm durations the dunes start to slump, which greatly interferes with eroded volume. If the slumping did not occur, alongshore variations in eroded dune face might become more present. For instance, see Figure 35 at t = 20 hrs. Slumping did not happen yet and slight alongshore differences in eroded volume can be observed.

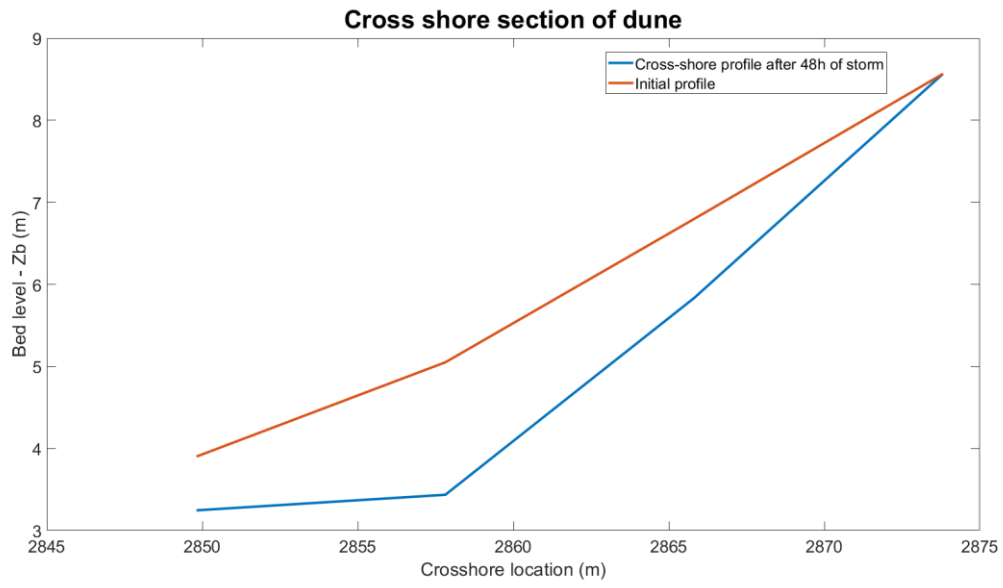


Figure 36 - Illustration of the surface area between initial and post-storm profile

5.3 Model results of wave conditions based on Egmond storm

Visualisations and observations of the model output from the three artificial bathymetries computed with the Egmond storm will be reviewed in this chapter. Please note that observations based on the near-shore bathymetry already stated in chapter 5.2 will not be discussed again. The main focus is the change in wave conditions, namely the 30-degree angle of incidence. The results will be compared with the reference case in chapter 5.4.

5.3.1 Bed level change of the full grid at storms end

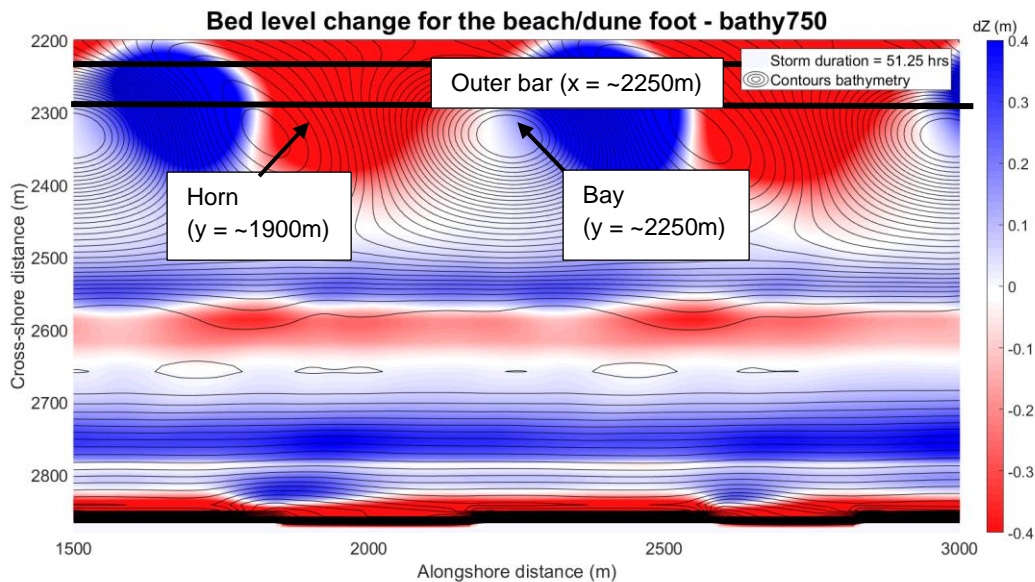


Figure 37 – bathy750EG: Bed level change (dZ_b) after 48 hours for bathy375. Initial bed level is used as reference ($dZ_b = 0$)

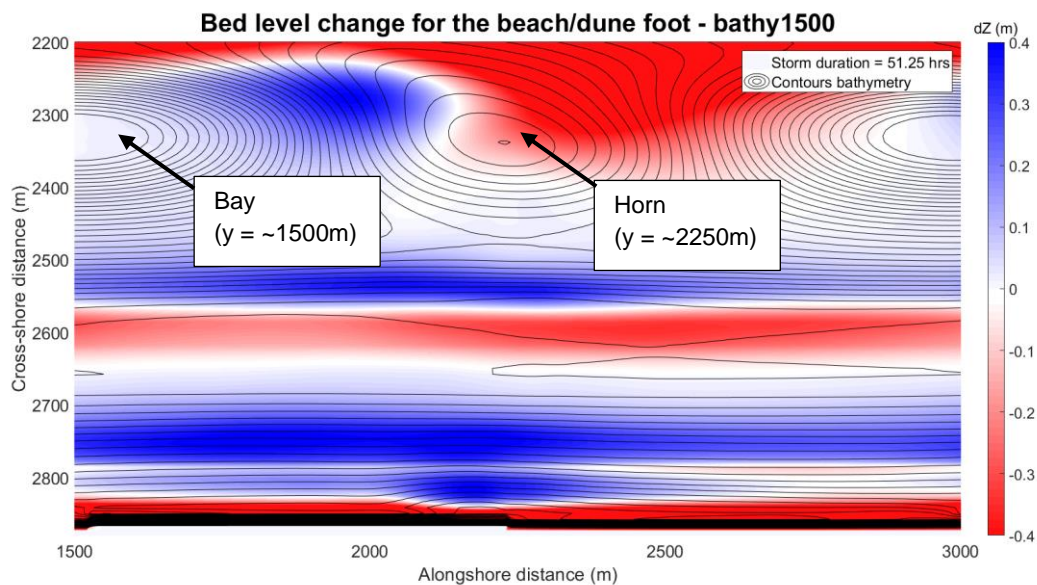


Figure 38 – bathy1500EG: Bed level change (dZ_b) after 48 hours for bathy750. Initial bed level is used as reference ($dZ_b = 0$)

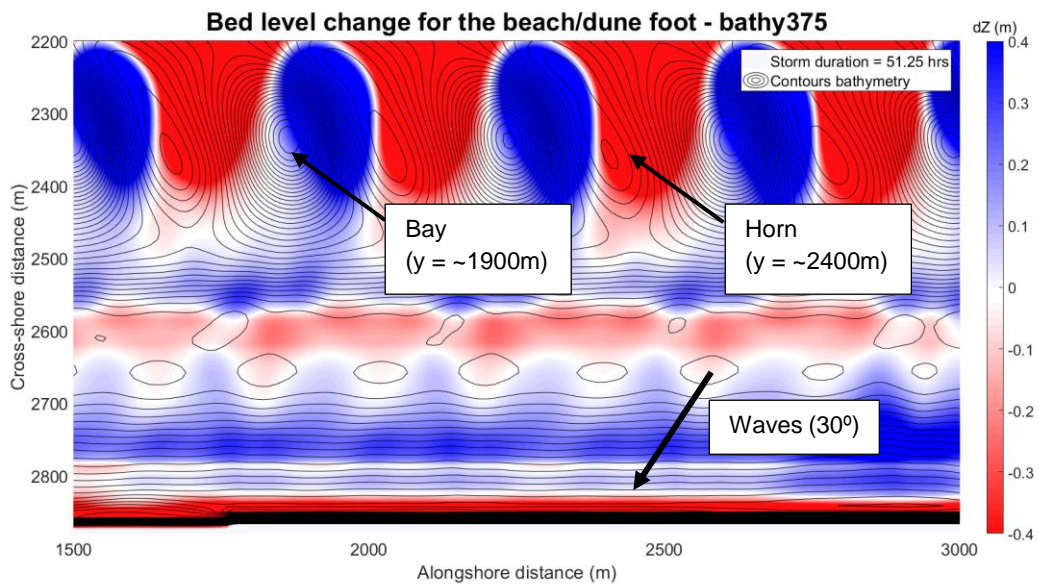


Figure 39 – bathy375EG: Bed level change (dZ_b) after 48 hours for bathy1500. Initial bed level is used as reference ($dZ_b = 0$)

Alongshore variations in dune erosion are once again difficult to see on these full grid plots. However, the impact of the change in incoming wave angle is noticeable. It can be observed that the outer bars migrate left (south) due to the waves arriving with a 30-degree angle of incidence towards north (e.g. see outer bar in Figure 37). There are some erosional hotspots visible for every bathymetry, a further clarification about alongshore variations in dune erosion is given in section 5.3.2. For the Egmond storm these locations are positioned behind the outer-bar horns as well, but shifted south. Furthermore, the double wavelength of the outer-bar crescentic pattern morphological coupling seems to be less present in bathy375EG. For all three bathymetries, the dune foot is very unstable at the end of computation due to slumping. The slumping of the dunes behaved differently compared to the Truc Vert storm. This is furtherly observed and discussed in sections 5.3.2 and 5.3.4.

5.3.2 Dune foot change over time

The scales of the colourbar and other dimensions of the timestack plots remained unchanged for the Egmond storm. By keeping the scaling uniform, better observations about similarities and differences can be made.

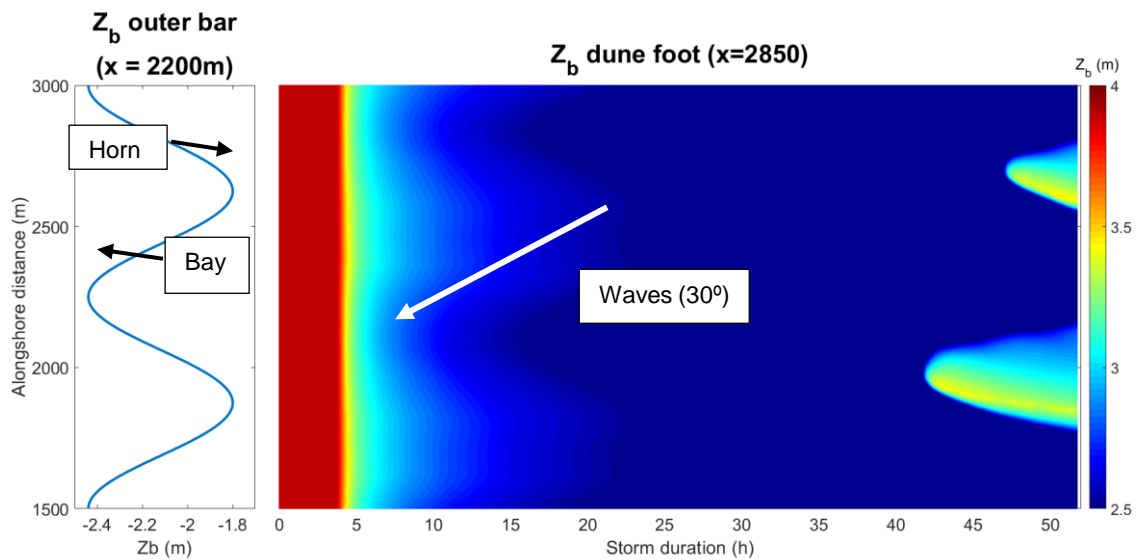


Figure 40 – bathy750EG: Timestack of dune foot change with the outer bar dimensions as reference

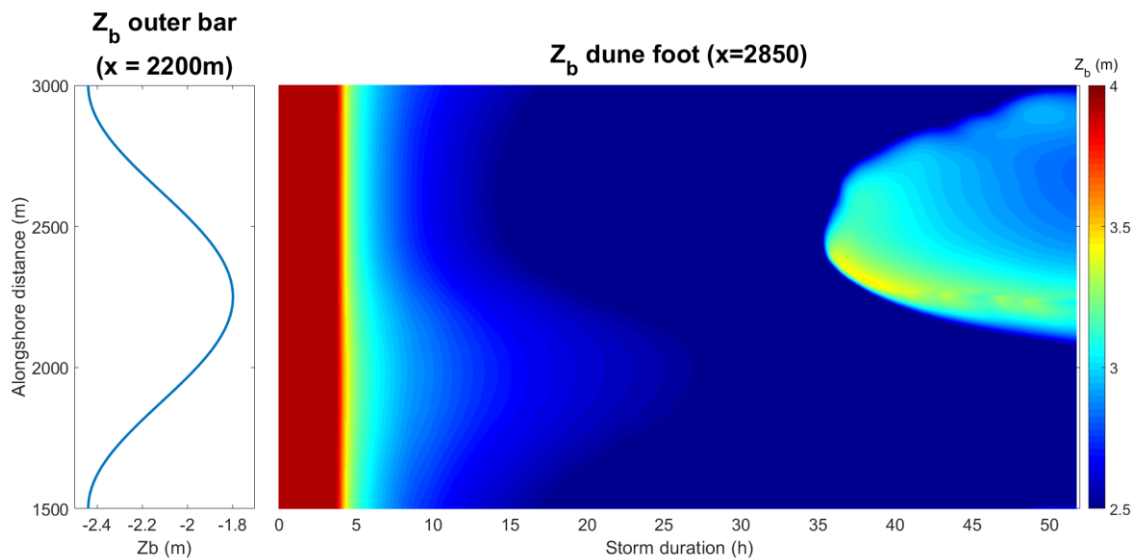


Figure 41 – bathy1500EG: Timestack of dune foot change with the outer bar dimensions as reference

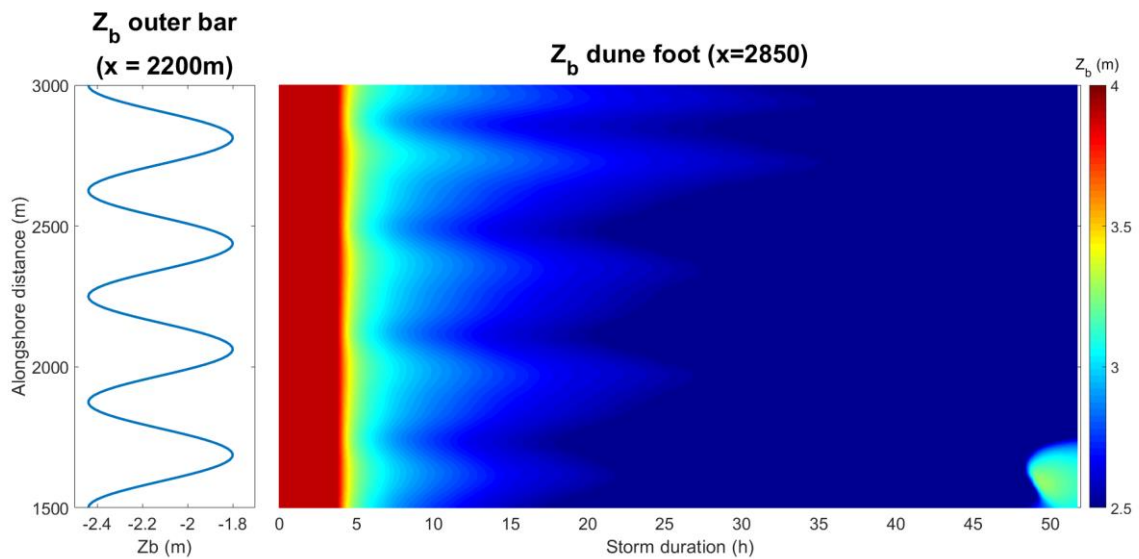


Figure 42 – bathy375EG: Timestack of dune foot change with the outer bar dimensions as reference

For the first 24 hours of storm, clear alongshore variations in dune foot height can be seen for all bathymetries. Slumping of the dune face occurs after 35 hours or later. The southward shift (downward in these plots) of the alongshore difference in dune foot height, compared to the alongshore location of the outer-bars is nicely visible. It appears to be that alongshore variations in dune foot are smoothed out after about 25-30 hours of storm. However, this is not the case. The colourbar only goes till a value of $Z_b = 2,5$ m, while the dune foot of all three bathymetries modelled with the Egmond storm drop to about $Z_b = 2,0$ m, with the same alongshore variable pattern. See appendix 8.3.

Bathy750EG (Figure 40) two alongshore areas (between $y = 1700$ & 1900 m and $y = 2400$ & 2600 m) of the dune foot are clearly positioned higher compared to other parts of the dune foot. These are related to the outer-bar pattern. After about $t = 42$ hrs the dunes start to slump behind the cross-shore location of the outer-bar horns. At storms end, the dunes are still slumping and it is expected they will continue to do so if the model was computed longer.

Figure 41 shows very clear alongshore variations in dune foot height, once again related to the outer-bar horn. Almost a 40 cm difference in dune foot height between $y = \sim 2000$ m and ~ 2750 m. Furthermore, after about $t = 36$ hrs the dunes start to slump, in the same trend as bathy750EG.

In Figure 42 the morphological coupling with the outer bars at half the wavelength of the crescentic pattern is not clearly visible. About 4 areas ($y = 1600, 2000, 2400, 2800$ m) can be observed which are positioned higher than other parts of the dune foot, again linked to outer-bar horns. Interesting to note is that slumping occurs only at the very end of the storm, behind the most southern outer-bar horn.

5.3.3 Hydrodynamics and sedimentation

The figures containing five subplots have the same lay-out as in chapter 5.2.3. The only differences are scaling among the Y-axis and quiver arrows. Since the wave period is lower (from 12 sec to 8 sec), the magnitude of infragravity and short wave height is lower as well (subplot b and c). The maximum of IG wave height is about 0,4 m, compared to 0,8 m for the Truc Vert storm. However, the short wave height only goes from 0,8 m to 0,6 m. As expected, the decrease in wave period has a larger impact on infragravity wave height. See appendix 0 for full grid plots of these cross-sections.

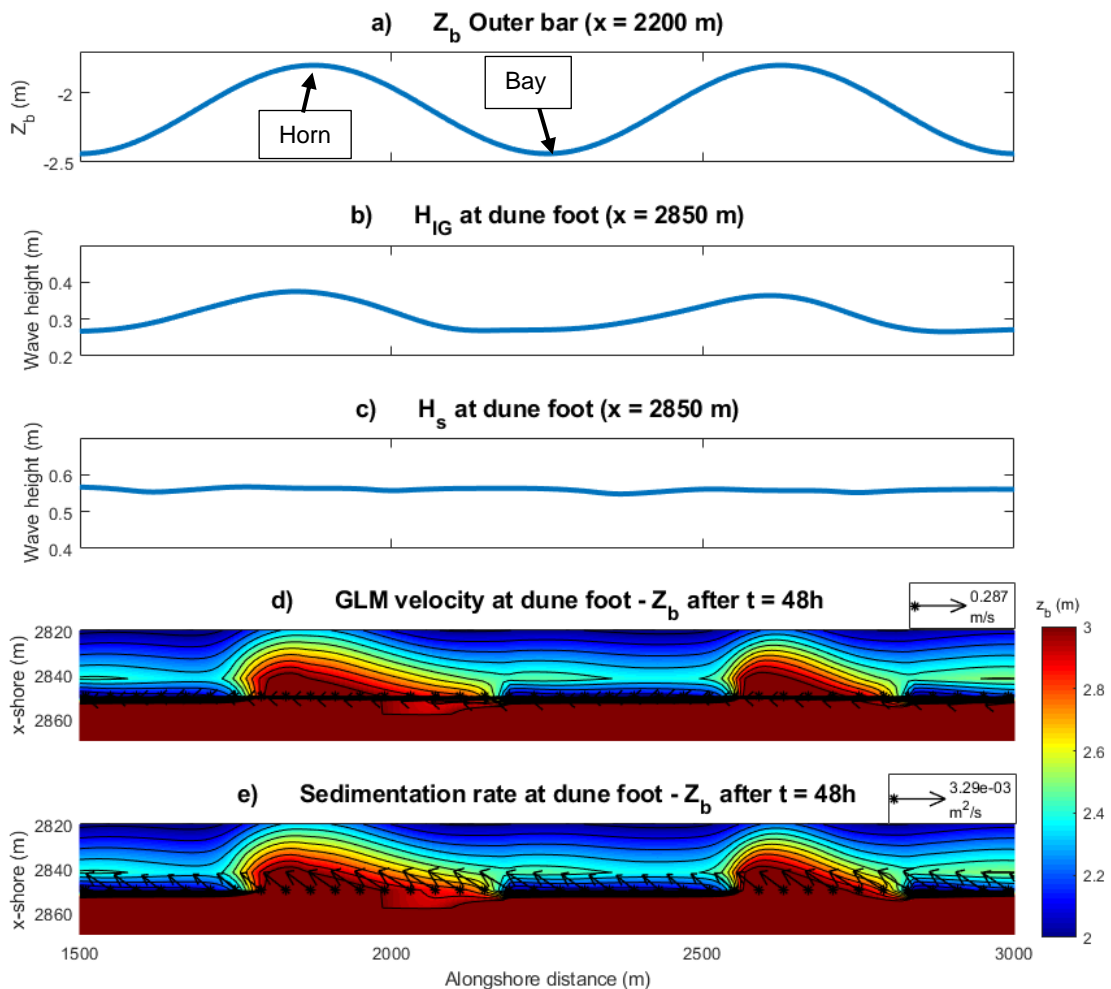


Figure 43 - bathy750EG: Five subplots containing wave heights, wave induced currents and sedimentation rate, with the outer-bar as reference

Bathy750EG (Figure 43) shows some interesting patterns in hydrodynamics and sedimentation. The alongshore shift to the south (left) that was visible in dune foot height does not correspond to the infragravity wave height pattern, which follows the trend of the outer-bar without a shift. The bed level is difficult to interpret, since slumping just started at storms end. However, the wave induced currents and sedimentation rate (d & e) clearly converge to the south. For the currents it is a 90-degree angle with the dune foot towards south with no circulations visible, which is caused by the 30-degree incoming wave angle. The sedimentation moves south with an angle of 45 degrees with the collision regime (x = 2850m).

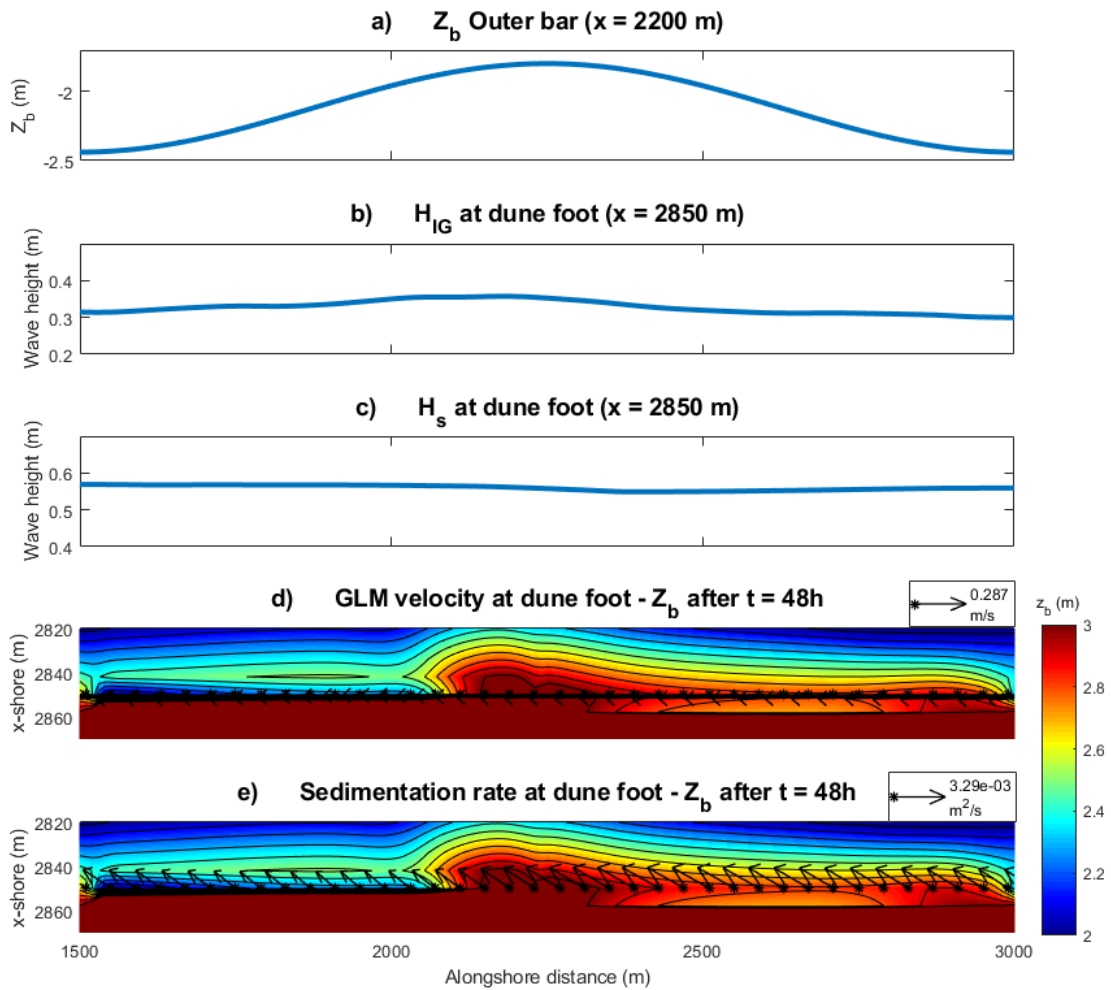


Figure 44 – bathy1500EG: Five subplots containing wave heights, wave induced currents and sedimentation rate, with the outer-bar as reference

Figure 44 and Figure 43 show similar trends in terms of currents and sedimentation rate. Furthermore, the dune face also just started slumping behind the outer bar ($y = 2250m$) as discussed before. However, the infragravity wave height (b) shows minimal to none along variations. Its magnitude is about 5 cm higher behind the outer-bar horn, compared to the bays. It can be that due to the relatively large size of the outer-bar horn together with 30-degree incoming wave angle, the IG wave height differences are more spread out alongshore and thus hardly present.

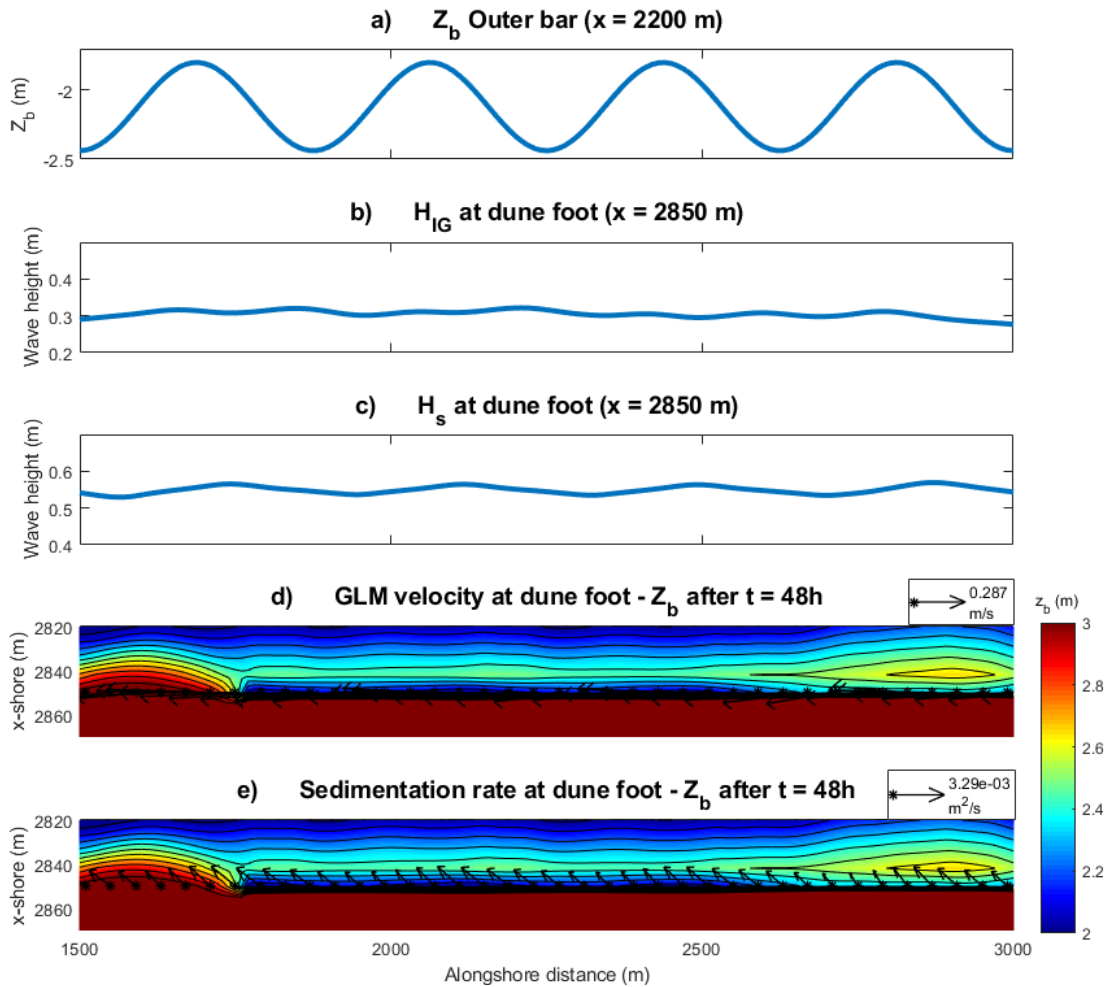


Figure 45 – bath375EG: Five subplots containing wave heights, wave induced currents and sedimentation rate, with the outer-bar as reference

Bathy375EG (Figure 45) shows very similar trends to bathy1500TV. Moreover, the infragravity wave height (b) does not show any noticeable variations alongshore. This is probably caused by the lower outer-bar crescentic wavelength of 375 metres. Differences in IG wave height are spread out due to the 30-degree angle of incidence.

5.3.4 Dune foot eroded volume over time

The eroded volume is calculated using the same method as in chapter 5.2.4, from a cross-shore section between $x = 2850$ & 2874 over the complete alongshore distance. See Figure 36 for a cross section. The surface area between the two profiles has been calculated for each timestep to quantify the amount of eroded sand of the dune foot per metre alongshore (m^3/m). Note that the colourbar scale of eroded volume remained the same for both storms.

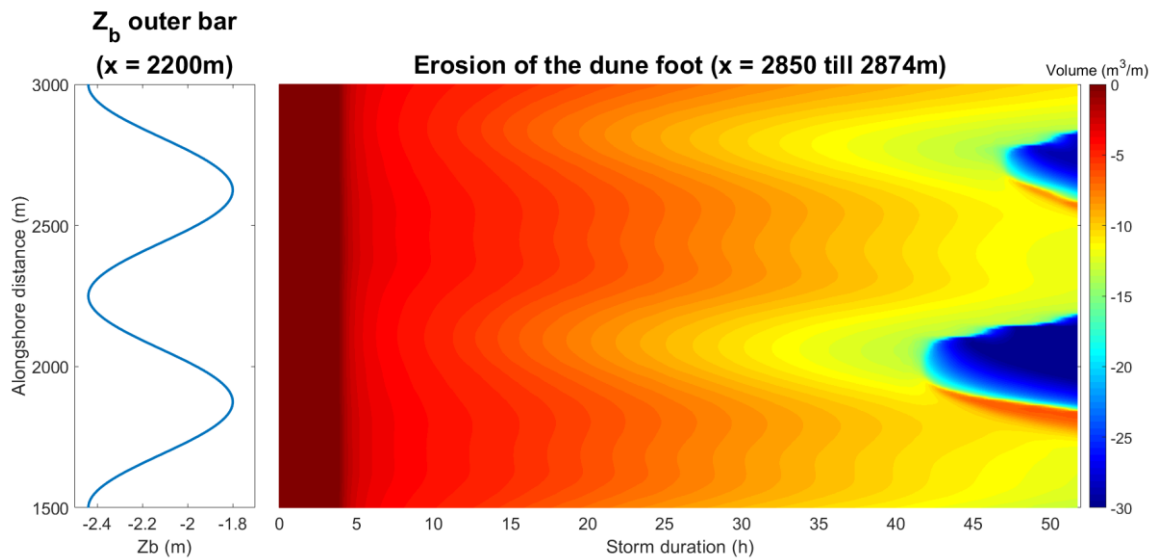


Figure 46 – bathy750EG: accumulated eroded volume of the dune face

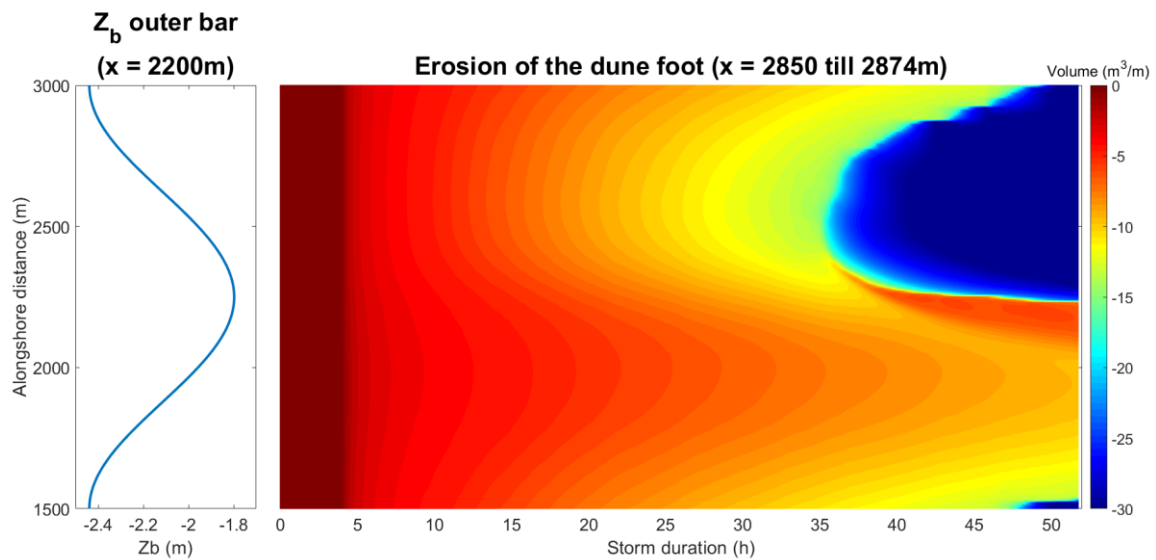


Figure 47 – bathy1500EG: accumulated eroded volume of the dune face

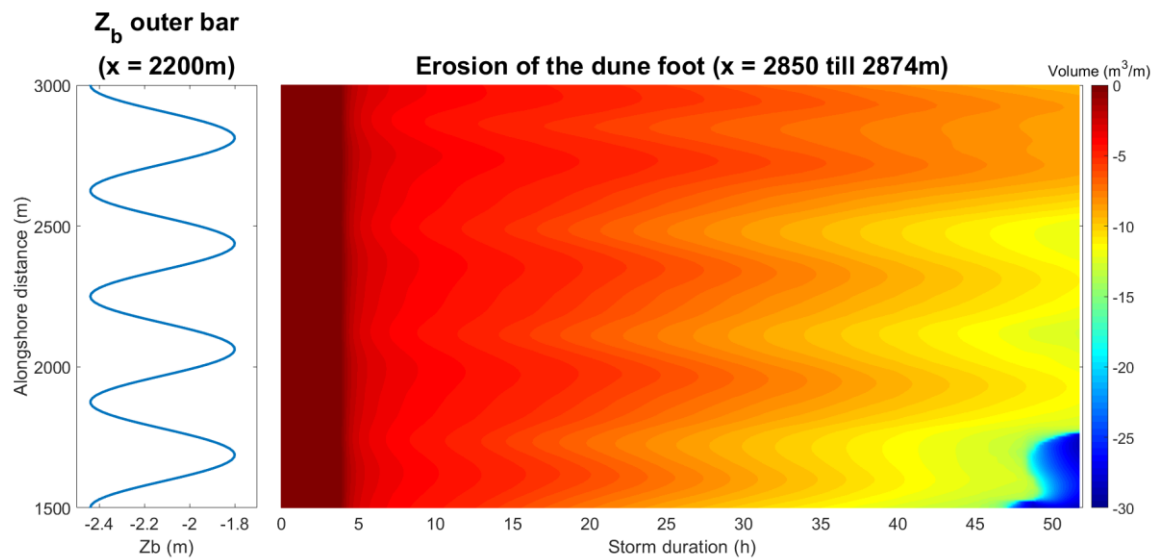


Figure 48 – bathy375EG: accumulated eroded volume of the dune face

Due to the angle of incidence being 30 degrees north the erosional hotspots do not line up with shallow and deep parts of the outer-bar, as they did for the Truc Vert storm. Quantifying and comparing specific cross-shore sections like in the table of section 5.2.4 are not relevant, since the so-called erosional hotspots are shifted south (downward for the figures above). However, alongshore differences in eroded volume are clearly visible for all three bathymetries. Figure 47 for example shows very distinct variations in eroded volume, especially at $t = 17$ hrs and beyond. The area affected by the outer-bar horn ($y = \sim 2000\text{m}$) eroded for about $5,0 \text{ m}^3/\text{m}$ at $t = 17$ hrs, while the area behind the bay ($y = \sim 2750\text{m}$) eroded for about $7,5 \text{ m}^3/\text{m}$. Variations of this magnitude can also be visible in Figure 46, for bathy375EG (Figure 48) these variations are less present due to its shorter distance between outer-bar horns.

5.4 Comparison between results & reference case

As expected, both the Truc Vert & Egmond storm modelled with an alongshore uniform grid resulted in no erosional hotspots (see section 5.1). With the three varying bathymetries, alongshore variations in erosion can certainly be observed. However, the magnitude of the variation is relatively low. The dune foot located at these erosional hotspots (behind outer-bar horns for the Truc Vert case) is only situated about 20-30 centimetres lower than the dune foot behind outer-bar horns (shifted south for Egmond case). Furthermore, alongshore variations in eroded volume of the dune face are only significantly present for the Egmond storm.

A notable difference between Truc Vert & Egmond storm for the alongshore uniform grid, is the erosional behaviour. Even though they both remain alongshore uniform, the dunes for the Egmond storm are significantly eroded heavier at storms end, because of the slumping event after about 24 hours (see section 5.1). For the Truc Vert reference case no slumping occurs, the dune foot gradually evolves to an equilibrium (see Figure 22 & Figure 23). Furthermore, if Figure 22 & Figure 23 are compared in terms of eroded volume, the difference in magnitude is an interesting observation. BathyUniTV erodes much more intense from $t = 4$ hrs and $t = 24$ hrs compared to bathyUniEG. However, after this time-step bathyUniEG suddenly slumps alongshore uniform, resulting in a higher eroded volume at storms end. Even though the waves are stronger for bathyUniTV (longer period), the dunes do not slump. Furthermore, the total eroded volume of the dune has been calculated just as in chapter 5.2.4 for both reference cases. It is important to consider landward parts above the dune foot as well when quantifying dune erosion. Since eroded sand from above the dune foot is deposited on top of it. This will affect the evolution of the dune foot, if the upper parts are eroded significantly more. Meaning that analysing just a single alongshore section of the dune foot is not sufficient.

Bathy750 has been chosen for a comparison because the erosional patterns are more or less symmetrical for this case, and thus interpretation of results becomes less difficult. As said before, during both storms slumping takes place for bathy750. Before this event (e.g. $t = 10$ hrs in Figure 27 & Figure 40) less erosion behind the outer-bar horns can be observed. For the Egmond storm this is shifted south (left) due to the angle of incidence. The alongshore variation (before slumping, $t = 10$ hrs) in dune foot erosion is about 15 cm for both storms. Furthermore, for both cases slumping of the dunes begins behind the outer-bar horns. Overall, the eroded dune face volume is significantly more for the Egmond storm at $t = 10$ hrs. However, the magnitude of variations in erosional hotspots between the storms are minimum. Only the location differs.

The eroded sand of the dunes, as said before, is deposited on the beach. For the Truc vert storm the sedimentation rate clearly converged towards the outer-bar horns, while for the Egmond storm sediment moves southwards. The following figures display how the eroded sand is deposited and distributed alongshore on the beach, for a cross-shore section between $x = 2720$ and 2820 m.

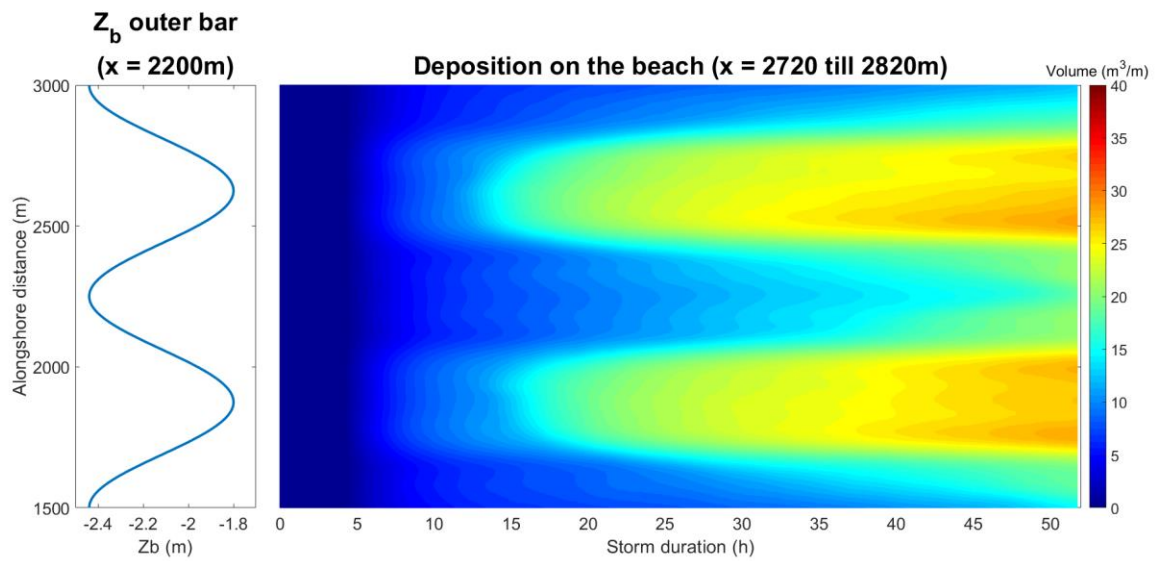


Figure 49 – bathy750TV: accumulated deposited volume on the beach

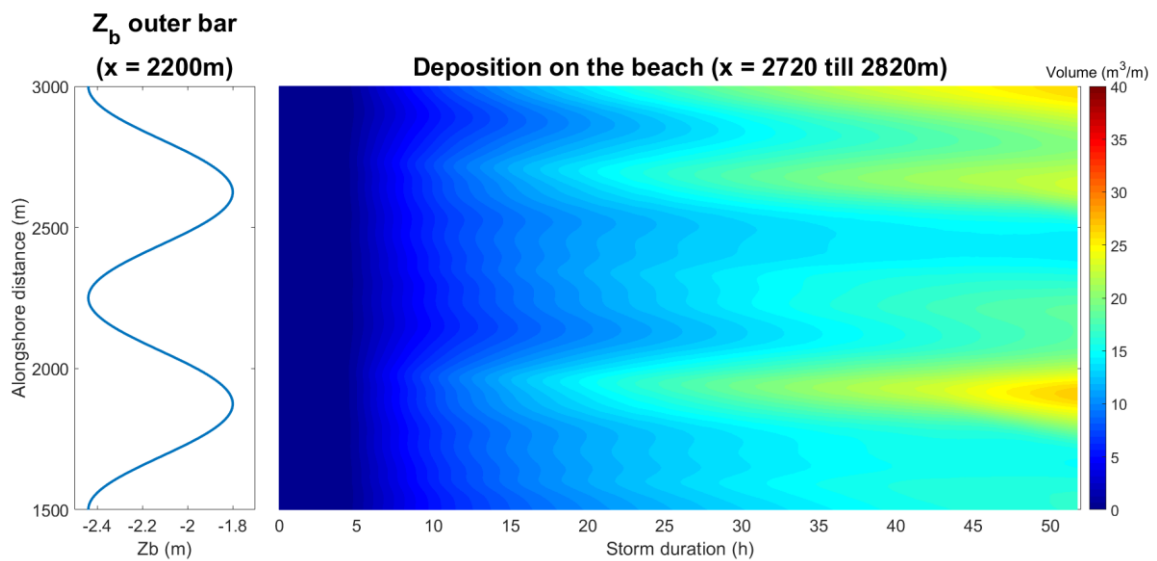


Figure 50 – bathy750EG: accumulated deposited volume on the beach

One significant difference between bathy750TV & EG can be observed, namely the amount of deposited sand on the beach is much larger for bathy750TV behind the outer-bar horns. This corresponds with the sedimentation magnitude and direction from Figure 30, where they converge towards $x = 2100$ & 1900m . In Figure 43 all sedimentation moves towards the south under a 45-degree angle. Resulting in a more evenly spread out deposition on the beach, clearly visible in Figure 50 for $t = 35$ hrs, compared to Figure 49. This difference in deposition on the beach area is also visible for bathy1500 & bathy375. See appendix 8.2 & 8.3.

6. Discussion

Three X-, Y-, Z-grids containing three different bathymetries were generated and modelled with two different storm conditions with a duration of 52 hours, including 4 hours of spin-up time. The result was a grid of 281 x-points by 333 y-points (including boundary) containing 208 entries of data for each grid point, corresponding to measured values for every 15 minutes. XBeach provided data about bed level, water level, wave height, currents and sedimentation. All this data was visualized in chapter 5, and will now be interpreted and compared to previous studies in the following chapter. Furthermore, certain findings will be further explained, and new research topics will be considered.

6.1 Alongshore variable dune erosion

Alongshore differences in erosion, wave conditions and current patterns are visible in the results of all the six different cases. However, the magnitude of differences in dune erosion are hardly noticeable. For all artificial bathymetries the dune foot eroded about 20-25 cm more, compared to locations behind outer-bar horns. These so-called erosional hotspots are located a few hundred metres apart, which makes a 20-25 cm difference in bed level relatively small. Even though the erosional differences are not as prominent as expected, they did behave as expected and show similarities with previous studies. A clear coupling between outer-bar horns and beach/dune response was visible in all results. Although it was not as significant as, for instance, the coupling studied by Castelle et al. (2015), but still relatively visible that it should be noted. As stated before, double the wavelength of the outer-bar crescentic pattern coupling with the dune foot was observed for bath375TV. The regime when this occurs corresponded to the findings of Castelle et al. (2009, part1). Claudino-Sales et al. (2008) and Houser et al. (2008) used XBeach to study alongshore differences in erosion and suggested that it is mainly driven by offshore bathymetry differences. For example, transverse ridges on the inner shelf that locally focus wave energy which result in erosional hotspots. This is in line with the results of this study. Furthermore, Galal & Takewaka (2011), Thornton (2007) and Mulligan (2018) found that the location of rip channels is related to erosional hotspots. Moreover, the XBeach model computed by de Winter et al. (2015) resulted in a dune erosion between 5 and 40 m³/m. This is of similar magnitude from the results modelled for this study (see chapters 5.2.4 & 5.3.4) The significance of angle of incidence is not discussed in these studies. The sensitivity and validity of angle of incidence within XBeach models will be addressed in section 6.2

To study the sensitivity of the magnitude of alongshore variable dune erosion, two parameters have been varied again to compare with previous results. Namely, the wave period and depth difference between the outer-bar horns and deep parts of the bar (from 4m originally to 2m). Bathy750 has been chosen here again to examine the sensitivity of these two parameters, because erosional hotspots are the most prominent here and thus influenced more by changes in model conditions.

The Truc vert storm was modelled with a $H_s = 5$ m, $T_p = 12$ s & $\theta = 0^\circ$, while the Egmond storm conditions were $H_s = 5$ m, $T_p = 8$ s & $\theta = +30^\circ$. If the period of the Truc Vert storm is altered to eight seconds, the 30-degree angle of incidence remains its only variable between the two. Similar timestacks as in chapters 5.2.2 & 5.3.2 are used to investigate the influence and validation of a 30-degree angle of incidence within the storm conditions of a XBeach model.

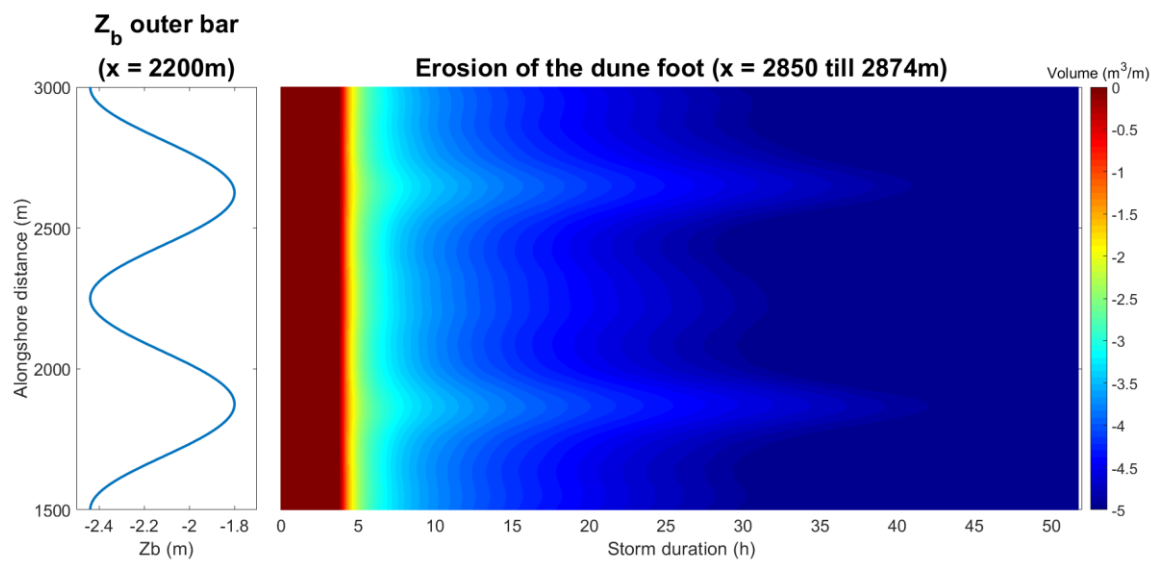


Figure 51 – bathy750TV8: eroded dune over time - Truc Vert storm with $T_p = 8$ seconds.

Figure 51 is compared with Figure 46 (bathy750EG) and Figure 33 (bath750TV) in terms of eroded volume of the dune at an erosional hotspot. Note the change in colourbar scale for bathyTV8. The value is taken from $t = 10$ hrs (including spin-up). The reason for this is because slumping did not take place yet after said duration. Slumping does not occur for some locations and situations, making it an unreliable variation in terms of a general comparison. For the Truc Vert storm the location of erosional hotspots are the same, while they are shifted south for the Egmond storm.

Total eroded volume of the dune foot at erosional hotspot (m^3/m)	<i>Bathy750TV8</i> ($y = 2600m$)	<i>Bathy750TV12</i> ($y = 2600m$)	<i>Bathy750EG</i> ($y = 2500m$)
<i>After $t = 10$ hrs</i>	3,28	4,72	4,01
<i>After $t = 52$ hrs</i>	5,27	30,85	16,59

With the cross-sections of the dune foot and total eroded volume, some interesting differences can be noted. The Truc Vert storm with a period of eight seconds, has a significantly lower eroded volume than that with a period of twelve seconds. Which is expected, since a lower period means weaker waves and thus less erosion. Furthermore, alongshore variations in dune foot erosion are slightly lower with a period of eight seconds. If Figure 50 and Figure 33 are compared at $t = 10$ hrs, bathyTV8 varies 16,9 centimetres between crest and trough at this timestep, while the dune foot height of bathyTV12 varies 22 centimetres (see appendix 8.2.1 & 8.2.4).

However, the Egmond storm case also has a wave period of eight seconds but shows more eroded volume than bathy750TV8. It can be said that this is caused by the angle of incoming waves, because the 30-degree angle of incidence is the only adapted condition. An explanation for this is the southward directed sedimentation rate observed in chapter 5.3.3. This resulted in less deposition on the beach behind the outer-bar horns, stated in chapter 5.4. The sediment is transported south, instead of directly off-shore with a shore normal incoming wave angle. A lower buffer on the beach can result in more instability of the dunes, and thus meaning more erosion of the dunes. Furthermore, test runs showed that XBeach produced

questionable results with higher incoming wave angles (for instance, 45 degrees). The boundary interfered significantly with the research area, where hydrodynamic and morphodynamics behaviour is unrealistic due to the edges of the grid (see chapter 4.3). It can be that a 30-degree incoming wave angle is also affected by the boundary and edges of the grid.

For the second case, alongshore depth differences of the outer-bar have been changed. From four meters for all the previous runs, to two metres for this situation. The new grid is modelled with storm conditions of Truc Vert with a wave period of twelve seconds. Also important to note, due to the change in depth difference the overall depth of the outer-bar becomes deeper as well. This is an unwanted liability when generating artificial bathymetries, but the results will still be viable to globally study alongshore variations in dune erosion.

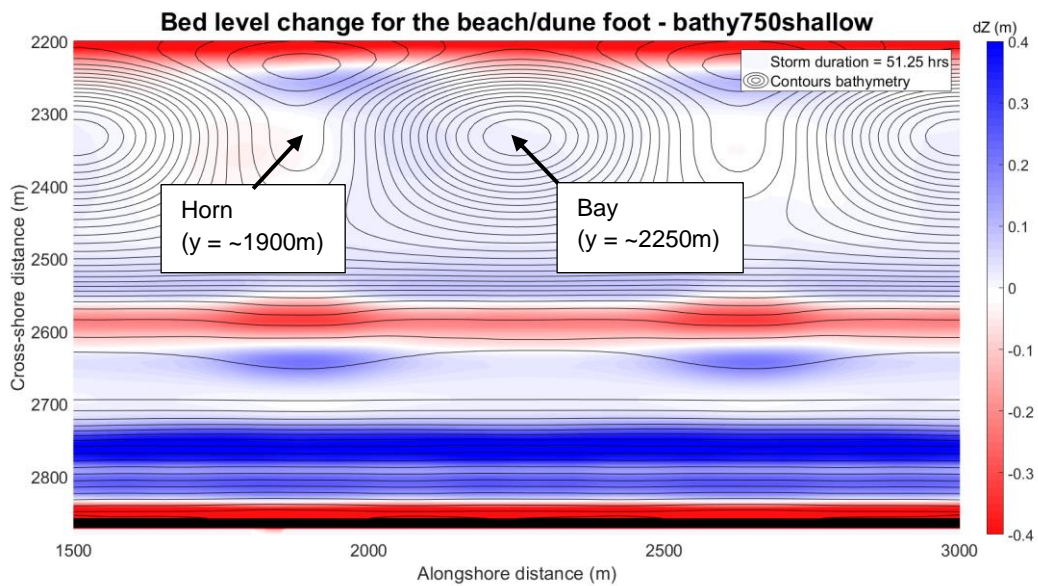


Figure 53 - bathy750shallow: Bed level change (dZ_b) after 48 hours. Initial bed level is used as reference ($dZ_b = 0$) - Truc Vert storm with $T_p = 12$ seconds

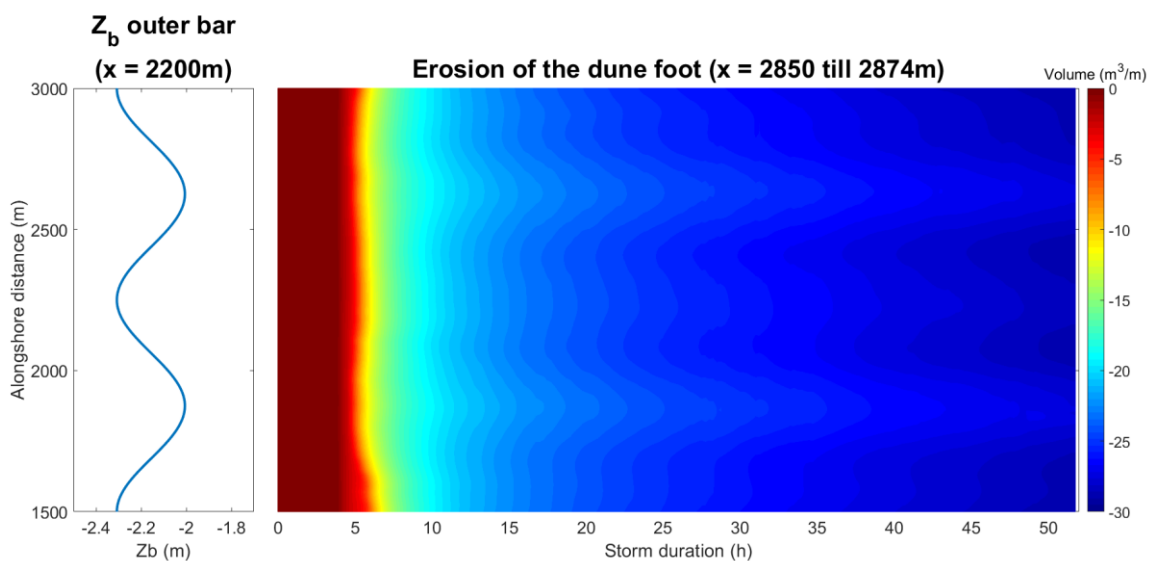


Figure 52 – bathy750shallow: eroded dune over time - Truc Vert storm with $T_p = 12$ seconds.

First off, as a result of the deeper average depth of the outer bar, more erosion takes place after $t = 10$ hrs (Figure 52). The dune has eroded for $17,88 \text{ m}^3/\text{m}$ for this time-step, which is almost three times as much as bathy750TV12. Furthermore, the decrease in alongshore depth differences of the outer-bar are clearly visible in erosional hotspots. The alongshore maximum difference between dune foot height is only $8,2$ centimetres. Some of it may also be caused by the deeper position of the outer-bar, but mostly by the depth difference of the outer-bar horns and shallow parts in-between.

6.2 XBeach limits & validity

As stated before, a large angle of incidence seems like a clear limitation of the XBeach modelling method used for this research. Some test runs have been done with an incoming wave angle of up to 45 degrees, which gave even more unrealistic results. The validity of angle of wave incidence within a 2DH XBeach model where no over-wash occurs is uncertain. Next to incoming wave angle, there are multiple other factors which can cause errors within a XBeach model. Namely grid dimensions, boundaries & spacing. In an ideal situation the modelled research area is unaffected by the grid boundaries and edges. But the boundaries cannot be endlessly large, otherwise the computation time would be unrealistic. In what way the boundary influences results and if the boundary used in this research is sufficient is hard to say. To put this statement to the test, measured storm data and bed level change could be compared to modelled results. Furthermore, the artificial grids created and used as model input can be improved. In a global perspective the model works as intended and results match the hypothesis and findings from previous studies. But, it is still somewhat unclear why, for instance, slumping occurs for certain model runs. To examine this, a better understanding of erosion models used by XBeach needs to be obtained. The XBeach manual states a certain equation about avalanching. To account for the slumping of sandy material from the dune face to the foreshore during storm-induced dune erosion avalanching is introduced to update the bed evolution. Avalanching is introduced via the use of a critical bed slope for both the dry and wet area. It is considered that inundated areas are much more prone to slumping and therefore two separate critical slopes for dry and wet points are used. The default values are 1.0 and 0.3 respectively. Since the dune foot used in this research is inundated, slumping seems very likely based on these statements. Overall, a 2DH XBeach model seems most likely viable to study alongshore differences in dune/bed level response during extreme storms when over-wash does not occur. To assess these findings, a quick test run has been done with a measured grid of a coastal profile near Truc Vert. It was modelled with a related extreme storm ($H_s = 5\text{m}$, $T_p = 12 \text{ s}$ & $\theta = \text{shore normal}$, surge = 2m).

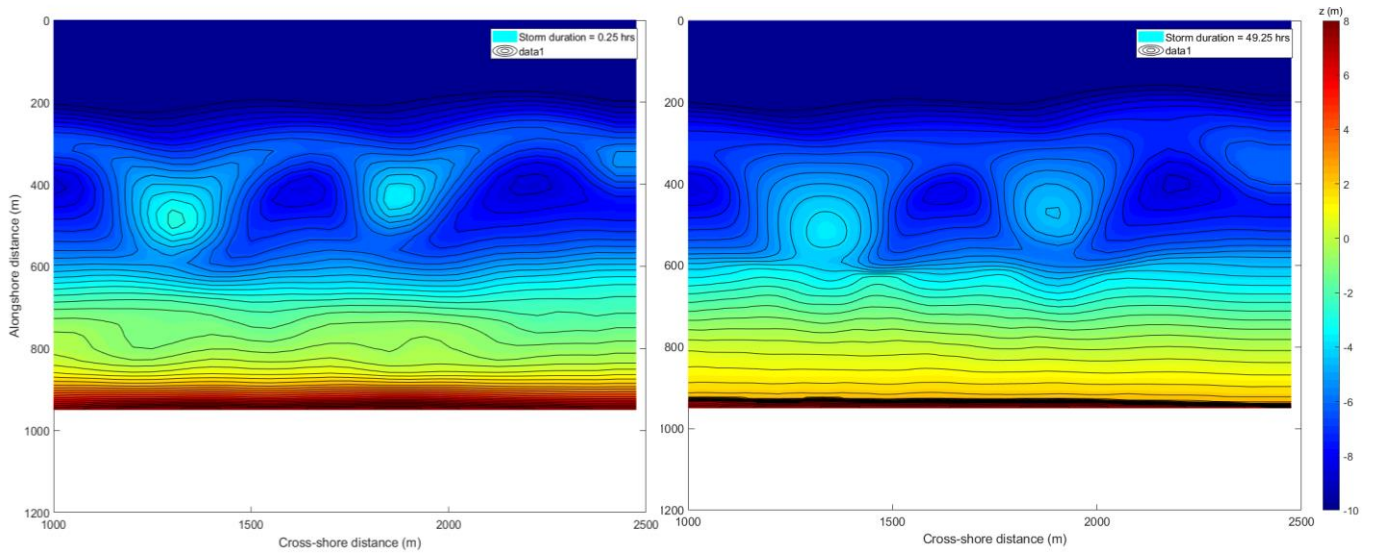


Figure 55 - Bed level response after a 48 hour Truc Vert storm of measured bathymetry + beach dune profile

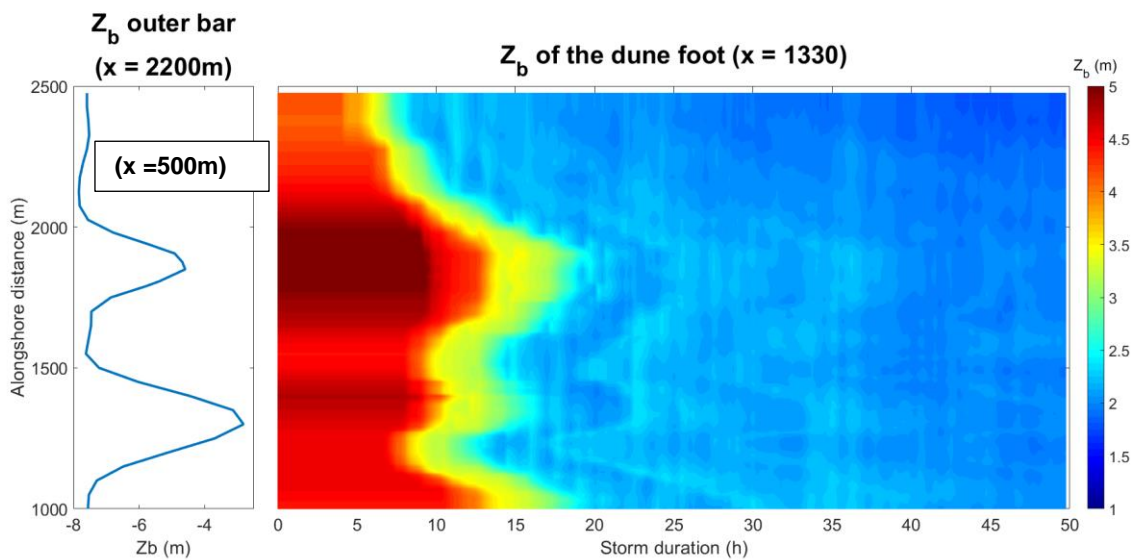


Figure 54 – Dune foot change over time, with the outer-bar profile as reference

It can be seen that the initial dune/beach profile show some alongshore variations (Figure 54). However, at storms end these initial alongshore variations in dune profile are more or less smoothed out. The initial dune profile is clearly related to the outer-bar pattern. It can be that the initial variations in dune foot are caused by calm weather, and are flattened out by the extreme storm. Nevertheless, this is a test run with a minimal boundary, a higher morfac and relatively long storm conditions with no changes in wave characteristics. Using XBeach for investigating dune response with no over-wash can be a great additional tool, if more research is conducted about the true validity of these type of 2DH XBeach models. Copying storm conditions from occurred events, with varying wave conditions over time, modelled with an improved artificial grid can be an interesting step towards new research. By doing this, the grid, including boundaries and grid spacing, can be optimized and compared to observations. General rules & tips that come with these findings can efficiently assist the generation of XBeach models in the future.

7. Conclusion

Modelling alongshore variations in dune erosion in the collision regime using a 2DH XBeach model is a relatively new approach. What dominantly drives these so-called erosional hotspots has not been generalized yet. This research is defined to two potential drivers of alongshore variable dune erosion; the nearshore bathymetry and wave characteristics.

As stated in the discussion, the angle of incoming waves is a compartment that is sensitive to errors within XBeach. A finding that is expected and valid, is a southern/northern shift in erosional hotspots that is in line with the magnitude of the wave angle of incidence. Furthermore, an overall higher erosion due to the 30-degree incoming wave angle is also present. Sedimentation moves southward due to this angle. However, the wave period does seem to influence alongshore variations in dune erosion. The overall erosion decreases with a lower period (see chapter 6.1), but the alongshore variability reduces as well. Making the wave period a considerable factor in terms of alongshore variable dune erosion.

In terms of near-shore bathymetry, the outer-bar bays are clearly related to erosional hotspots. The magnitude is smaller than expected, but the wave height, currents and sedimentation showed related behaviour. An interesting finding was the infragravity wave height. The peaks in IG wave height are at exact opposite locations of erosional hotspots (see section 5.2.3). Therefore, these results imply that infragravity waves do not steer erosional hotspots, but counteract it. Looking at sedimentation rate, the figures in section 5.2.3 show that sedimentation converges towards the outer-bar horns. Resulting in deposition on the beach behind the horns, creating an in-phase morphological coupling with the outer-bars. Except for bathy375TV, where are double the outer-bar wavelength coupling occurs. Section 5.3.2 show a sedimentation rate southward, giving a more spread out deposition on the beach. These findings correspond to the deposition on the beach area in chapter 5.4.

Overall, the near-shore bathymetry dominantly steers alongshore variable dune erosion. Wave characteristics play a role as well, but wouldn't matter at all if there are not prominent outer-bar horns present. Erosional hotspots scale with alongshore depth difference of the outer-bar, general depth of the horns and sea-ward position of the outer-bar. Furthermore, a XBeach 2DH model seems like a viable option to consider when modelling dune erosion of for instance, the Dutch and French coast, in the collision regime. However, further research about the validity of incoming wave angle within a 2DH XBeach model should be considered.

References

- De Winter, R. C., Gongriep, F., & Ruessink, B. G. (2015). Observations and modeling of alongshore variability in dune erosion at Egmond aan Zee, the Netherlands. *Coastal Engineering*, 99, 167-175.
- Castelle, B., Guillot, B., Marieu, V., Chaumillon, E., Hanquiez, V., Bujan, S., & Poppeschi, C. (2018). Spatial and temporal patterns of shoreline change of a 280-km high-energy disrupted sandy coast from 1950 to 2014: SW France. *Estuarine, Coastal and Shelf Science*, 200, 212-223.
- Castelle, B., Marieu, V., Bujan, S., Splinter, K. D., Robinet, A., Sénéchal, N., & Ferreira, S. (2015). Impact of the winter 2013–2014 series of severe Western Europe storms on a double-barred sandy coast: Beach and dune erosion and megacusp embayments. *Geomorphology*, 238, 135-148.
- Castelle, B., & Ruessink, B. G. (2011). Modeling formation and subsequent nonlinear evolution of rip channels: Time-varying versus time-invariant wave forcing. *Journal of Geophysical Research: Earth Surface*, 116(F4).
- Castelle, B., Ruessink, B. G., Bonneton, P., Marieu, V., Bruneau, N., & Price, T. D. (2010). Coupling mechanisms in double sandbar systems. Part 1: Patterns and physical explanation. *Earth Surface Processes and Landforms*, 35(4), 476-486.
- Castelle, B., Ruessink, B. G., Bonneton, P., Marieu, V., Bruneau, N., & Price, T. D. (2010). Coupling mechanisms in double sandbar systems. Part 2: impact on alongshore variability of inner-bar rip channels. *Earth Surface Processes and Landforms: The Journal of the British Geomorphological Research Group*, 35(7), 771-781.
- Splinter, K. D., Kearney, E. T., & Turner, I. L. (2018). Drivers of alongshore variable dune erosion during a storm event: Observations and modelling. *Coastal Engineering*, 131, 31-41.
- Splinter, K. D., Carley, J. T., Golshani, A., & Tomlinson, R. (2014). A relationship to describe the cumulative impact of storm clusters on beach erosion. *Coastal engineering*, 83, 49-55.
- Den Heijer, C. (2013). The role of bathymetry, wave obliquity and coastal curvature in dune erosion prediction (Vol. 12). IOS Press.
- Van Thiel de Vries, J. S. M. (2009). Dune erosion during storm surges.
- Roelvink, D., Reniers, A., Van Dongeren, A. P., de Vries, J. V. T., McCall, R., & Lescinski, J. (2009). Modelling storm impacts on beaches, dunes and barrier islands. *Coastal engineering*, 56(11-12), 1133-1152.
- Roelvink, D., McCall, R., Mehvar, S., Nederhoff, K., & Dastgheib, A. (2018). Improving predictions of swash dynamics in XBeach: The role of groupiness and incident-band runup. *Coastal Engineering*, 134, 103-123.

Masselink, G., & Gehrels, R. (Eds.). (2014). Coastal environments and global change. John Wiley & Sons.

Cohn, N., Ruggiero, P., de Vries, S., & Kaminsky, G. M. (2018). New insights on coastal foredune growth: the relative contributions of marine and aeolian processes. *Geophysical Research Letters*, *45*(10), 4965-4973.

Karunaratna, H., Pender, D., Ranasinghe, R., Short, A. D., & Reeve, D. E. (2014). The effects of storm clustering on beach profile variability. *Marine Geology*, *348*, 103-112.

Price, T. D., Ruessink, B. G., & Castelle, B. (2014). Morphological coupling in multiple sandbar systems-a review. *Earth Surface Dynamics*, *2*(1), 309-321

Price, T. D., Castelle, B., Ranasinghe, R., & Ruessink, B. G. (2013). Coupled sandbar patterns and obliquely incident waves. *Journal of Geophysical Research: Earth Surface*, *118*(3), 1677-1692.

Price, T. D., & Ruessink, B. G. (2013). Observations and conceptual modelling of morphological coupling in a double sandbar system. *Earth Surface Processes and Landforms*, *38*(5), 477-489.

Price, T. D. (2013). *Morphological coupling in a double sandbar system*. Utrecht University.

Ruessink, B. G., Boers, M., Van Geer, P. F. C., De Bakker, A. T. M., Pieterse, A., Grasso, F., & De Winter, R. C. (2012). Towards a process-based model to predict dune erosion along the Dutch Wadden coast. *Netherlands Journal of Geosciences*, *91*(3), 357-372.

Van de Lageweg, W. I., Bryan, K. R., Coco, G., & Ruessink, B. G. (2013). Observations of shoreline-sandbar coupling on an embayed beach. *Marine Geology*, *344*, 101-114.

Sallenger Jr, A. H. (2000). Storm impact scale for barrier islands. *Journal of Coastal Research*, *16*(3).

De Bakker, A. T. M., Brinkkemper, J. A., Van der Steen, F., Tissier, M. F. S., & Ruessink, B. G. (2016). Cross-shore sand transport by infragravity waves as a function of beach steepness. *Journal of Geophysical Research: Earth Surface*, *121*(10), 1786-1799.

Mulligan, R. P., Gomes, E. R., Miselis, J. L., & McNinch, J. E. (2019). Non-hydrostatic numerical modelling of nearshore wave transformation over shore-oblique sandbars. *Estuarine, Coastal and Shelf Science*, *219*, 151-160.

Stockdon, H. F., Sallenger Jr, A. H., Holman, R. A., & Howd, P. A. (2007). A simple model for the spatially-variable coastal response to hurricanes. *Marine Geology*, *238*(1-4), 1-20.

Galal, E. M., & Takewaka, S. (2011). The influence of alongshore and cross-shore wave energy flux on large-and small-scale coastal erosion patterns. *Earth Surface Processes and Landforms*, *36*(7), 953-966.

Harley, M. D., Turner, I. L., Short, A. D., Bracs, M. A., Phillips, M. S., Simmons, J. A., & Splinter, K. D. (2015). Four decades of coastal monitoring at Narrabeen-Collaroy Beach: the past, present and future of this unique dataset. In *Australasian Coasts & Ports Conference 2015: 22nd Australasian Coastal and Ocean Engineering Conference and the 15th Australasian Port and Harbour Conference* (p. 378). Engineers Australia and IPENZ.

Houser, C., Hapke, C., & Hamilton, S. (2008). Controls on coastal dune morphology, shoreline erosion and barrier island response to extreme storms. *Geomorphology*, *100*(3-4), 223-240.

Nilin, J., Pestana, J. L. T., Ferreira, N. G., Loureiro, S., Costa-Lotufo, L. V., & Soares, A. M. (2012). Physiological responses of the European cockle *Cerastoderma edule* (Bivalvia: Cardidae) as indicators of coastal lagoon pollution. *Science of the Total Environment*, *435*, 44-52.

Schupp, C. A., McNinch, J. E., & List, J. H. (2006). Nearshore shore-oblique bars, gravel outcrops, and their correlation to shoreline change. *Marine Geology*, *233*(1-4), 63-79.

Davidson, M. A., Splinter, K. D., & Turner, I. L. (2013). A simple equilibrium model for predicting shoreline change. *Coastal Engineering*, *73*, 191-202.

Senechal, N., Coco, G., Castelle, B., & Marieu, V. (2015). Storm impact on the seasonal shoreline dynamics of a meso-to macrotidal open sandy beach (Biscarrosse, France). *Geomorphology*, *228*, 448-461.

Claudino-Sales, V., Wang, P., & Horwitz, M. H. (2008). Factors controlling the survival of coastal dunes during multiple hurricane impacts in 2004 and 2005: Santa Rosa barrier island, Florida. *Geomorphology*, *95*(3-4), 295-315.

Bender, C. J., & Dean, R. G. (2003). Wave transformation by two-dimensional bathymetric anomalies with sloped transitions. *Coastal Engineering*, *50*(1-2), 61-84.

Palmsten, M. L., & Holman, R. A. (2012). Laboratory investigation of dune erosion using stereo video. *Coastal engineering*, *60*, 123-135.

Splinter, K. D., & Palmsten, M. L. (2012). Modeling dune response to an East Coast Low. *Marine Geology*, *329*, 46-57.

Daly, C., Roelvink, D., van Dongeren, A., de Vries, J. V. T., & McCall, R. (2012). Validation of an advective-deterministic approach to short wave breaking in a surf-beat model. *Coastal Engineering*, *60*, 69-83.

Vousdoukas, M. I., Wziatek, D., & Almeida, L. P. (2012). Coastal vulnerability assessment based on video wave run-up observations at a mesotidal, steep-sloped beach. *Ocean Dynamics*, *62*(1), 123-137.

Martínez, M. L., & Psuty, N. P. (2004). *Coastal dunes*. Berlin: Springer.

8. Appendix

8.1 Parameter files XBeach models

```

%%%%%%%%%%%%%%%%%%%%%%%%%%%%%%%%%%%%%%%%%%%%%%%%%%%%%%%%%%%%%%%%%%%%%%%%
%%%%%%%%%%%%%%%%%%%%%%%%%%%%%%%%%%%%%%%%%%%%%%%%%%%%%%%%%%%%%%%%%%%%%%%%
%%% XBeach parameter settings input file
%%%
%%%
%%% date:      04-Jul-2019 14:06:19
%%%
%%% function:  xb_write_params
%%%
%%%%%%%%%%%%%%%%%%%%%%%%%%%%%%%%%%%%%%%%%%%%%%%%%%%%%%%%%%%%%%%%%%%%%%%%
%%%%%%%%%%%%%%%%%%%%%%%%%%%%%%%%%%%%%%%%%%%%%%%%%%%%%%%%%%%%%%%%%%%%%%%%

%%% Grid parameters
%%%%%%%%%%%%%%%%%%%%%%%%%%%%%%%%%%%%%%%%%%%%%%%%%%%%%%%%%%%%%%%%%%%%%%%%

depfile      = bed.dep
posdwn       = 0
nx           = 280
ny           = 332
vardx        = 1
xfile        = x.grd
yfile        = y.grd
xori         = 0
yori         = 0.000000
thetamin     = -180
thetamax     = 180|
dtheta       = 20

%%% Initial conditions
%%%%%%%%%%%%%%%%%%%%%%%%%%%%%%%%%%%%%%%%%%%%%%%%%%%%%%%%%%%%%%%%%%%%%%%%

zs0          = 4

%%% Model time
%%%%%%%%%%%%%%%%%%%%%%%%%%%%%%%%%%%%%%%%%%%%%%%%%%%%%%%%%%%%%%%%%%%%%%%%
%

tstop        = 187200

%%% Morphology parameters
%%%%%%%%%%%%%%%%%%%%%%%%%%%%%%%%%%%%%%%%%%%%%%%%%%%%%%%%%%%%%%%%%%%%%%%%

morfac       = 2
morstart     = 14400

```

params.txt file for all model runs - only the z-values of 'ny' and 'nx' are changed - part 1

```

%%% Physical processes
%%%%%%%%%%%%%%%%%%%%%%%%%%%%%%%%%%%%%%%%%%%%%%%%%%%%%%%%%%%%%%%%%%%%%%%%

morphology    = 1

%%% Sediment transport parameters
%%%%%%%%%%%%%%%%%%%%%%%%%%%%%%%%%%%%%%%%%%%%%%%%%%%%%%%%%%%%%%%%%%%%%%%%

sws           = 1
lws           = 1
bulk          = 0

%%% Wave boundary condition parameters
%%%%%%%%%%%%%%%%%%%%%%%%%%%%%%%%%%%%%%%%%%%%%%%%%%%%%%%%%%%%%%%%%%%%%%%%

instat        = jons_table

%%% Wave breaking parameters
%%%%%%%%%%%%%%%%%%%%%%%%%%%%%%%%%%%%%%%%%%%%%%%%%%%%%%%%%%%%%%%%%%%%%%%%

break         = roelvink2
gamma         = 0.450000

%%% Wave-spectrum boundary condition parameters
%%%%%%%%%%%%%%%%%%%%%%%%%%%%%%%%%%%%%%%%%%%%%%%%%%%%%%%%%%%%%%%%%%%%%%%%

bcfile        = JONSWAP1.txt

%%% Output variables
%%%%%%%%%%%%%%%%%%%%%%%%%%%%%%%%%%%%%%%%%%%%%%%%%%%%%%%%%%%%%%%%%%%%%%%%

outputformat  = netcdf
tintm         = 900
tintg         = 10
tstart        = 0

nglobalvar    = 1
zs

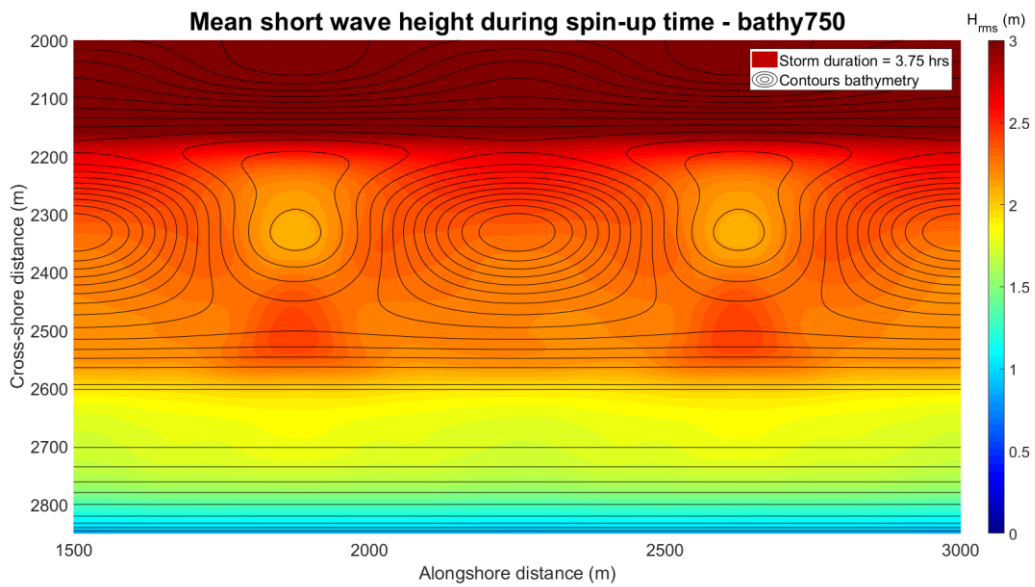
nmeanvar      = 7
H
zs
zb
v
u
Svtot
Sutot

```

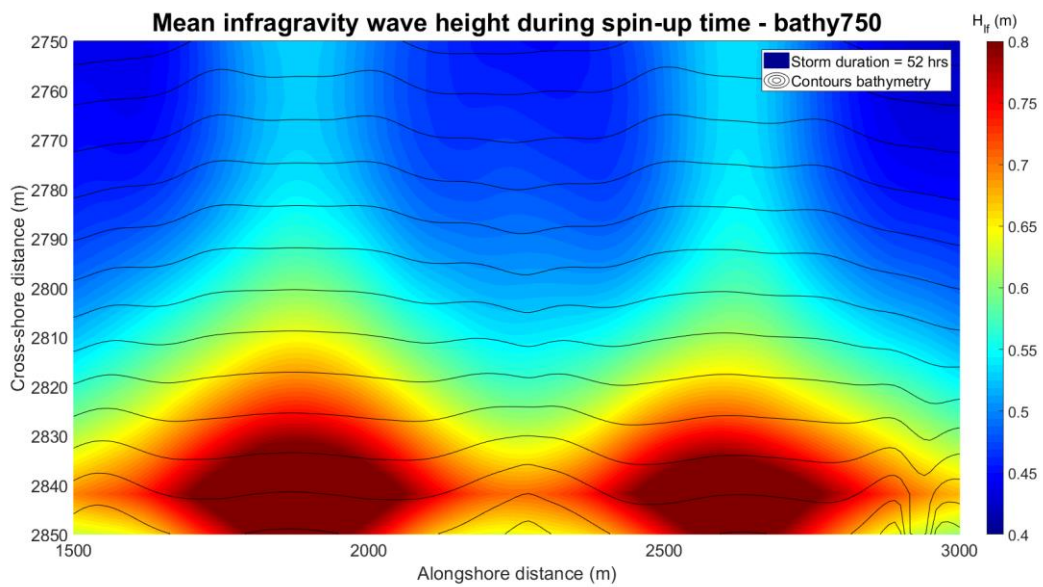
params.txt file for all model runs - only the z-values of 'ny' and 'nx' are changed - part 2

8.2 Truc Vert storm

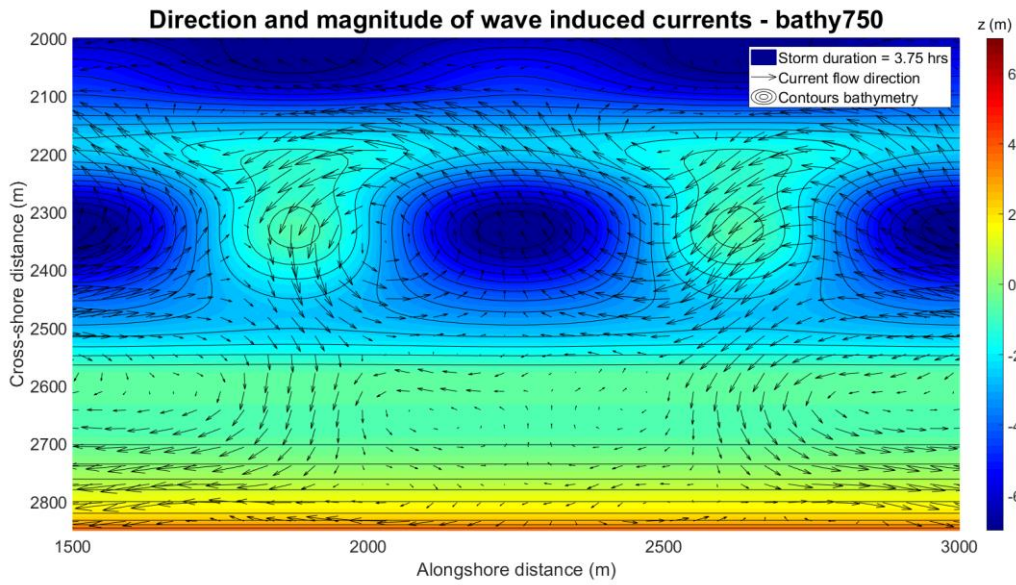
8.2.1 Bathy750 TV12



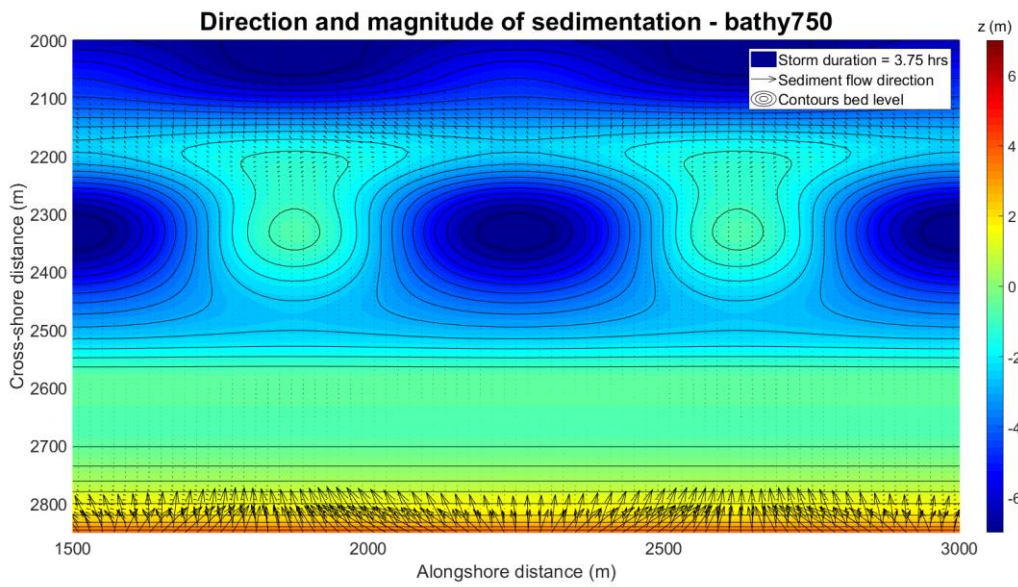
H_{rms} between outer bar and coastline for bathy750



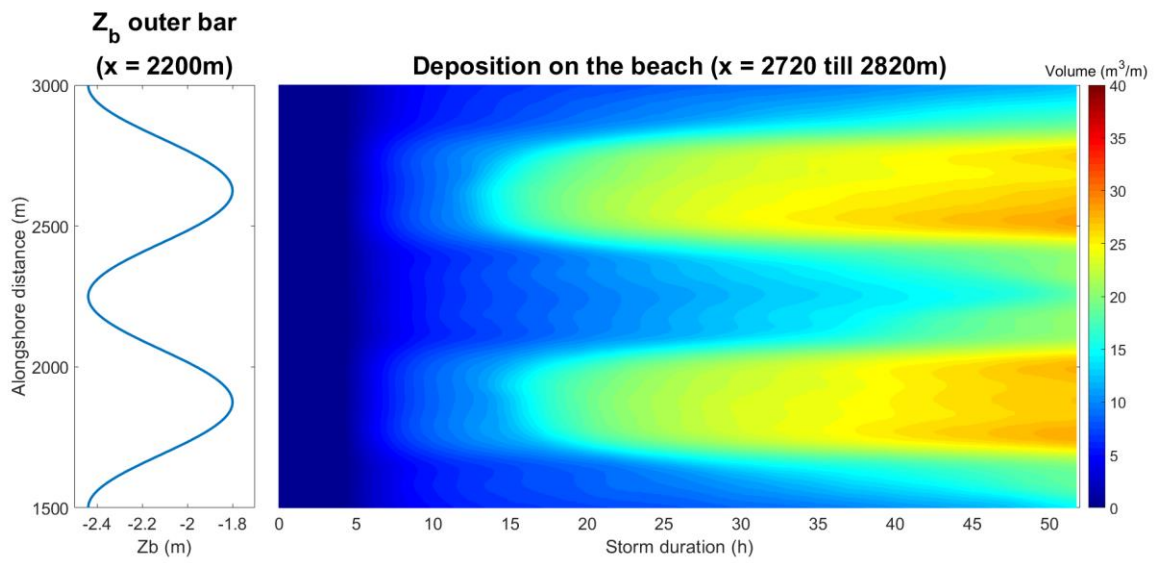
Low frequency wave height, close-up of the beach of bathy750



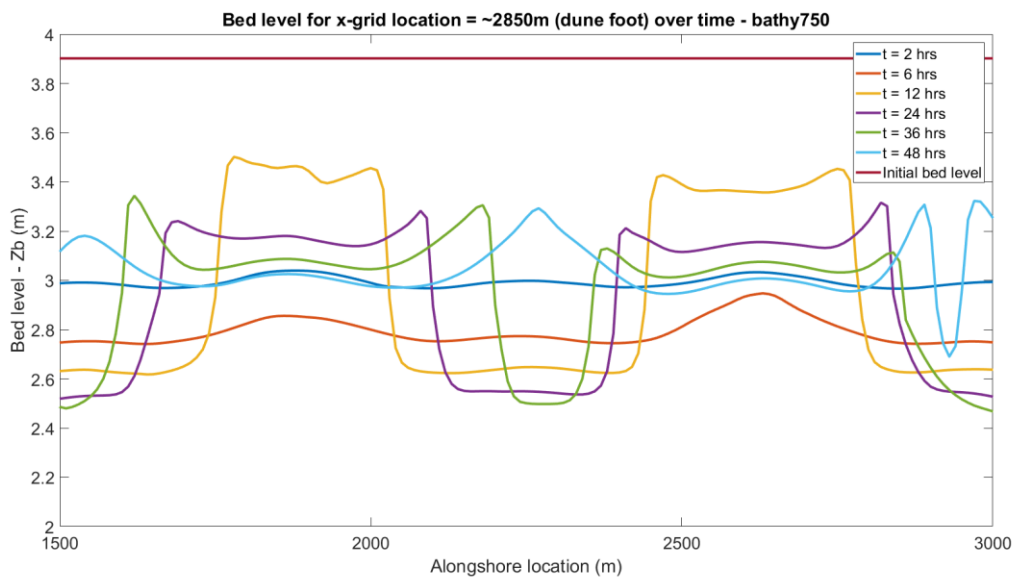
Wave induced currents at the near-shore bathymetry



Total sedimentation magnitude and direction

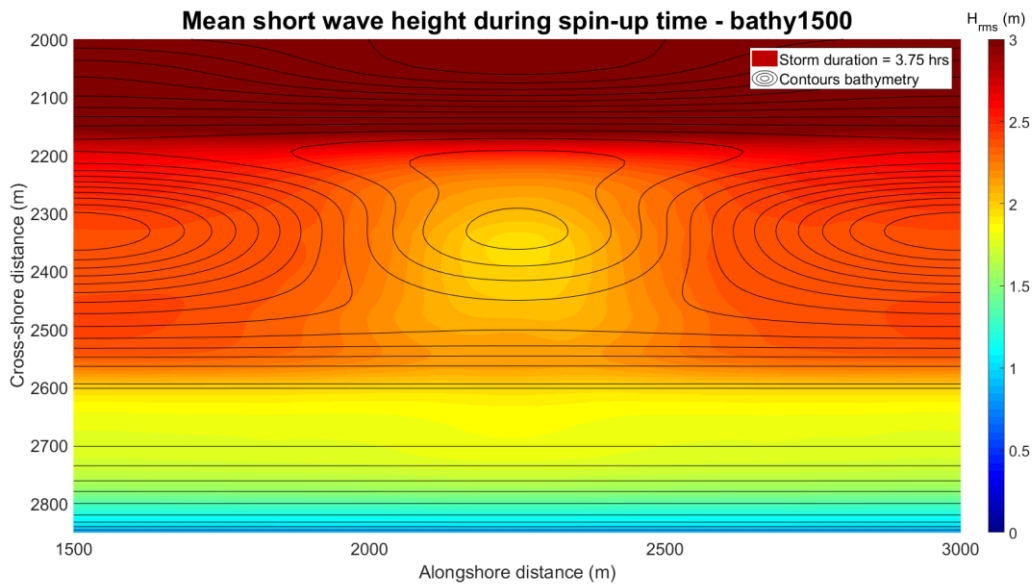


Deposited volume on the beach area

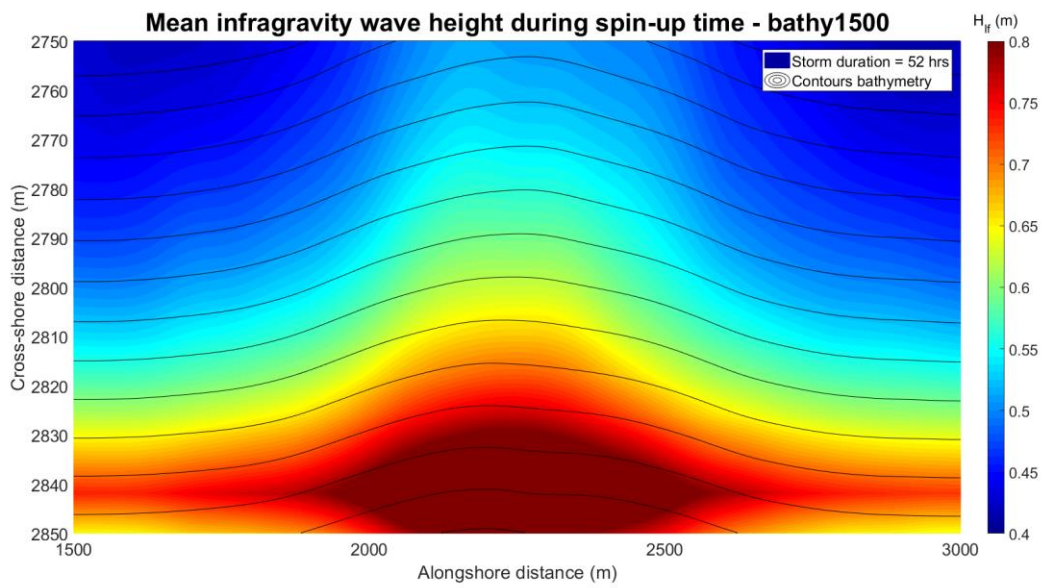


Alongshore section of the dune foot

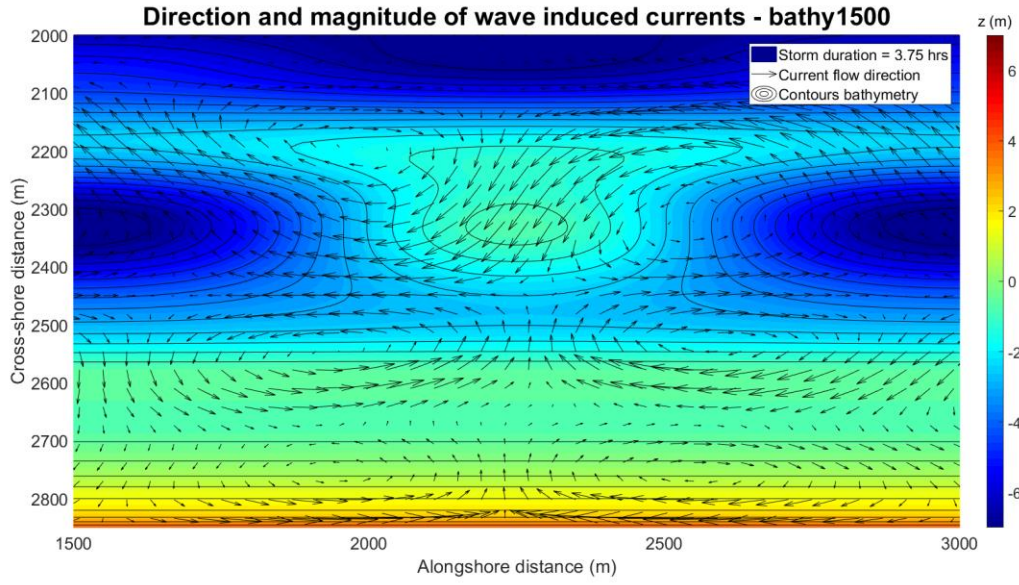
8.2.2 Bathy1500 TV12



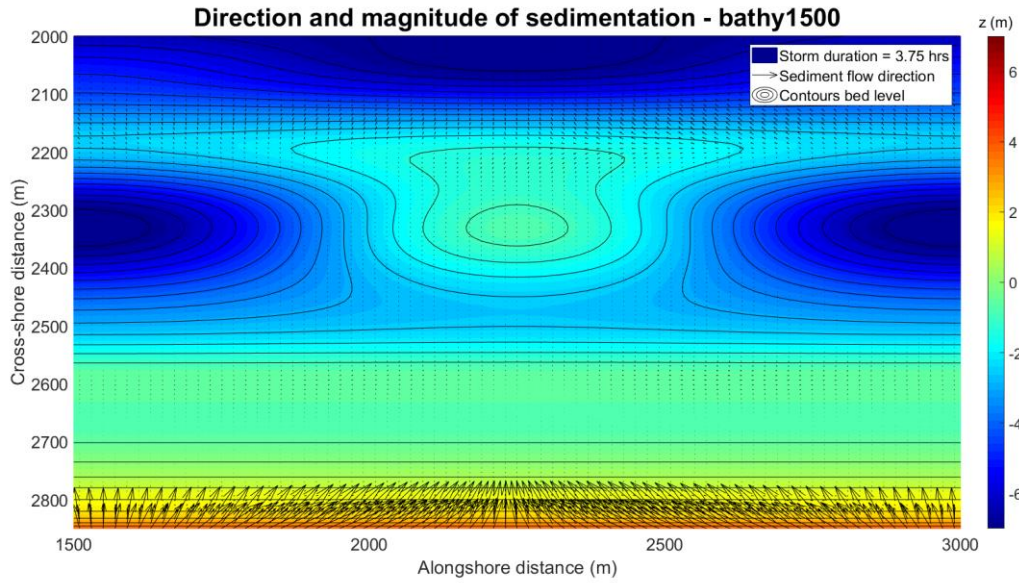
H_{rms} between outer bar and coastline for bathy1500



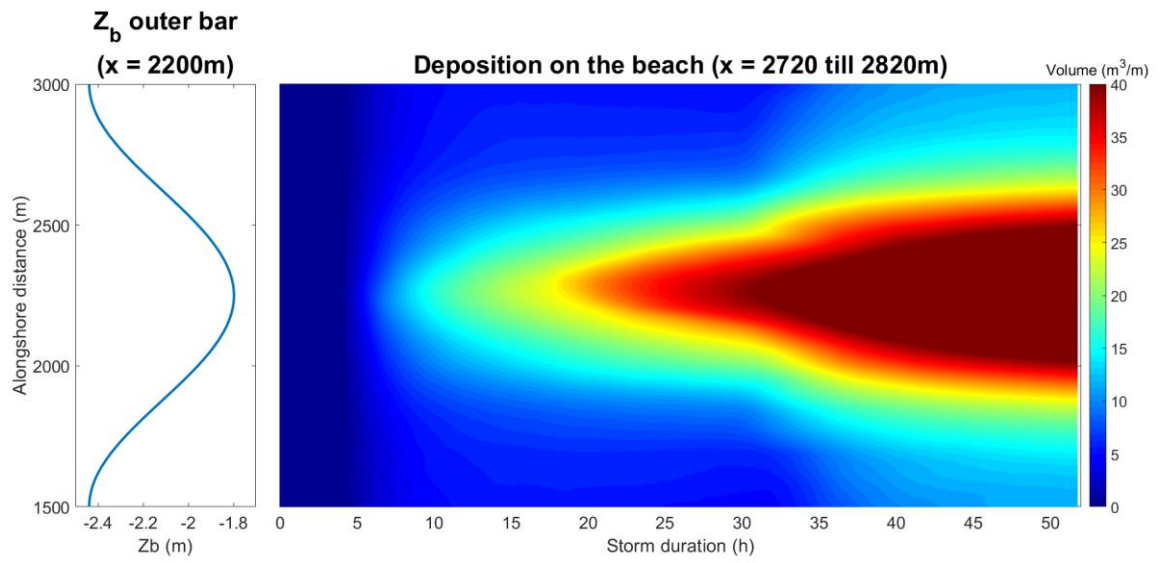
Low frequency wave height, close-up of the beach of bathy1500



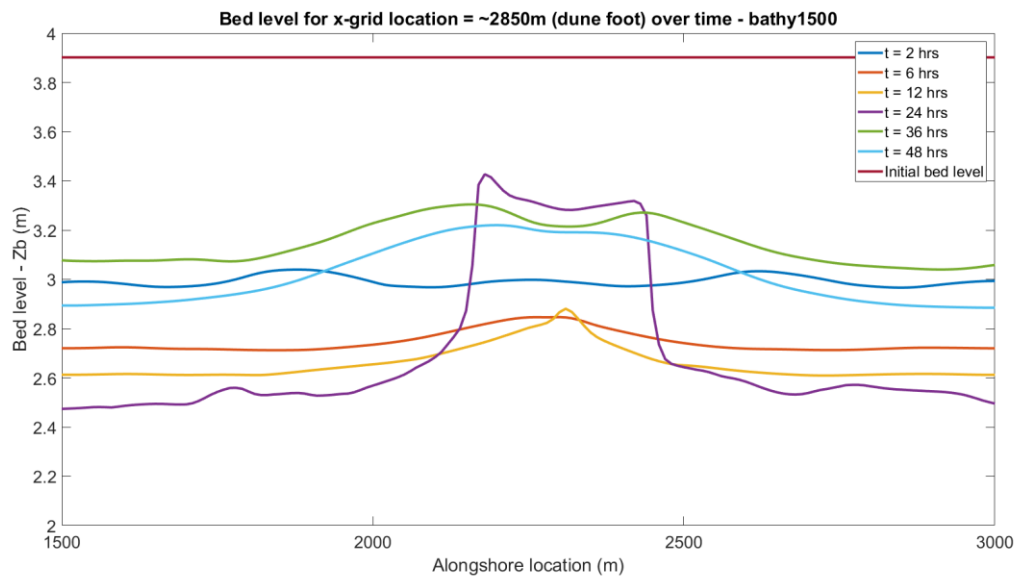
Wave induced currents at the near-shore bathymetry



Total sedimentation magnitude and direction

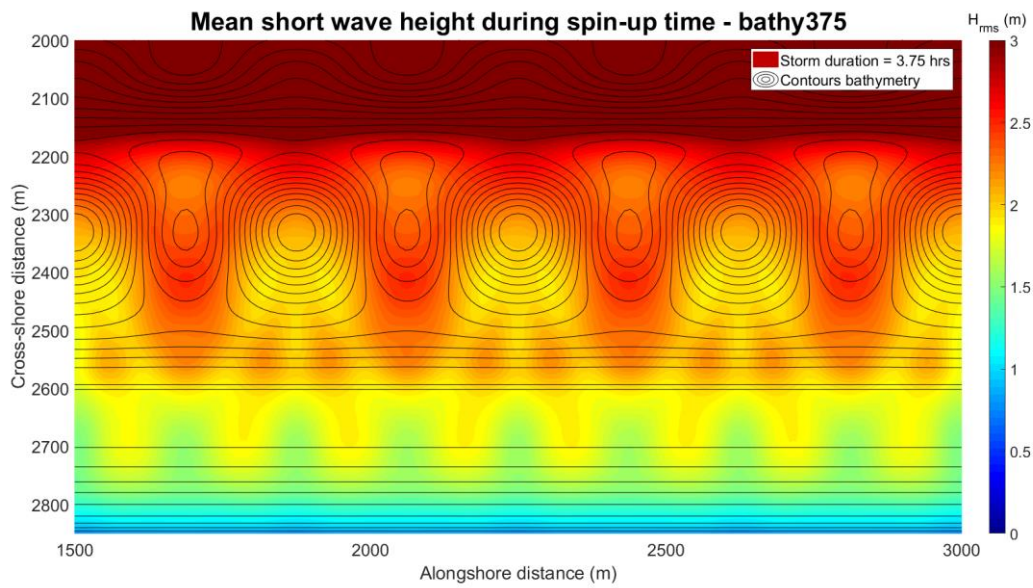


Deposited volume on the beach area

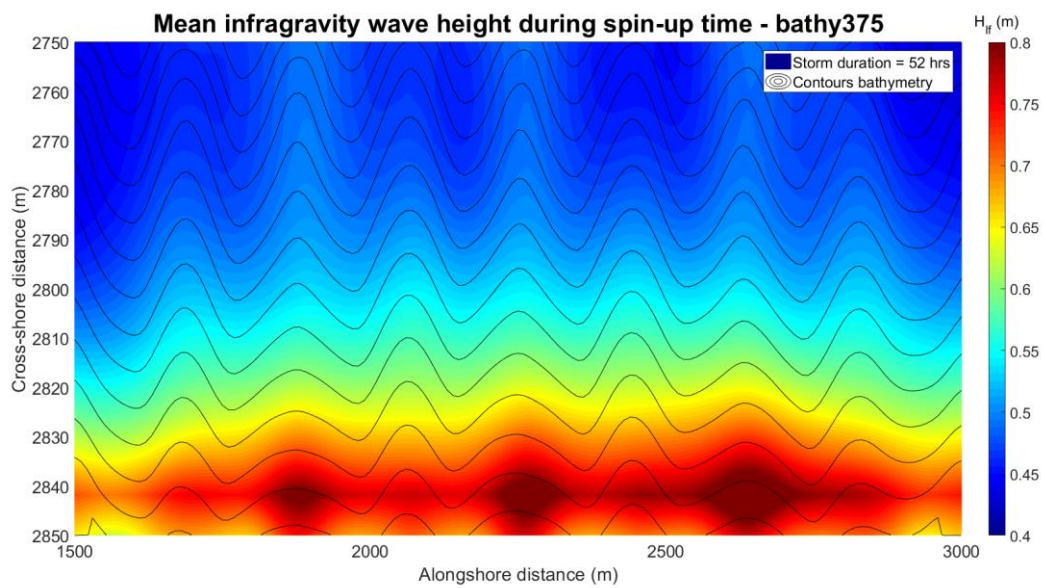


Alongshore section of the dune foot

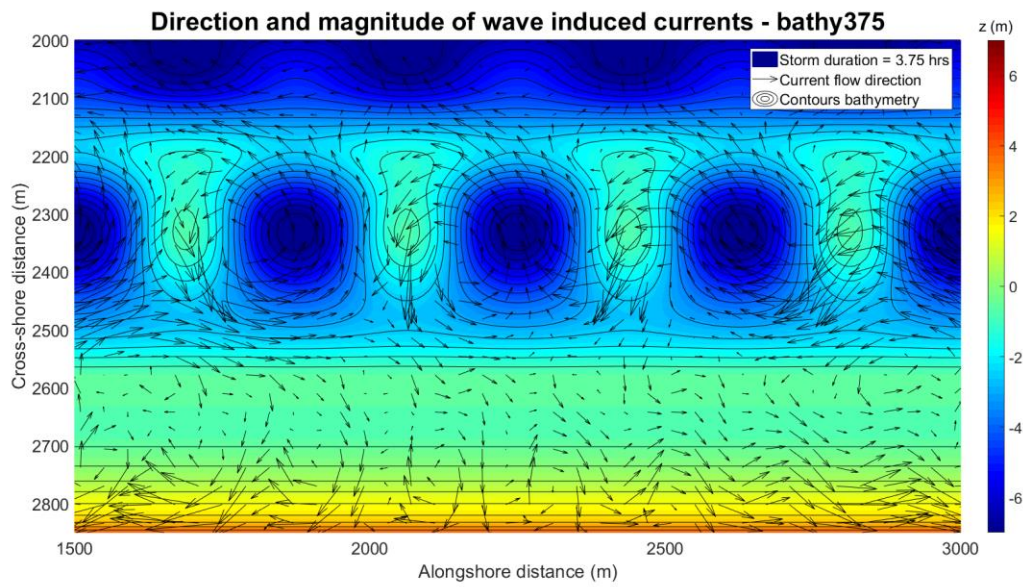
8.2.3 Bathy375 TV12



H_{rms} between outer bar and coastline for bathy375



Low frequency wave height, close-up of the beach of bathy375



Wave induced currents at the near-shore bathymetry

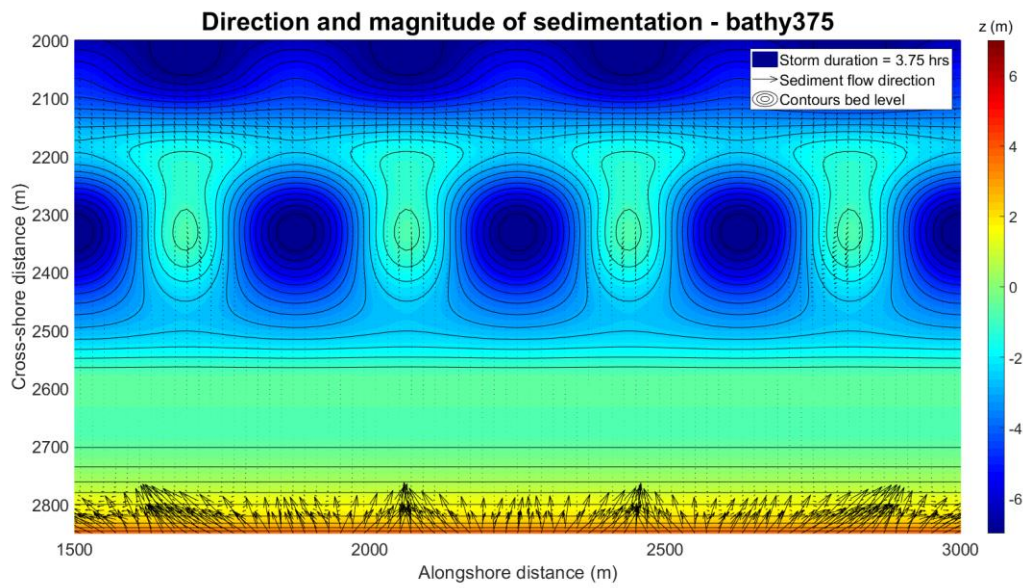
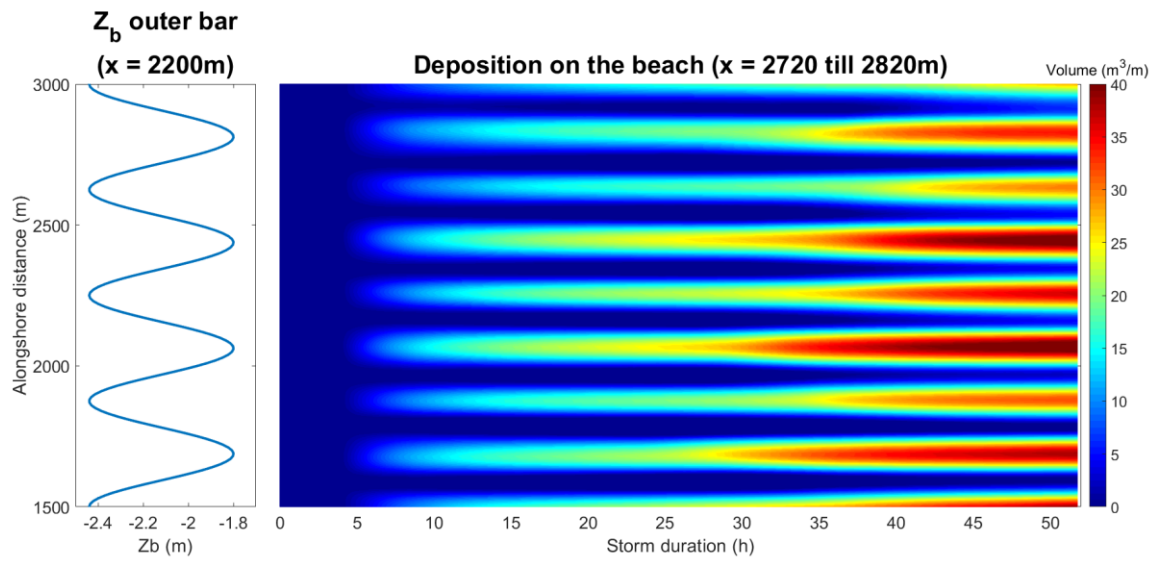
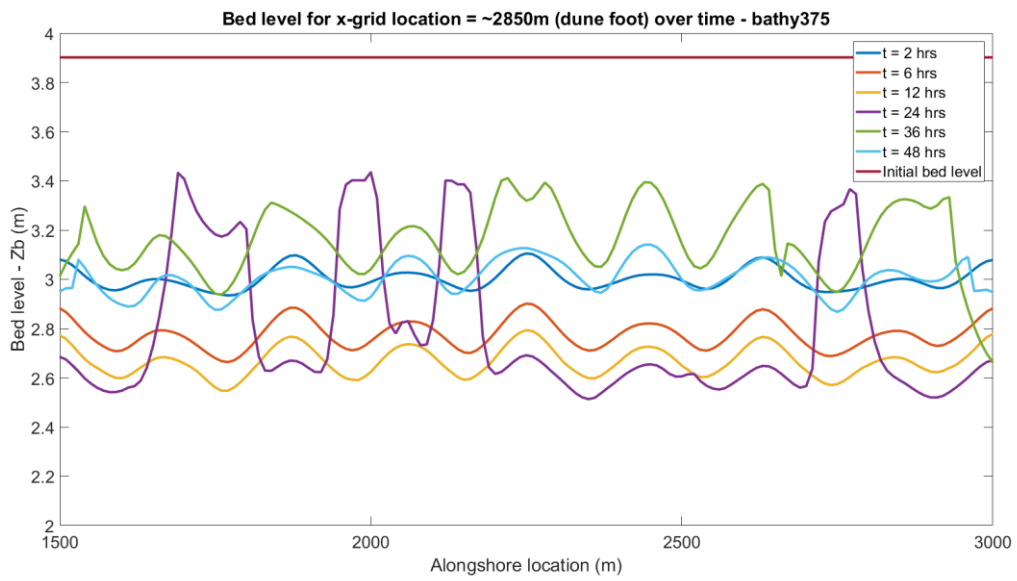


Figure 56 - Total sedimentation magnitude and direction

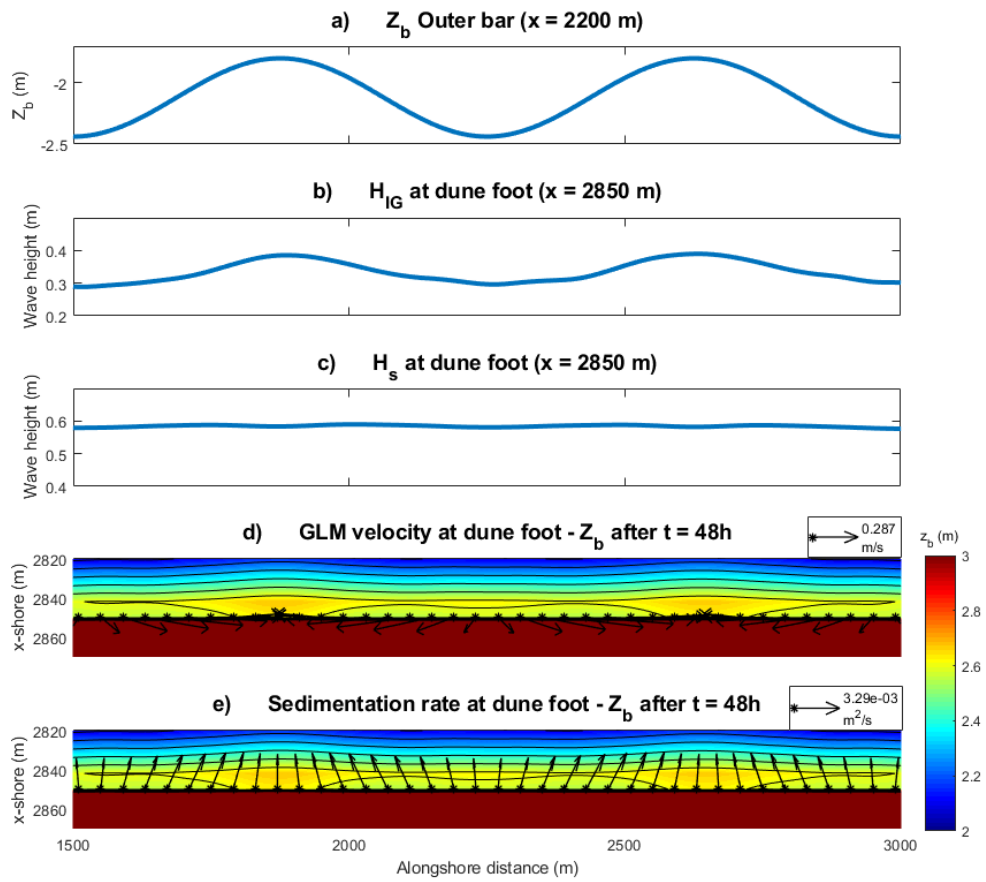


Deposited volume on the beach area

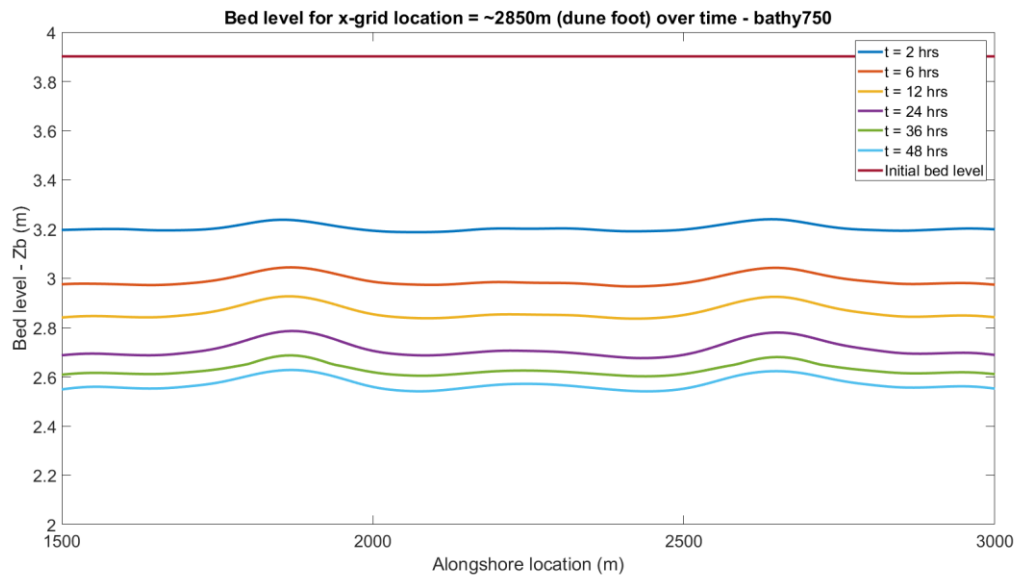


Alongshore section of the dune foot

8.2.4 Bathy750 TV8

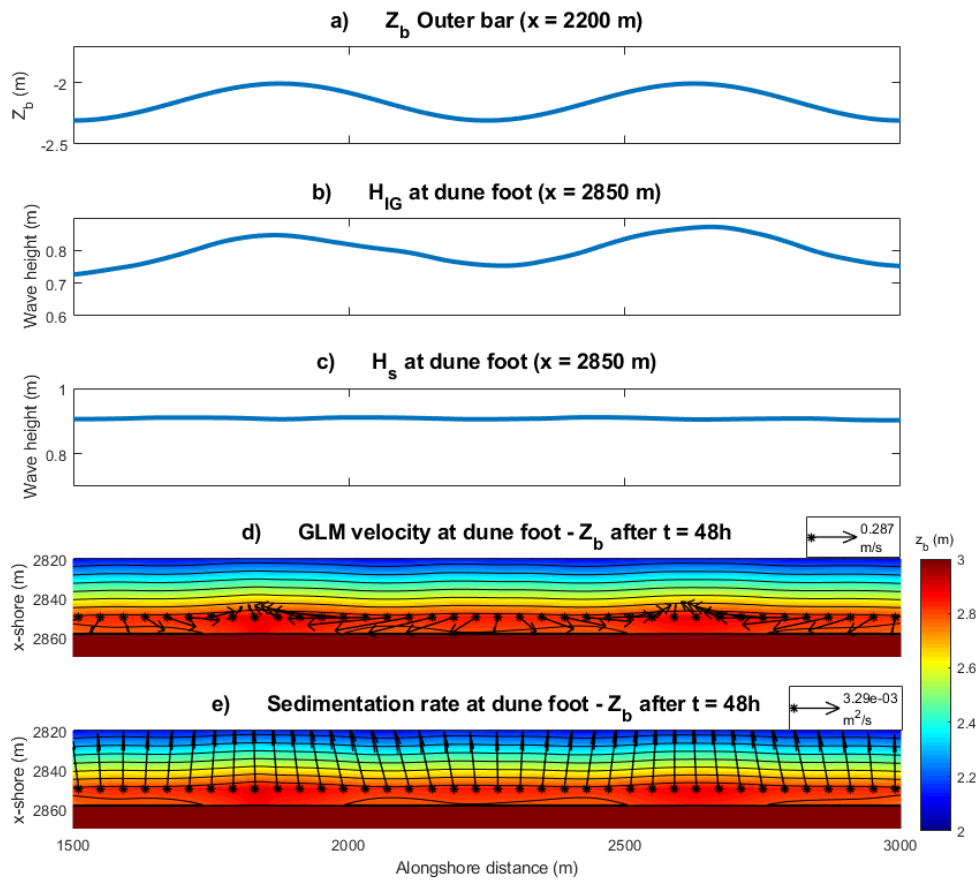


bathy750TV8: Five subplots containing wave heights, wave induced currents and sedimentation rate, with the outer-bar as reference

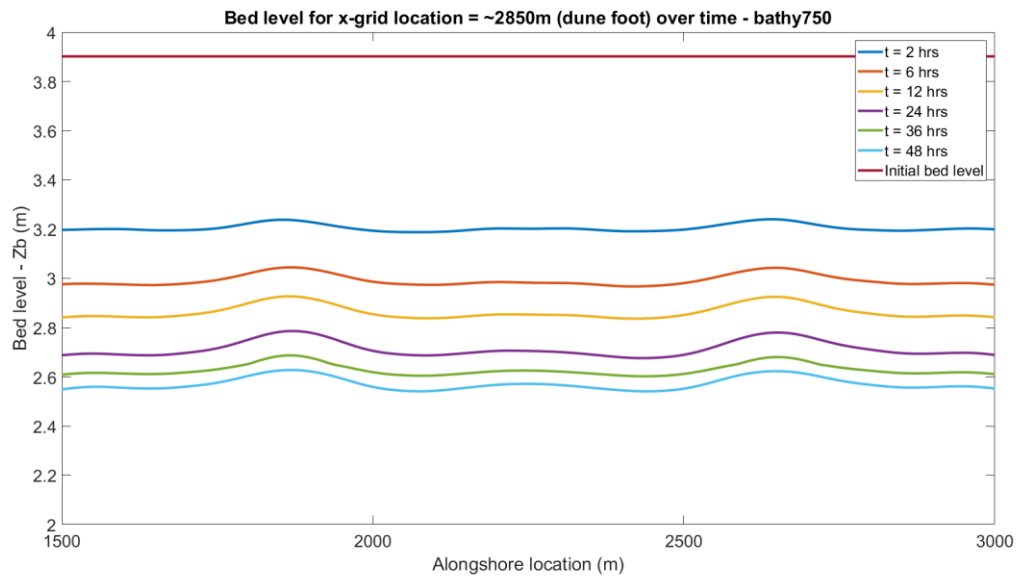


Alongshore section of the dune foot

8.2.5 Bathy750shallow



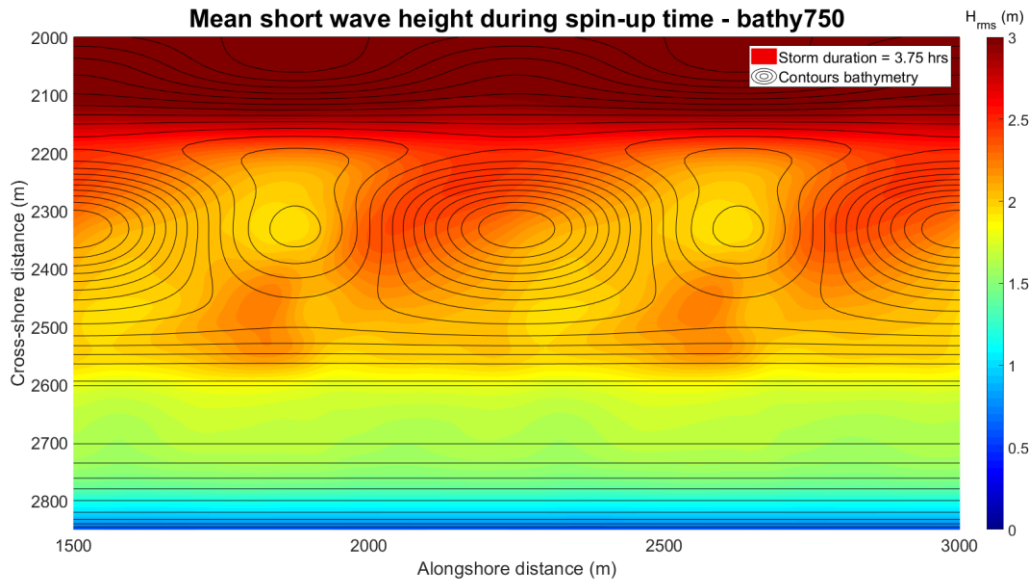
bathy750TV8: Five subplots containing wave heights, wave induced currents and sedimentation rate, with the outer-bar as reference



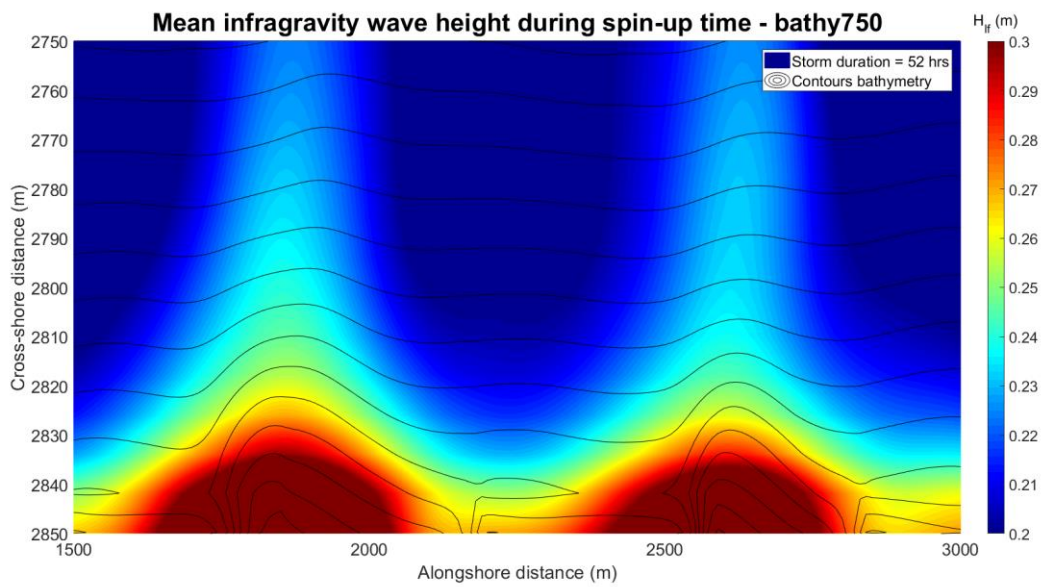
Alongshore section of the dune foot

8.3 Egmond storm

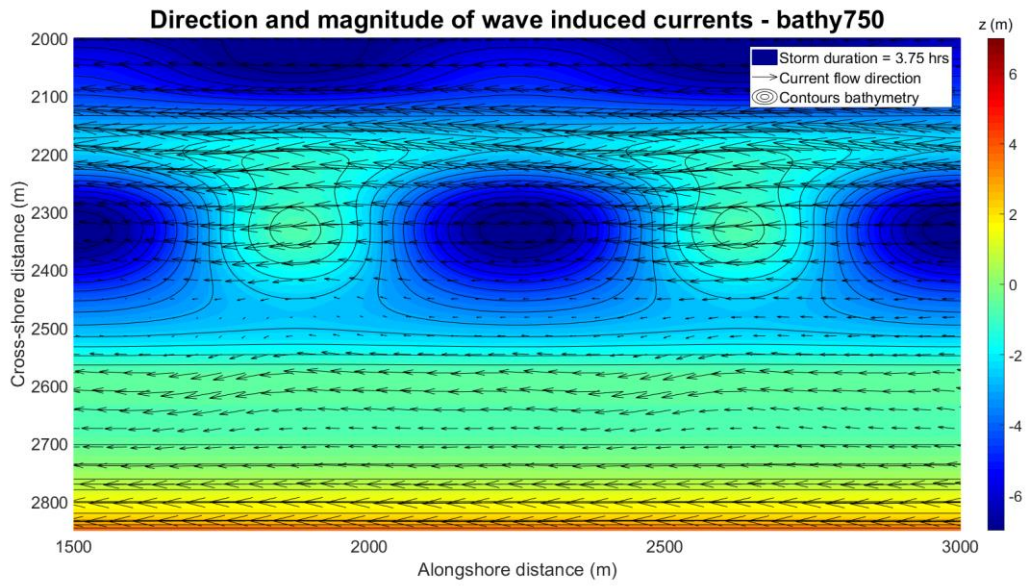
8.3.1 Bathy750 EG



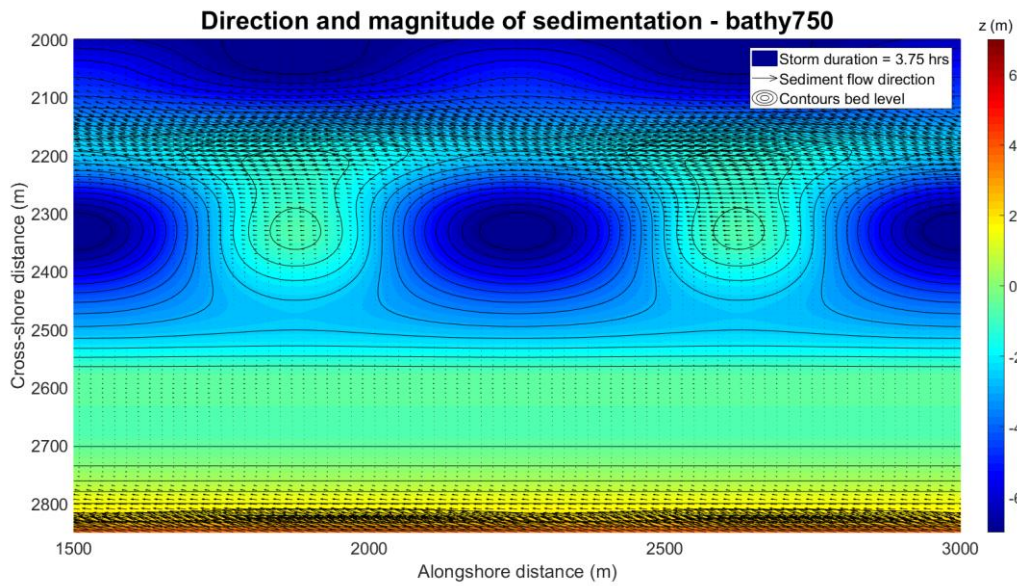
H_{rms} between outer bar and coastline for bathy750



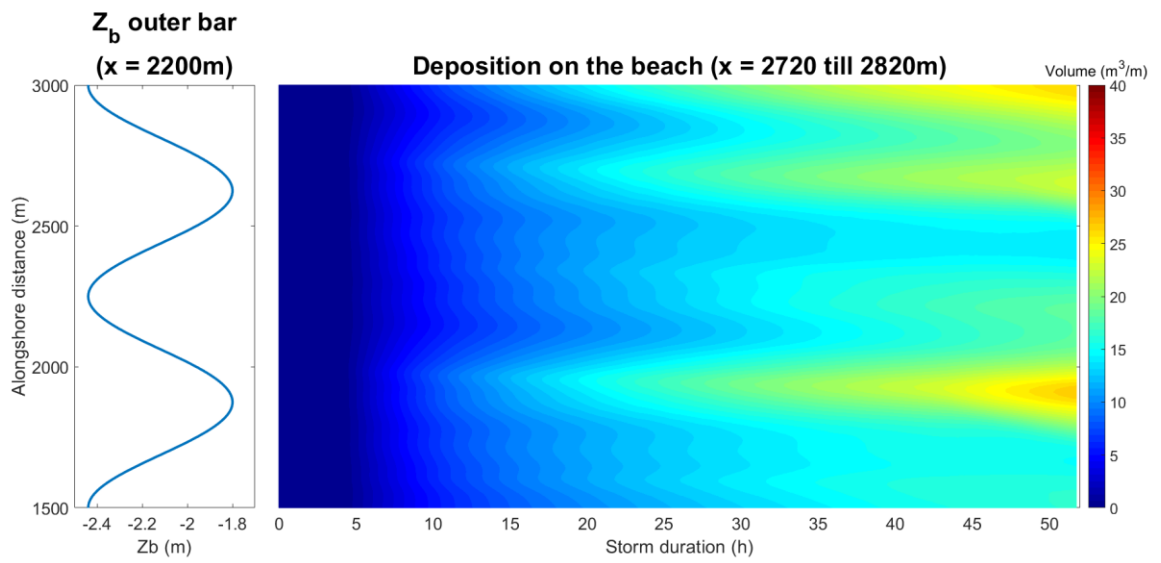
Low frequency wave height, close-up of the beach of bathy750



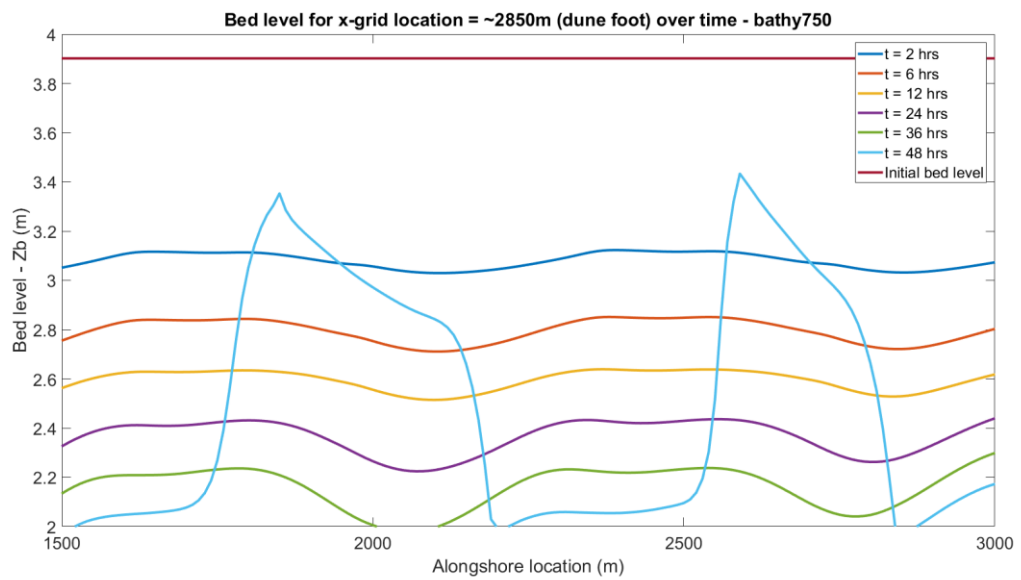
Wave induced currents at the near-shore bathymetry



Total sedimentation magnitude and direction

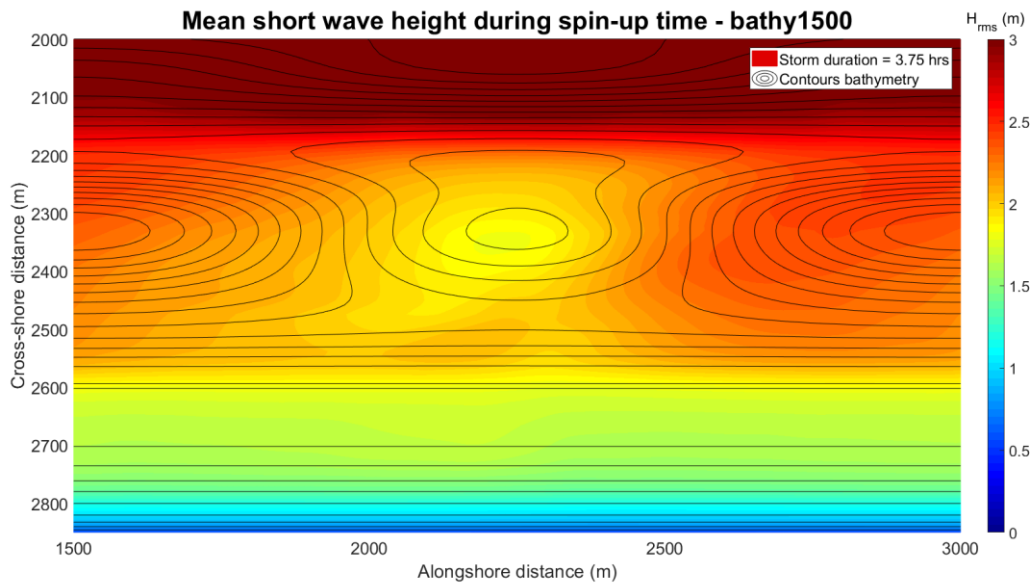


Deposited volume on the beach area

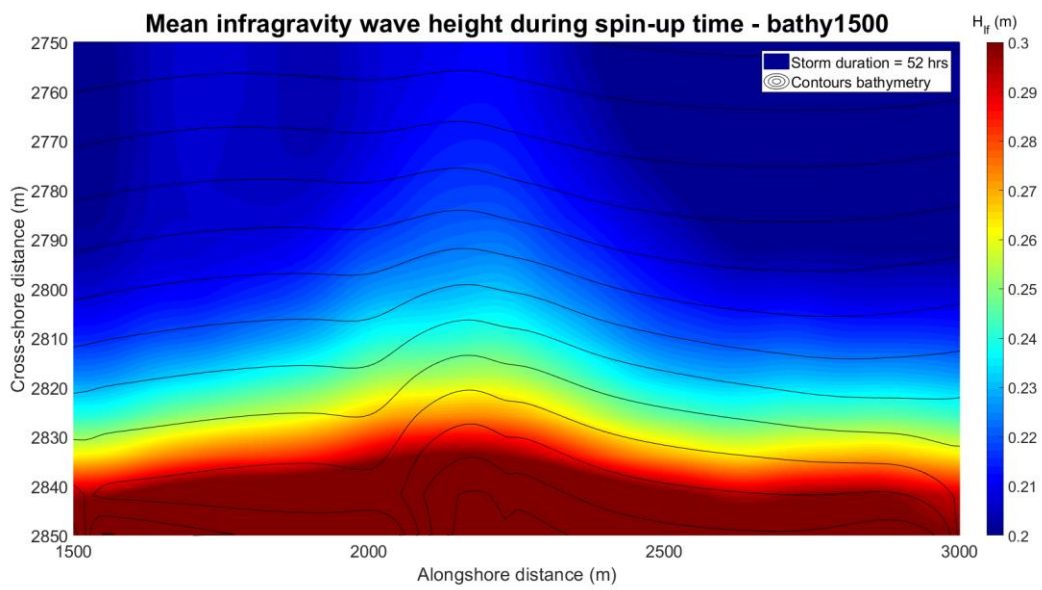


Alongshore section of the dune foot

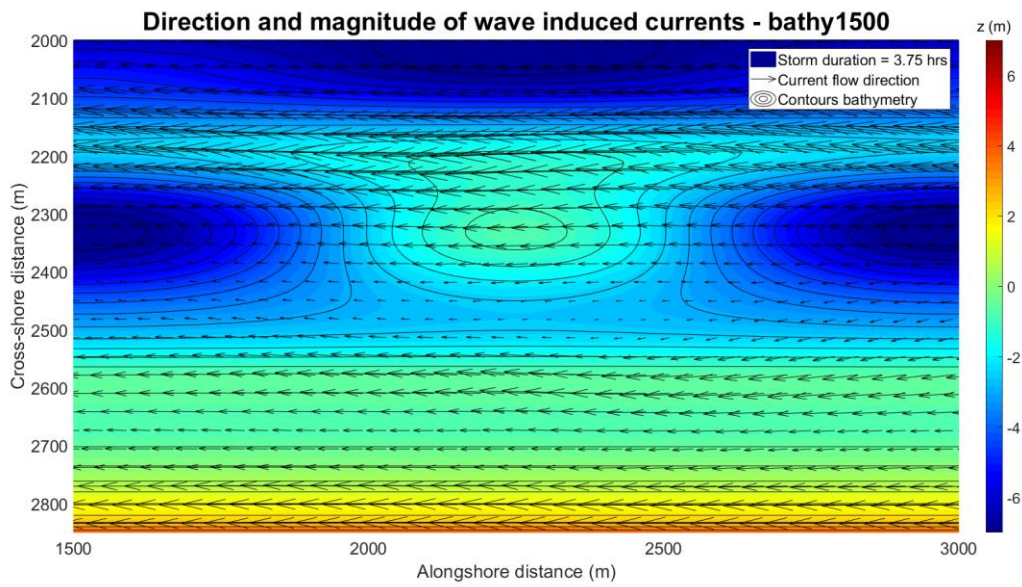
8.3.2 Bathy1500 EG



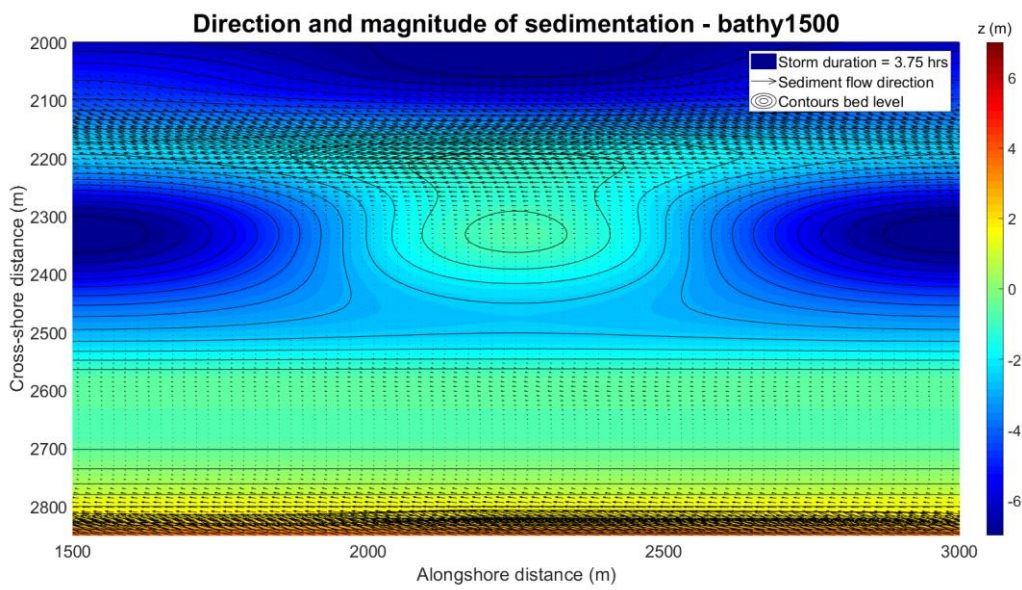
H_{rms} between outer bar and coastline for bathy1500



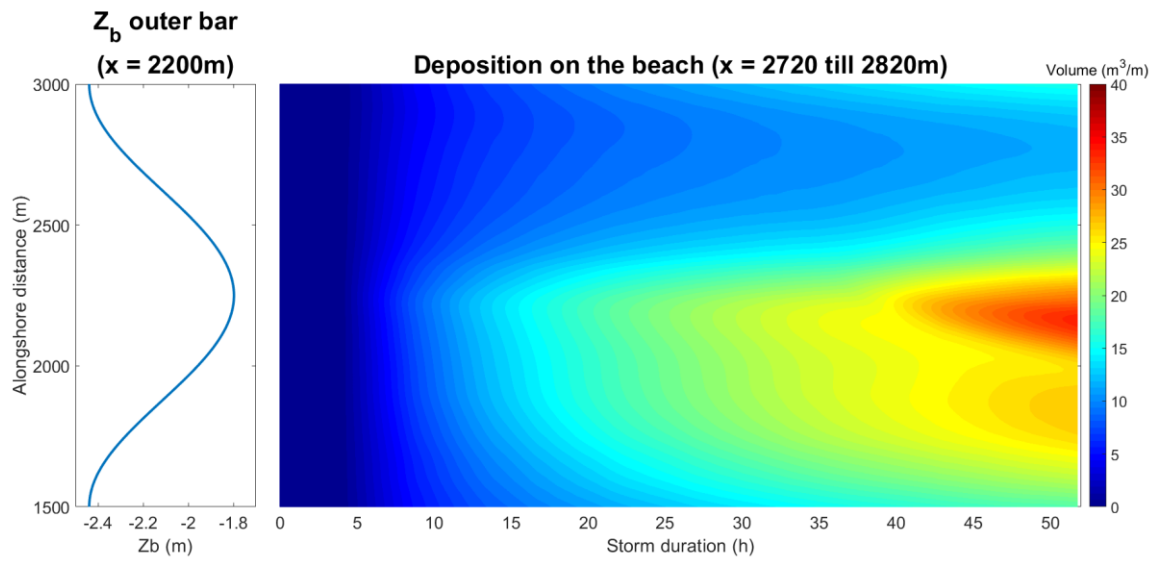
Low frequency wave height, close-up of the beach of bathy1500



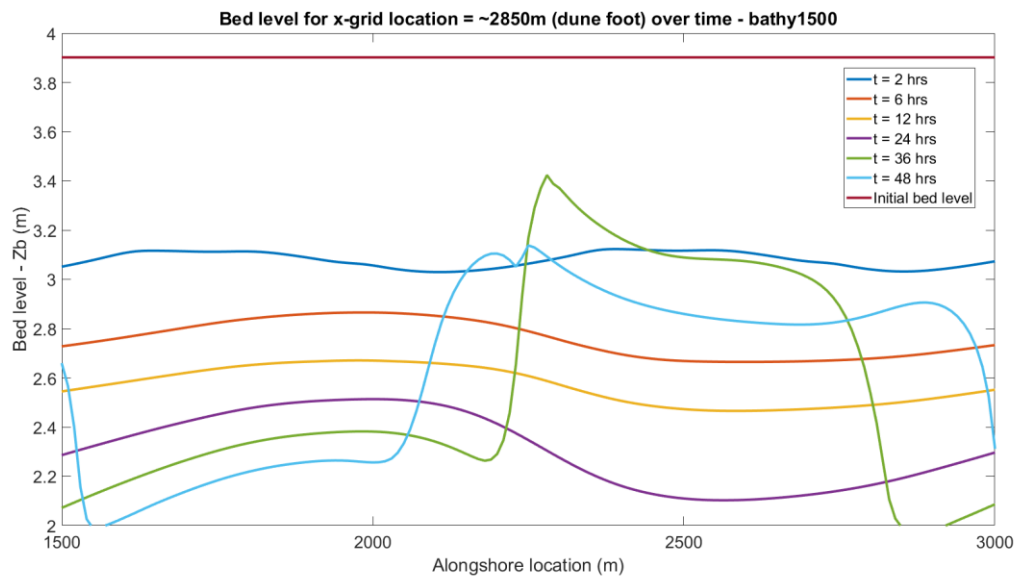
Wave induced currents at the near-shore bathymetry



Total sedimentation magnitude and direction

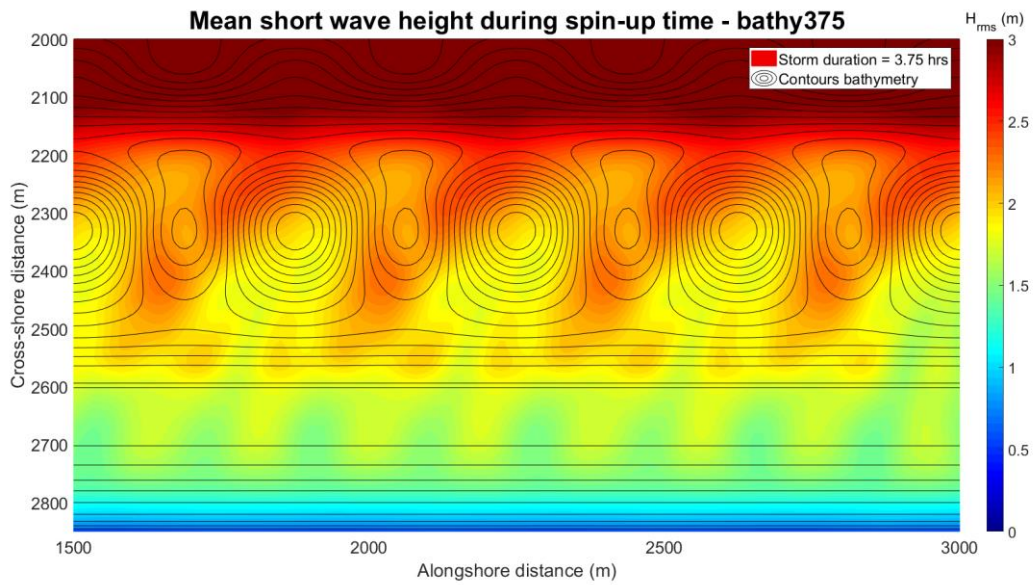


Deposited volume on the beach area

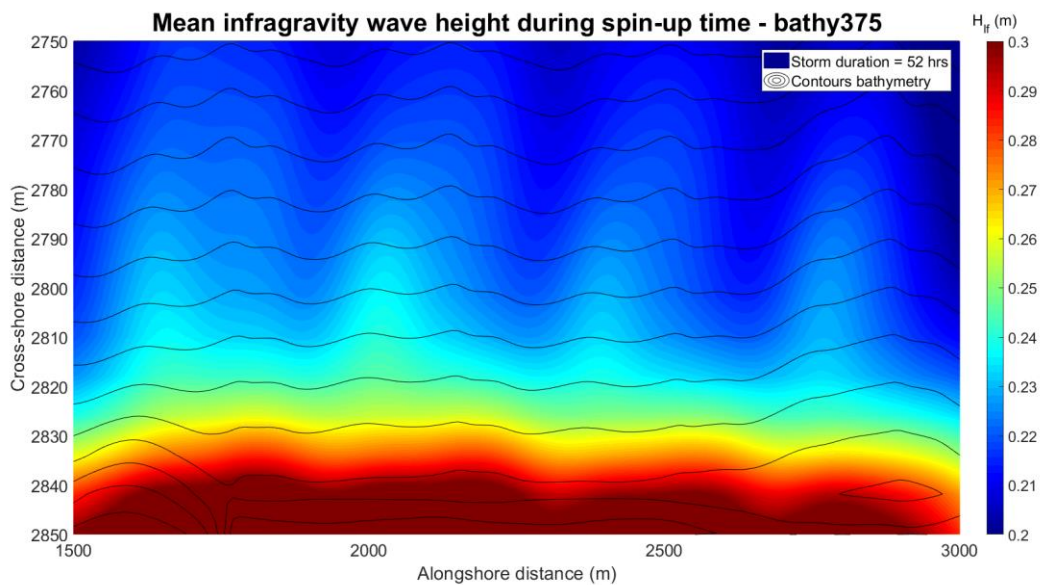


Alongshore section of the dune foot

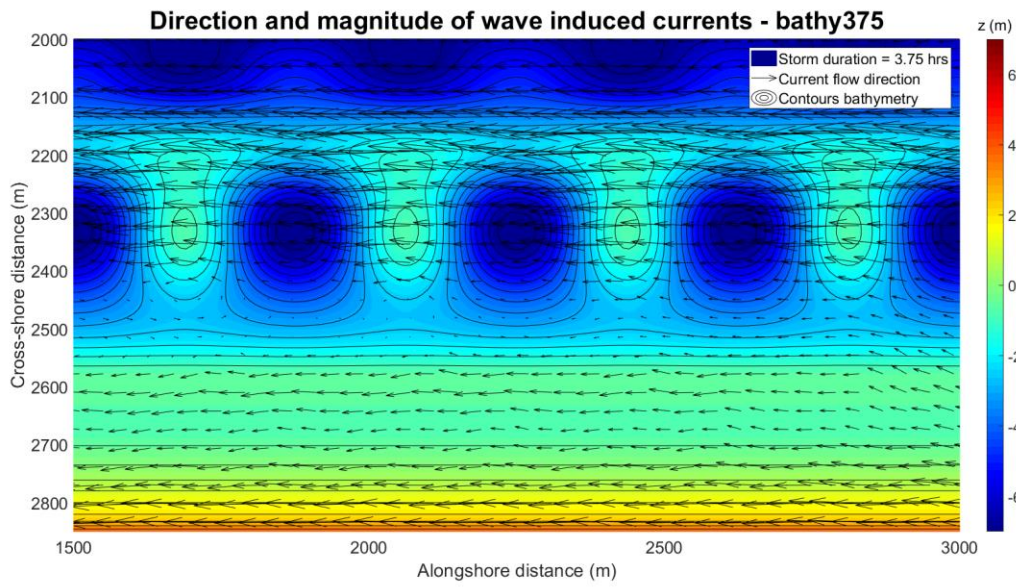
8.3.3 Bathy375 EG



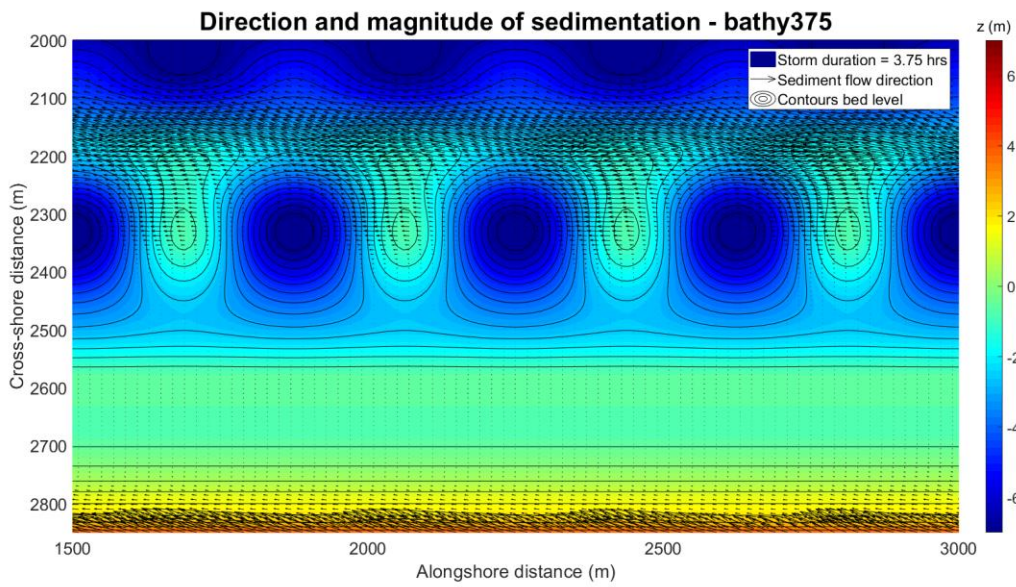
H_{rms} between outer bar and coastline for bathy375



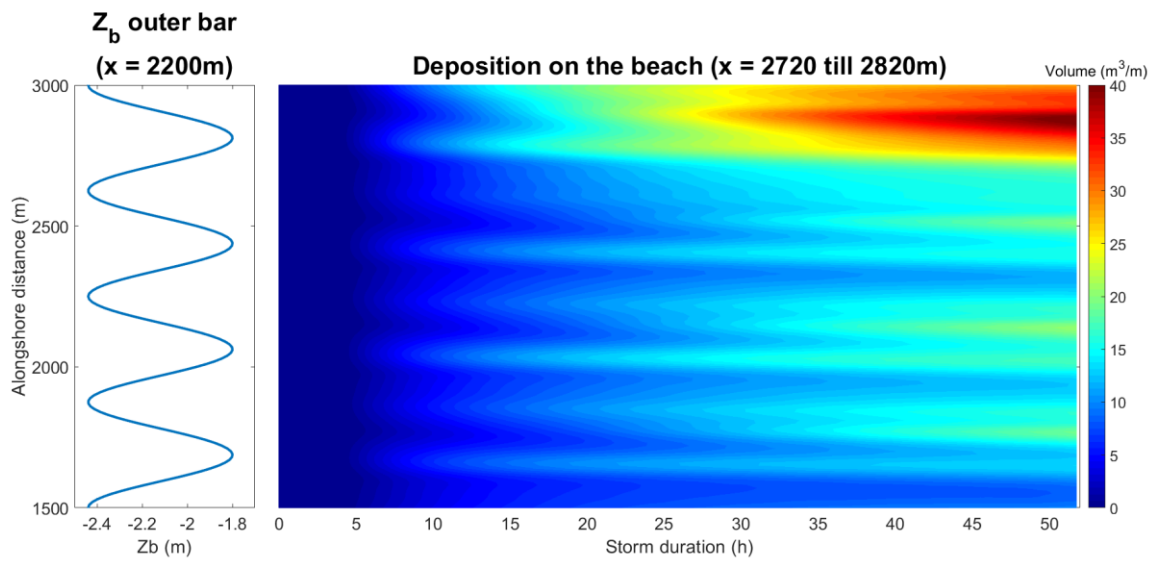
Low frequency wave height, close-up of the beach of bathy375



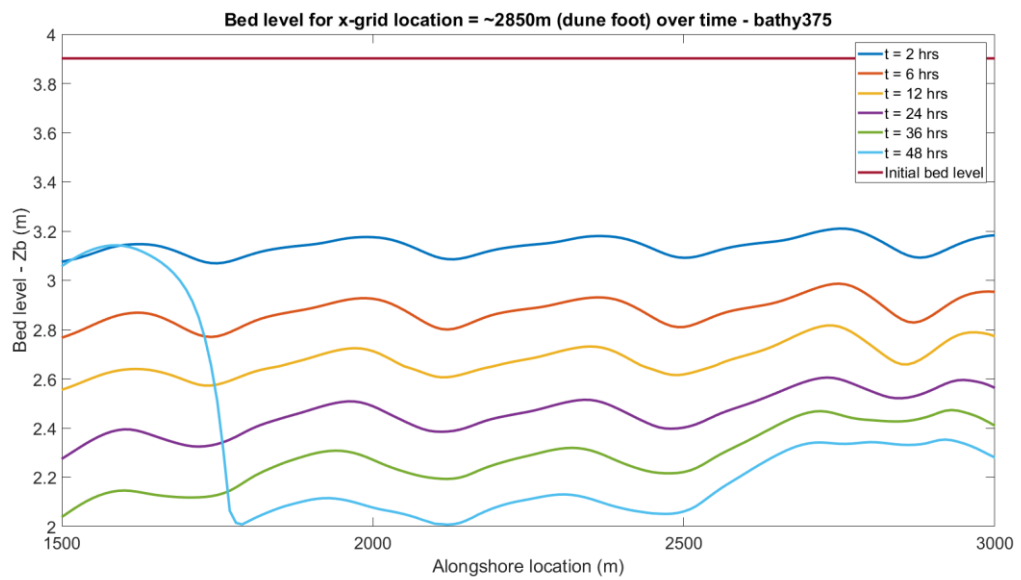
Wave induced currents at the near-shore bathymetry



Total sedimentation magnitude and direction



Deposited volume on the beach area



Alongshore section of the dune foot